TOWARD A COMPUTATIONAL THEORY OF SHAPE

Benjamin B. Kimia

Department of Electrical Engineering
McGill University, Montréal

A thesis submitted to the Faculty of Graduate Studies and Research
in partial fulfillment of the requirements for the degree of
Doctor of Philosophy

August 1990

Abstract

Although the shape of objects is a key to their recognition, viable theories for representing and describing shape have been elusive. We propose a framework that unifies competing approaches to shape. The basis for our approach is an analysis of deformations of shape designed to induce a topology over shapes suitable to support object recognition. We show that deformations classify into *constant motion* and *curvature motion*, which intriguingly lead to *conservation laws* for shape. These conservation laws are nonlinear and lead to singularities. A notion of entropy for shape is developed which limits the singularities of shape to *shocks*. The formation of shocks and their classification under arbitrary deformations is the basis of our representation for shape. The space of deformations leads to a *reaction-diffusion* space for shape in which the formation of shocks is studied. This leads us to propose *parts*, *protrusions*, and *bends* as the computational elements of shape. A notion of *scale* on these elements then naturally emerges, which is captured by the *entropy scale-space*. Any particular shape is finally described as the interaction between processes for computing parts, protrusions, and bends, the perceptual reality of which is illustrated via qualitative experiments.

Résumé

Quoique la forme des objets soit un élément clé dans le processus de reconnaissance de ceux-ci, une théorie viable de représentation et de description des formes est restée évasive jusqu'à ce jour. Nous proposons une théorie qui unifie des approches rivales de la description des formes. La base de notre approche est une analyse des déformations morphologiques conçue pour induire une topologie sur l'ensemble des formes appropriée pour la reconnaissance d'objets. Nous montrons que les déformations se divisent en *mouvement constant* et en *mouvement courbe*, produisant ainsi des *lois de conservation* pour les formes. Ces lois sont non-linéaires et induisent des singularités. Une notion d'entropie pour les formes est développée limitant les singularités de forme à des *chocs*. La formation de chocs et leur classification, lorsque soumis à des déformations arbitraires, est la base de notre représentation. L'espace des déformations produit ce qu'on appellera un *espace de réaction-diffusion* pour les formes dans lequel la formation de chocs est étudiée. Ceci nous amène à proposer comme éléments de calcul de la forme les trois catégories suivantes, soit les *parties*, les *appendices* et les *plis*. Une notion d'*échelle* sur ces éléments se déduit naturellement et est caractérisée par l'*espace-échelle d'entropie*. N'importe quelle forme peut enfin être décrite par l'intéraction entre les processus de calcul des parties, des appendices et des plis. Enfin, leur plausibilité au niveau de la perception est illustrée par des expériences qualitatives.

Acknowledgements

I cherish the time that I spent with Steve Zucker as the supervisor of my graduate studies. I have learned a great deal, academically, and otherwise and I have truly enjoyed it. The times with him have been intellectually stimulating and challenging. He has been understanding, helpful, generous, kind, and sympathetic. To put my appreciations in black and white would take away from it.

I am grateful to Professor Levine who supervised me on a number of projects. He introduced me to computer vision and has given me unceasing support in my many years in this lab. I have especially enjoyed collaboration with Allan Tannenbaum whose energy and enthusiasm is never-ending. A note of thanks to my undergraduate teacher Professor Roth who thought me about mathematics. I also appreciate the help of Ciprian Foias, Bob Hummel, and Demetri Terzopoulos.

McRCIM is a special place. The environment is stimulating and I shall miss it. I would like to thank the McRCIMites for making it special, in particular Allan. Benoit, Cem, Daniel, der Mouse, Frederic, Frank, John, Gracy, Leei, Kamal, Margaret. Peta, Peter. Pierre(s). Yvan, and Toky. A special note to Benoit. Lee. and Pierre for help with so many things. I appreciate the encouragement and support of my personal friends Adrian. Cameron. Daniel. Frederic. Gracy. Kayvan. Moshe, and Sam.

Many thanks to Allan Dobbins. my officemate. for uncountable favors, stimulating discussions, and friendship.

This thesis is dedicated to my parents, my sisters Suzanne and Tania. and also to Steve Zucker. I would like to mention the emotional support that Morad, Phyllis, Dyan, Rena, Salim, and Dara Kimia have provided over the years.

The financial assistance of the NSERC and FCAR is greatly appreciated.

Contents

List of Tables

List of Figures

Chapter 1

Introduction

Animals rely heavily on vision to survive. They depend on it to find food, flee enemies, and reproduce. This everyday experience of vision comes to us instantly and effortlessly: as we open our eyes, the world is perceived in its full three dimensions. As a consequence, we navigate in it, avoid obstacles, escape danger, recognize and manipulate objects. It is not surprising then that vision is considered one of the most important components of an intelligent machine. Machine vision, however, has proved surprisingly elusive, tracing back to some fundamental questions in the psychology of perception, philosophy, and neurophysiology.

Vision is the process of inferring structure in the world from a sequence of images. Light emanates from light sources, strikes and bounces off objects in the scene, and then enters the eye (camera) to form an image on the retina (photosensitive array). These images may come from a pair of eyes and last over time. How is it that such a set of two-dimensional images can give rise to a stable three-dimensional interpretation that builds our sense of the external world [31]?

The purpose of vision may be as simple as differentiating between two hypotheses, e.g. foe or friend, or it may be as intricate as painting miniatures. Vision is used in a variety of tasks such as walking through a field or driving a car through a crowded downtown street, manipulating objects such as in carpentry or diamond cutting, or in the recognition of predator and prey. The problem of recovery of structure from images is necessarily dependent on the purpose for which this information is used.

This thesis in concerned with the perception of planar shapes. Even in the absence of other visual cues, shape is used for object recognition, manipulation, and navigation. While, it is possible to devise special-purpose algorithms e.g. for inspection tasks, the range of tasks and purposes requires a general framework.

1.1 What is a Shape, That an Algorithm May Know It, and an Algorithm, That It May Know a Shape?

What is a shape? Consider figure 1.1 which most people would immediately recognize as a cat [33]. This is despite a serious lack of other visual cues, such as color, stereo, motion, textures, shading, internal contours, etc. We have accomplished this recognition task based merely on the presentation of a patch of black (figure) on white (background). There are many instances where an object is recognized simply based on this kind of shape information [79]. We often recognize animals, trees, plants, fruits, landscapes, and clouds.

In addition to these natural objects, man-made objects are often recognized when the only visual cue is shape. This is principally because because components of these objects are flat to begin with, or are rotationally symmetric, leading to generic two-dimensional projections. Examples include tools, furniture, musical instruments, and vehicles. Shape is important in other images as well: medical images, (X-ray, PET, MRI, etc.), laser range images, radar images, and electron microscope images. Figure 1.2 displays images with easily recognizable shapes. We will use these examples throughout this thesis to demonstrate our approach.

A number of other fields are also interested in shape. For example, biologists

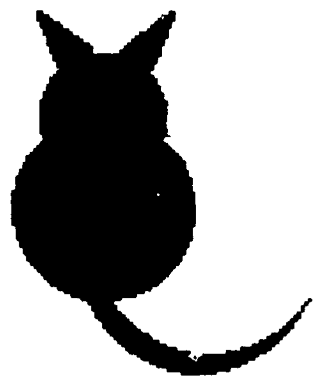

Figure 1.1: This figure is easily recognized despite the lack of visual cues such as color, stereo, motion, shading, texture, etc.

have used shape to infer taxonomic relations in plants and animals. More recently, measurement of biological shape has posed interesting questions [82, 81, 83, 14]. As another example, artists have long been interested in capturing the shape of things as one can observe in the ancient petroglyphs found in the caves of southern France.

In computer vision, numerous applications for the recognition and classification of shapes exist. Levine et. al. used the shape of cells to isolate, track, and classify the moving white blood cells [51]. There has been considerable activity in the area of detection and classification of tumors in X-ray images. Other applications include the study of the shape of clouds [59], assembly line inspection tasks, and optical character recognition. Shape has also been used in robotics to determine grasp points for objects.

All these fields are useful sources of information [44], not only as an aid in modeling and analysis of shape, but as mirrors on our unconscious internal representations. However, despite the wide interest in shape, its definition has remained elusive: Zusne claims there are as many definitions for shape as there are for love, [96]! If shape is so elusive, what then, is an algorithm that captures the essence of shape? Attneave et.

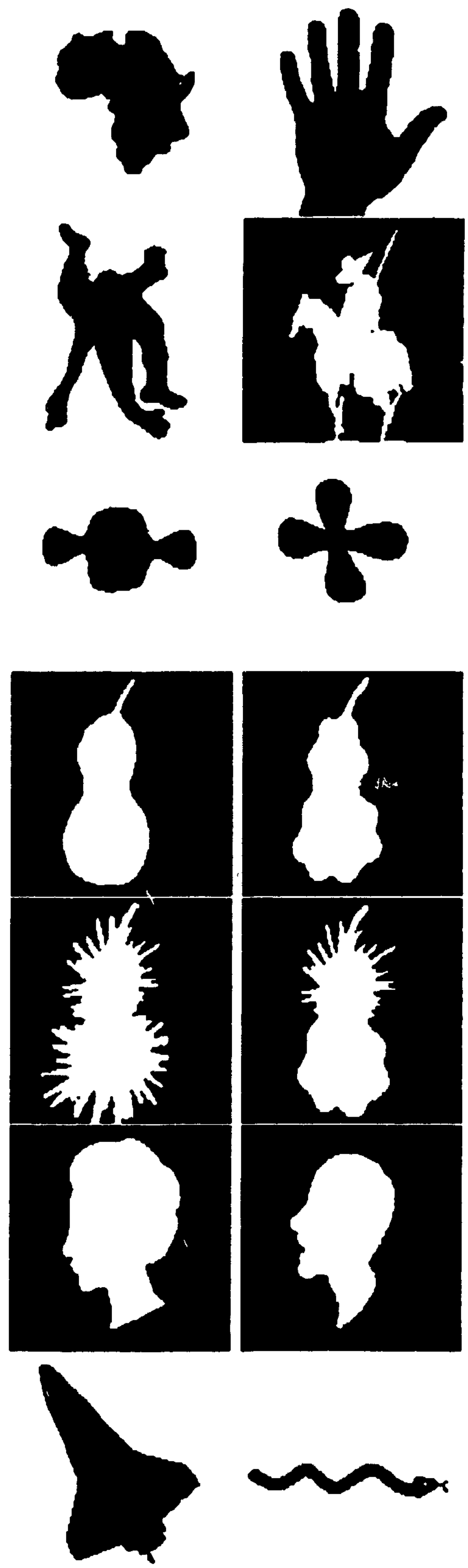

Figure 1.2:

al. suggested that shape, as a psychological quantity is multidimensional, although it was not clear how many dimensions would suffice to describe shape, or what these dimensions should have been [3]. In short, shape is an undefined, intuitive concept, and can perhaps only be defined in an operational manner. It is clear that a large part of the ambiguity surrounding shape is due to a serious lack of a natural language for describing shape [6].

We submit that the essence of shape is in considering the many attributes of it *simultaneously*: that shape is more than a curve, or a region. It is perceived locally, but also globally; one can focus in on a small feature, but then attend to the general shape of the object. It may be viewed as a composition of parts; at the same time it may look like it is the growth of another object, and yet it may look like the deformation of another. Furthermore, it is evident that a framework for shape defines shape operationally. As such, when building this framework, one should meet the purposes for which shape is used. Finally, for general purpose vision, we believe that insight into developing this framework can be attained by making it consistent with our perception of shape.

1.2 Need for a New Geometry

Objects come in all forms, deform, and grow, and as they do so incrementally, their shape does not change drastically. For example, a face with a pimple is still a face, i.e. our perception of the face is not drastically altered when a pimple grows on it. And, the perception of a tree with a flock of birds resting on it, has much in common with the perception of a tree. Similarly, an industrial tool that is slightly bent or chipped will be perceived exactly as we have just described it. In short, the primary perception is one of an object with modifications. This is so intrinsic to us that to mention it might appear redundant. Along a different direction, objects deform with motion, growth, erosion, etc. However, our perception is only slightly modified as figure 1.3 illustrates. There seems to be great stability of our visual sensation with regard to such changes.

Unfortunately, standard geometries of traditional and modern mathematics do not satisfactorily address these aspects of shape for the purposes of object recognition. Topology is so general that bounding contours of non-fractal physical objects (planar, closed, and simple) are equivalent. On the other hand, "Congruence geometries, such as Euclidean, affine, and projective geometries require an exact match, or some distance or area tolerance from it" [11]. Mumford questioned the success of a theory of shape description for recognition and categorization tasks without having first defined what is meant by a "nearby" shape [61]. In other words, what is needed is to define a space for shape and then to impose a topology on it. It is clear, however, that the Euclidean metric is not natural for shape, in the sense that "close" objects are perceived as different and "distant" objects are visually indistinguishable (as in figure 1.4). A number of other metrics, e.g. the Hausdorff metric, have been considered. Koenderink et. al. point out that useful notions of "partial order, similarity, and relatedness" have no equivalent in the usual geometrical shape theories. Indeed, without these notions, the task of object recognition seems impractical [44] . These ideas point to the need for a language that makes the morphogenesis of shape explicit.

A second problem concerns the treatment of singularities. Singularities have often been reduced to limits of highly bent structures. Attneave showed that the most salient portions of a shape are corners and the high curvature points [2]. However, Singularities do occur in nature, and they play a different role than their smoothed versions [55]. However, given our predisposition to highly developed geometrical descriptions of curves and surfaces, it is not surprising that smooth curves and surfaces

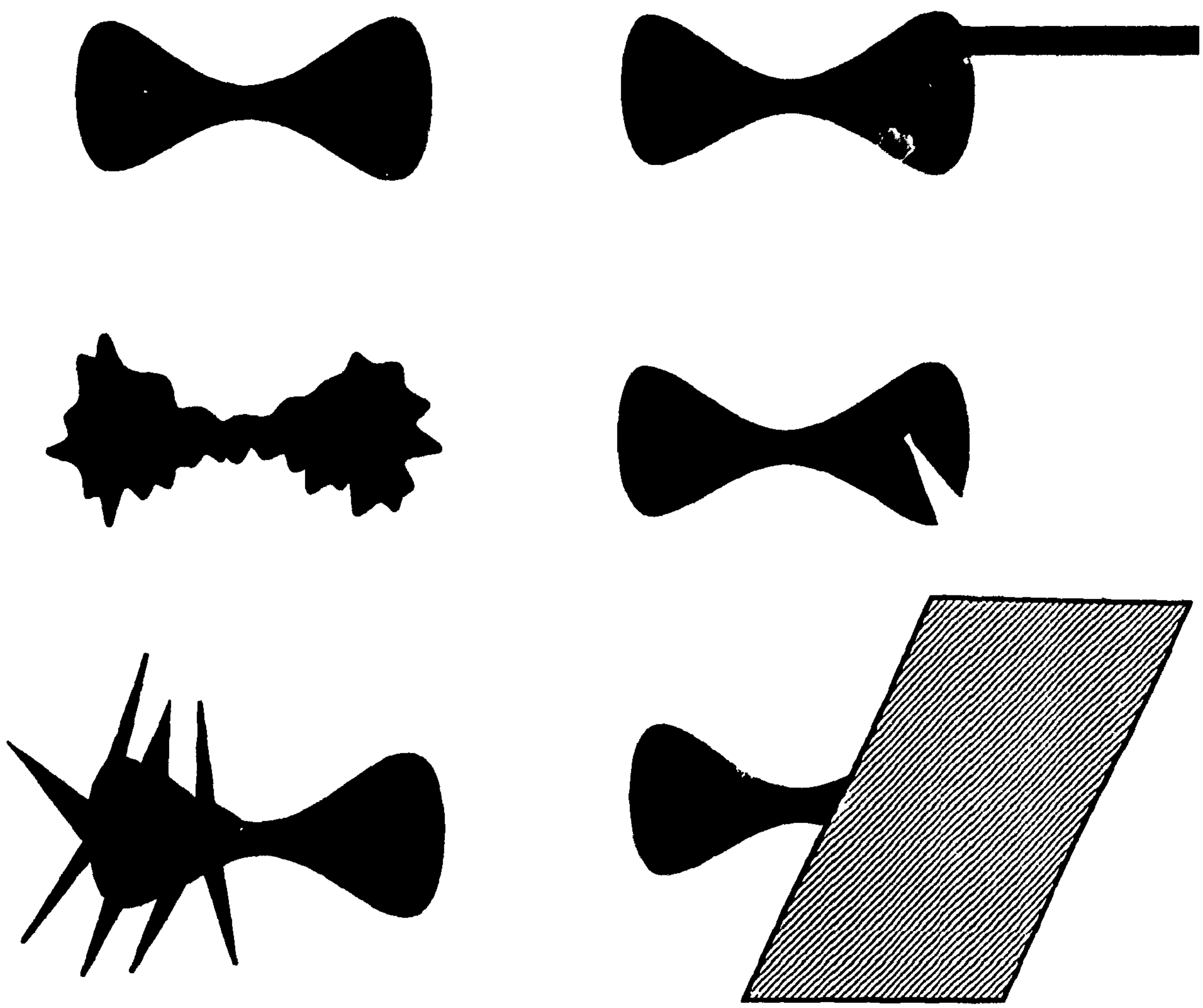

Figure 1.3: Shapes are categorized into classes in spite of their differences. This is partly due to our ability to abstract the shape of an object in the presence of occlusions, protrusions, chips, noise, and various degradations.

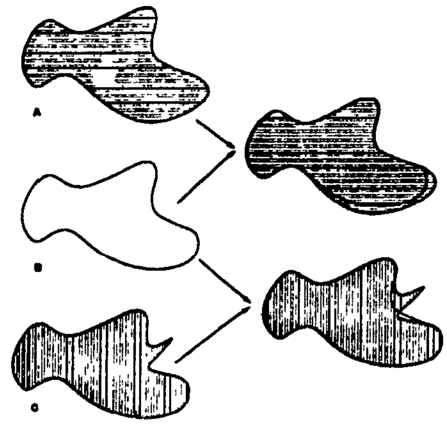

Figure 1.4: Standard geometries do not address the issues in shape. For example, the Euclidean metric ignores the perceptually significant protrusion in the bottom (C) and assign more differentiation to shape (A) when compared to figure (B), as depicted on the right hand side.

have been the common tools used in describing the visual world. Nevertheless, singularities must have an explicit place in a theory of shape, as well as in some other areas of vision.

What kind of geometry, then, do we require for shape? And, how does one define a metric and/or a topology for shape? What are our constraints and guidelines? It seems that one can not speak of likeness between two shapes, without having discovered a language for speaking about it. This thesis is concerned with a setting to describe shape; one in which it is possible to define similarity between two shapes, regardless of whether they arose as a composition of parts, or as a transformation of other shapes.

1.3 Issues

Shape is the bottleneck between low-level and high-level vision. Two paradigms have emerged for the early processing of visual information. First, the *edge detection* paradigm asserts that in order to isolate, detect and recognize objects in the scene, the contours in the scene must first be obtained. The *segmentation* paradigm, on other hand, focuses on the region defining the object as the primary concept of low-level vision. Whether we work with edges or regions, in representing shape we are faced with the question: What is the essence of shape? What re-presentation of the information is pertinent to shape and suitable for object recognition? What kind of description should our edge and region information be transformed into?

One might represent shape, fully and accurately, in a number of mathematically precise ways. For example, one may concentrate on the shape as a "curve" and represent the shape as the set of points describing the outline of the shape; or a chain code describing the orientation of the outline [26]; or the curvature of the outline as a function of the arc-length [1, 60], orientation, etc; or one might use the Fourier transform of the boundary [94, 34], or the interior and its the quadtree representation [6], etc. Although these representations are formal and mathematically faithful in isolation, they are inadequate for the purpose of recognition. This is precisely the bottle-neck of shape, figure 1.5. To represent shape is more than merely describing it, e.g. as a set of oriented edges. Part of the problem of shape is the isolation of the object itself. Also, the needs of object recognition must be taken into account.

1.3.1 Boundary vs Region

This leads us to examine the first issue, namely, whether to represent the shape by its *boundary* or by its interior *region*? The two approaches are equivalent in the sense that the interior is accessible via the boundary and vice versa. As such, most approaches concentrate on either representing the region or the boundary, as summarized in table 1.1. Nevertheless, representations make certain information explicit while implicitly encoding the remainder. For example, if the shape is represented by the boundary, the orientation information is explicit while closeness of points

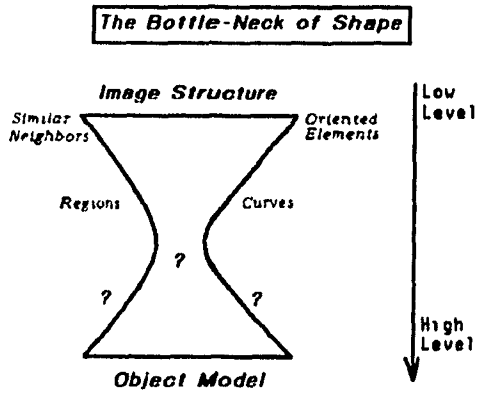

Figure 1.5: Low-level algorithms in vision often employ intensity differences across a contour, leading to the edge-detection paradigm, or grouping similar intensities to form regions, leading to the segmentation paradigm. On the way to the recovery of objects, there appears to be no intermediate level, or a language for speaking about shape.

along the "necks" and symmetry is implicit. In contrast, in a region-based representation, the orientation of the boundary tangent is implicit while the closeness of points through the region and object symmetry is explicit. A different trade-off may arise when considering computational complexity: boundary representations are one-dimensional and therefore inexpensive to process in contrast to an expensive two dimensional regional representation.

We submit that a simultaneous representation of the boundary and the interior is needed for a full understanding of shape. Throughout the rest of this thesis, when we refer to boundary-based, or region-based approaches, we intend the type of distinction in table 1.1. The distinction is in part semantic since one could always blur this distinction by basing region computation as a global boundary function (e.g. to derive an implicit characteristic function), and in part technical as will emerge in the sequel.

Boundary	Region
Strip Tree [5]	Quad Tree [73]
Chain Code [26]	SAT [11]
Fourier Descriptors [94, 31, 67, 85]	Fourier Descriptors [30]
Codon [70, 54]	Generalized Cylinders [10, 58], Superquadrics [61]

Table 1.1: Most methods concentrate on either the on the boundary or on the interior of the shape. However to fully capture shape a representation with a spectrum of local to global is needed.

1.3.2 Local vs Global

One method of shape classification is based on shape features. For example, the area and the centroid of a shape are used to differentiate one shape from another. Another feature is eccentricity (elongation), which may be defined in several ways, e.g. ratio of principal axes of inertia or the ratio of the length of maximum cord to maximum cord perpendicular to it. Other examples are the Euler number, compactness, shape numbers, and shape moments, among others [6, 71]. All shape features attempt to capture the shape by a few numbers and, as such, they are *global* approximations of the shape. In other words, information about the shape from *all* portions of it combine to form a global description. More powerful representations of shape can be global too. The Fourier representations of the shape [94, 31, 67, 85] are global representations in that each Fourier descriptor is dependent on all portions of the shape. Bolles et. al. introduced *focus features* where global relationships of local features are represented [13]. Hough transform techniques gather votes for certain features and, as such, can also be considered to be global.

The major problem with a global representation of a shape occurs in the presence of occlusions. When an object is partially occluded, all global descriptors change drastically. As such, these representations are not suitable for object recognition. Furthermore, a notion of approximation in the global domain does not correspond to that in the shape domain. For example, the shapes corresponding to a set of

Boundary-Based Primitives	Region-Based Primitives	Volume-Based Primitives
Codons [70]	Generalized Ribbons [15]	Generalized Cylinders [10, 58]
Arcs of circles [24]		Superquadrics [64]
Primitive Curvature Changes [1]	MLD parts [65]	Geons [9]
Polygons [69]	SAT [11]	Polyhedra[86]

Table 1.2: A review of shape primitives.

Fourier descriptors with or without some higher order terms do not resemble each other closely. *Local* features in isolation, on the other hand, do not give a global sense of shape and are sensitive to noise. The challenge is to capture the general shape of the object without losing its partial representations For object recognition, the representation must degrade gracefully as portions of the object are occluded.

1.3.3 Composition vs Deformation

Let us begin by picturing the process of building a doll out of clay. One might place a small chunk of clay (head) on top of a larger one (body); pull out some of the clay to mimic the nose, push another part in to depict the eye; take another chunk of clay, roll and attach to make the arm and bend it to represent the form. An exercise in arts and crafts reveals that objects may be *composed* to form new ones, or existing objects may be *deformed* to arrive at other objects.

The concept of composition is related to that of *primitives*. A large number of primitives have been proposed to fit and approximate the boundary, the region or the volume, table 1.2. Hoffman et. al. pointed out that each set of primitives is well suited to represent some shapes, but not others [36].

Composition suggests a notion of *part*. These parts are regions of the shape that will most likely belong to a distinct entity in the three dimensional world. Several arguments support the notion of parts. First, objects in the real world are, in fact, made out of parts. For example, as animals move, portions of their body stay intact, while some others move relative to each other. This relative motion is one of the factors giving rise to the head, the torso, and the legs, as parts. As the wind blows through trees, the leaves move relative to the tree. Second, objects are rarely seen in their entirety. Recognition must take place on partial information [9], as evidenced by the example of a tiger that is partially occluded by a bush. Indeed, object recognition in a world made out of parts would be a great deal more complex if one had to index on whole objects rather than their parts. Representing parts saves us from rediscovery of new instances that are combinations of the old. Third, there is often a neck-like joint between parts which is perceptually significant. For example, it can be used as a stable hold site. Or, the neck is where an object made of homogenous material would break if forced. One must however be careful to distinguish between the notion of *parts* and the primitives used to model those parts [36, 9], table 1.2.

Deformations, on the other hand, suggest change. For example, objects grow and shrink, bend and straighten, protrude and indent, stretch and squish. Leyton suggested that the relationship between shapes may be captured by studying the relationship between curvature extrema [54]. Specifically, a shape is related to another by a sequence of certain rewrite rules (*process*) in a shape grammar. Parts are claimed to be a certain type of process.

We view the above approaches of parts and process as two extremes in approaches to shape. Ideally, the relationship between shapes is represented when both composition and deformations are captured explicitly.

1.3.4 Scale and a Hierarchy of Significance

Scale is a way of assigning significance to various aspects of shape. This is necessary for several reasons. First, stability with noise requires that small features be given small weight in the representation.

In conclusion, shape has many attributes and to successfully represent it, these attributes must be represented simultaneously. Specifically, the shape must be represented along the axes of local and global, boundary and region, and composition and deformation, figure 1.6.

1.4 Deformations Underlying a Topology for Shape

Choosing a representation for shape makes certain relationships between shapes explicit. For many tasks, such as object recognition, it is desirable that shapes which are slightly deformed, occluded, chipped, or covered relate closely to the original shape. This is perceptually not unreasonable, since our perceptions do not abruptly change when objects undergo these transformations; see figure 5.1. Thus we begin with the following axiom:

Axiom 1.1 *Slight changes in the boundary of an object cause only slight changes to its shape.*

Thus we consider a shape represented by the curve $\mathcal{C}_0(s) = (x_0(s), y_0(s))$ undergoing a deformation. With the notation of section 2.1, let each point of this curve move by some arbitrary amount in some arbitrary direction, figure 1.7.

$$\begin{cases} \frac{\partial \mathcal{C}}{\partial t} & = \alpha(s,t)\vec{T} + \beta(s,t)\vec{N} \\ \mathcal{C}(s,0) & = \mathcal{C}_0(s), \end{cases} \tag{1.1}$$

where $\vec{T}$ is the tangent, $\vec{N}$ is the outward normal, κ is the Gaussian curvature, and α, β are arbitrary functions as in equation 2.1. This can be reduced to (see chapter 2, equation 2.2,

$$\begin{cases} \frac{\partial \mathcal{C}}{\partial t} & = \beta(s,t))\vec{N} \\ \mathcal{C}(s,0) & = \mathcal{C}_0(s), \end{cases} \tag{1.2}$$

Now, we concentrate on those deformations that depend on local information about the geometry of the curve, namely those dependent on the curvature [22],

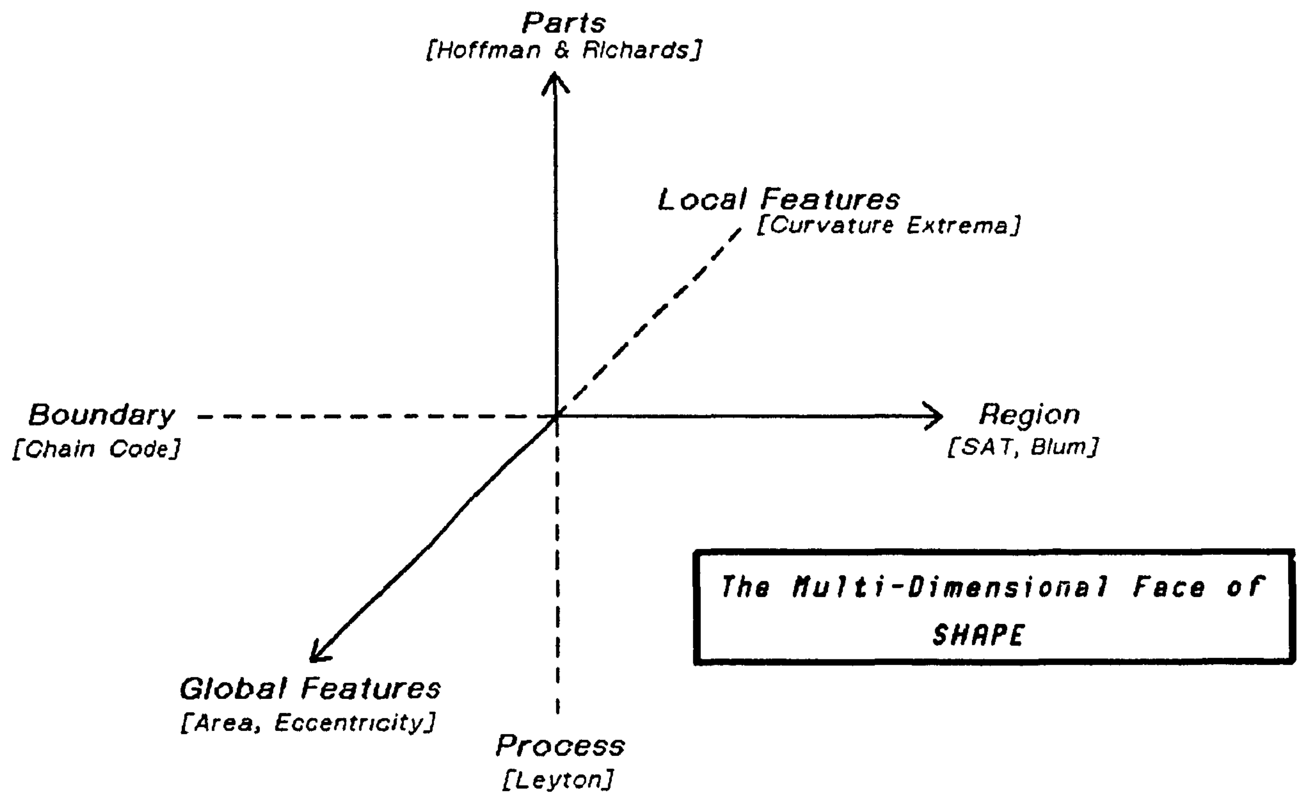

Figure 1.6: This figure depicts the multi-dimensional nature of shape: Shape has both boundary and regional features, which may be local or global. Further, shape may be the result of composition or deformation.

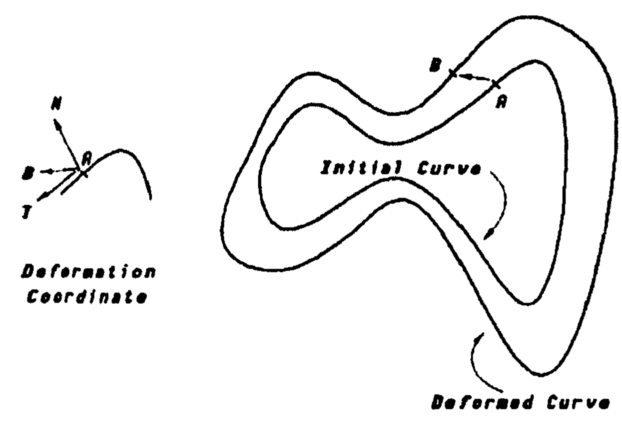

Figure 1.7: The point on the initial curve A move by some small but arbitrary amount in some arbitrary direction to B. With simple restriction, one can classify this deformation to *constant motion* and *curvature motion* along the normal.

$$\begin{cases} \frac{\partial C}{\partial t} & = \beta(\kappa(s,t)))\vec{N} \\ C(s,0) & = C_0(s). \end{cases} \tag{1.3}$$

Further, we propose that:

Axiom 1.2 *The similarity between a shape and its deformed version does not depend on the time of deformation.*

Then,

$$\begin{cases} \frac{\partial C}{\partial t} & = \beta(\kappa(s))\vec{N} \\ C(s,0) & = C_0(s). \end{cases} \tag{1.4}$$

To examine this deformation closely, expand $\beta(\kappa)$ into its Taylor expansion and consider the first order approximation

$$\begin{cases} \frac{\partial C}{\partial t} & = (\beta_0 - \beta_1\kappa)\vec{N} \\ C(s,0) & = C_0(s). \end{cases} \tag{1.5}$$

The remaining terms involving higher orders of κ qualitatively resemble κ as we will show.

The above equation contains two terms. The first term describes a deformation that is a constant motion along the normal, or *constant motion*. The second term, on the other hand, describes a deformation that is proportional to the curvature along the normal, or *curvature motion*. To summarize the above discussion of deformations, it has been shown that

Result 1.1 *Arbitrary local deformations of a curve in an arbitrary direction are qualitatively captured by a linear combination of two basis deformations, namely, the constant motion and curvature motion, of the curve along its normal.*

Such deformations will be fundamental to the remainder of this thesis, and will provide the basis forming a topology over shape.

1.5 The Multidimensional Nature of Shape

Earlier it was argued that a representation of shape ought to span a range of local to global, explicitly encode both boundary and region information, represent a notion of significance for shape, and should be expressed in a language that is appropriate for shape. Namely, a language in which one can break the shape into parts, perform boundary and regional deformations. In the previous section we introduced our basis deformations, *constant motion* and *curvature motion*, we now sketch how they are related to the various aspects of shape.

The basis deformations have drastically different but complementary effects on an initial curve: While constant motion requires no curvature information, or in other words local shape knowledge of the boundary, the curvature motion depends on it. In the course of this manuscript, we will show that the *entropy condition* of constant motion is a regional concept, in that it relates portions of the curves close in the plane.

but perhaps far along the boundary. As such entropy and constant motion deal directly with regional information. Curvature motion deals with boundary information, and hence is complementary according to our previous discussion.

While constant motion often creates singularities in the original, the curvature motion smoothes out singularities immediately and yields a progressively more rounded shape. In fact, the following theorem shows that this is precisely Gaussian smoothing of the curve coordinates.

Theorem 1.1 *Consider the family of curves $C(s,t)=(x(s,t), y(s,t))$ satisfying*

$$\begin{cases} \frac{\partial C}{\partial t} & = -\kappa(s,t)\vec{N} \\ C(s,0) & = C_0(s), \end{cases} \tag{1.6}$$

where $C_0(s) = (x_0(s), y_0(s)$ is the initial curve, s is some arbitrary parameter along the curve, t is time, κ is curvature, and $\vec{N}$ is the normal. Then the coordinates satisfy the diffusion equation

$$\begin{cases} \frac{\partial x}{\partial t} & = \frac{\partial^2 x}{\partial \hat{s}^2} \qquad x(\hat{s},0) = x_0(\hat{s}) \\ \frac{\partial y}{\partial t} & = \frac{\partial^2 y}{\partial \hat{s}^2} \qquad y(\hat{s},0) = y_0(\hat{s}), \end{cases} \tag{1.7}$$

where $\hat{s}$ is the arc-length parameter along the curve.

This being an introductory chapter, the proof is presented in the context of a scale-space for shape in chapter 7. Rather, we emphasize that the effect of Gaussian convolution is smoothing, which takes complicated shapes to simpler ones and eventually to a rounded blob. More rigorously, embedded curves shrink to a rounded point without creating self-intersections [28, 35]. The smoothing properties of Gaussians have been utilized to build a scale-space representation of shape [60]; see chapter 7 for an extensive treatment of a scale-space for shape.

One may contrast the local-global properties of curvature and constant motions from yet another perspective. While curvature motion operates *globally* on the curve, the constant motion spans a *local* neighborhood of the curve. To illustrate this, consider a finite deformation time and Theorem 1.1. Now, based on the curvature motion, a smooth initial curve will evolve to a curve whose every point is determined by information from all along the curve, weighted by a Gaussian. In contrast, in the same duration, the support for a point in the evolved curve (the portion of curve affecting its outcome) for local motion is a finite segment of the curve, this follows from Huygens' principle [29].

It is also interesting to note that while Gaussian smoothing and the heat equation are linear, the constant motion is nonlinear. In fact, linear processes retain the smoothness of the initial curve, while nonlinear processes can lead to singularities. Figure 1.8 summarizes the contrasting but complementary properties constant motion and curvature motion.

1.6 Overview

There are several distinct aspects to this thesis, a reflection on the nature of shape itself. The essence of shape is in its connectivity with other shapes. Therefore composition and deformations play an important role in the representation of shapes. Observe that a slightly deformed curve looks similar to the original. We have already shown that arbitrary deformations break down to two kind of deformations: 1) constant speed motion along the normal (***constant motion***) and 2) motion along the normal whose speed at any point is proportional to the curvature at that point (***curvature motion***). In chapter 2 evolution equations are derived for the tangent, normal, metric, curvature, and length under arbitrary deformations. Then, we obtain bounds for length, total curvature, and the distance a curve can travel. Based on these results, our key mathematical result is an existence theorem for evolution up to and including the time when a shape develops a *shock*. The implication is that visible

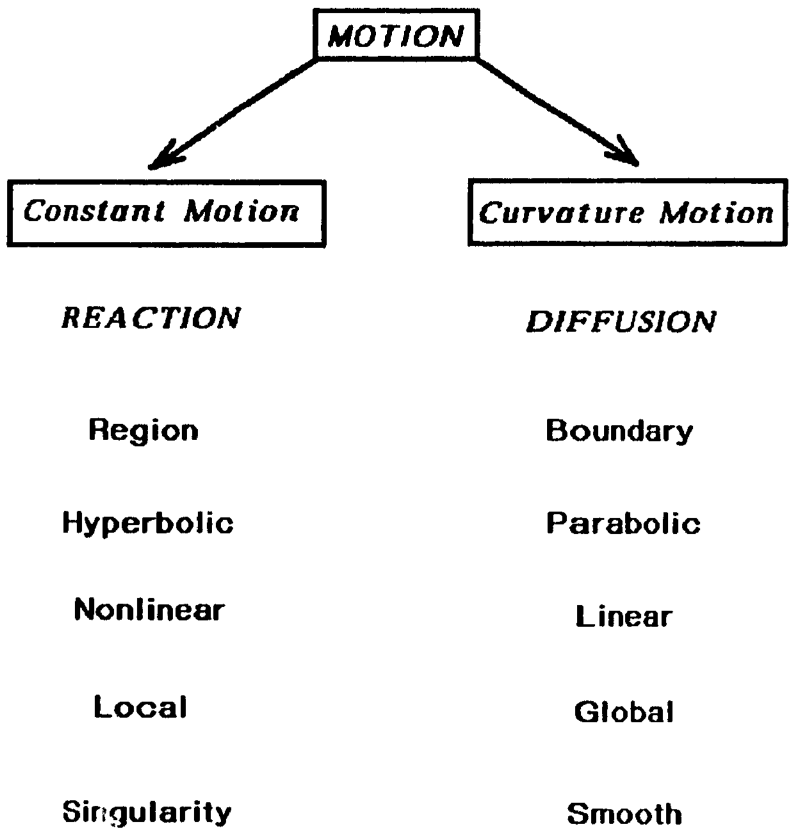

Figure 1.8: This figure summarized the contrasting but complementary properties of constant motion and curvature motion. These extremes in isolation are not sufficient to capture an understanding of shape. Rather, a spectrum of these attribute, e.g. from local to global, must be considered. It is in this context that the basis motions are relevant to shape, figure 1.6.

shapes will evolve to characterizable limiting shapes even in the presence of shocks.

It is intriguing that combinations of constant motion and curvature motion satisfy a *viscous conservation law*, as we will show in chapter 3. Hyperbolic conservation laws capture the dynamics of a number of physical applications and have been well studied. The viscous conservation law presents interaction between two extremes of conservation, or *reaction* and viscosity, or *diffusion*. Combinations of these two extremes together with time constitute the *reaction-diffusion* space for shape, chapter 5. This space represents the spectrum of extremes: local to global, boundary and region, composition and deformation.

One of the significant aspects of conservation laws is that they are nonlinear and, as opposed to linear systems, develop singularities. To deal with these singularities, we use notions of shocks and entropy in chapter 4. Various types of shocks form in the reaction-diffusion space, which leads us to our proposed computational elements of shape: *parts*, *protrusions* and *bends*, in chapter 6. The reaction-diffusion space is a particular implementation of a more abstract framework for understanding shape. In chapter 8, we propose the *shape triangle*, in which shape is perceived as the result of competition/cooperation between certain processes that are biased to perceive parts, bending, or protrusion. Qualitative perceptual experiments motivate and test the reality of proposed approach. As a consequence of the reaction-diffusion implementation, we build the entropy scale-space for shape, chapter 7, which encompasses certain morphological and Gaussian smoothing methods as special cases. It is from the entropy scale-space that a topology of shape begins to emerge and we illustrate this by showing how to place shapes in the shape triangle based on the structure of the entropy scale-space.

1.7 Contributions of the Thesis

This thesis makes a number of contributions. It brings together a number of seemingly disparate approachs to shape under a unifying framework. In addition, a mathematical framework is suggested which will perhaps have implications for other areas of vision. In summary, the specific contributions are:

- Introducing *conservation laws* and *reaction-diffusion* equations to the study of shape in vision.
- Characterized deformations of shape as combinations of *constant motion* and *curvature motion*.
- Proposed computational elements for shape: *parts*, *protrusions* and *bends* as they emerge from the formation of *shocks* in the *reaction-diffusion* space.
- A hierarchy of significance and a novel notion of scale for shape in the *entropy scale-space*.
- The *Shape Triangle* as the set of three shape processes that describe shape in terms of compositions, boundary deformations, and regional deformations, in cooperation or in competition.

Chapter 2

On General Curve Deformation

2.1 Motivation

In this chapter, we study certain evolution equations of embedded plane curves where the speed of the deformation is a function of the curvature, and whose direction is in the normal direction.

The curve evolution problem is relevant in applied sciences. The study of immersed closed curves evolving as functions of their curvature has been carried out for crystal growth [46, 8], flame propagation [75, 76, 63], and curve shortening [28, 35]. We would like to investigate properties of the classical solutions of these evolution equations. In a sequel we plan to consider the weak solutions when shocks develop [49, 48, 63].

The research has been motivated by the study of certain problems in computer vision. Specifically, in the context shape perception, it becomes essential to study the process of deforming the boundary of shapes, especially when singularities form. This chapter is primarily concerned with providing a rigorous basis for the process of deformation. First, the basic notation for tangent, normal, orientation, curvature, length and total Gaussian curvature is defined. Second, evolution equations are derived for these entities. Third, bounds are derived for length, curvature, and the travelled distance. Finally, ...

2.2 Notation

We will now set up some of the basic notation and concepts which we will need in what follows.

Let $C(s,t) : S^1 \longrightarrow \mathbf{R}^2$ be a family of embedded curves where t denotes time and s parameterizes each curve. We assume that this family evolves according to the evolution equation

$$\begin{cases} \frac{\partial C}{\partial t} & = \alpha(s,t)\vec{T} + \beta(s,t)\vec{N} \\ C(s,0) & = C_0(s), \end{cases} \tag{2.1}$$

where $\vec{N}$ is the outward normal, κ is the Gaussian curvature, and α, β are arbitrary functions. For each deformation $\{\alpha, \beta\}$, there exists another deformation $\{0, \beta'\}$ such that the resulting traces of curves are equivalent [27]. Furthermore, we constrain the deformations to be determined by the local geometry of the curve, i.e., β should be a function of curvature. Therefore, we consider the case $\alpha(s,t) = 0$ where β is typically of the form $\beta(\kappa) = 1 - \epsilon\kappa$. Assume that $C_t = C(.,t)$ is a C^2-classical solution on some interval $[0,t')$, $(t' < \infty)$. Thus we are considering C^2 solutions of the system

$$\begin{cases} \frac{\partial C}{\partial t} & = \beta(\kappa(s,t))\vec{N} \\ C(s,0) & = C_0(s), \end{cases} \tag{2.2}$$

(Note that we do not rule out the possibility that a C^2-solution may exist for all $t \geq 0$.)

Let,

$$g(s,t) := |\frac{\partial C}{\partial t}| = [x_s^2 + y_s^2]^{1/2}, \tag{2.3}$$

denote the *metric* along the curve. The arc-length parameter $\hat{s}$ is then defined as

$$\hat{s}(s,t) := \int_0^s g(\xi,t)\, d\xi.$$

Let the positive orientation of a curve be defined so that the interior is to the left when traversing the curve. The *tangent, curvature, normal, orientation* and *length* are defined in the standard way. We will take the normal to be pointing outwards, where the inward or outward is determined by the interior, or equivalently by the orientation of the curve. We then have that

$$\begin{aligned}
\vec{T} &:= \frac{\partial C}{\partial \tilde{s}} = \frac{1}{g}\frac{\partial C}{\partial s}, \\
\kappa &:= |\frac{\partial \vec{T}}{\partial \tilde{s}}| = \frac{1}{g}|\frac{\partial \vec{T}}{\partial s}|. \\
\vec{N} &:= \frac{-\frac{\partial \vec{T}}{\partial \tilde{s}}}{|\frac{\partial \vec{T}}{\partial \tilde{s}}|} = \frac{-1}{\kappa g}\frac{\partial \vec{T}}{\partial s}. \\
\theta &:= \angle(\vec{T}, \vec{x}) \\
L(t) &:= \int_0^{2\pi} g(s,t)\, ds
\end{aligned}$$

We also define a quantity which we will call *length-squared* by

$$L^{(2)}(t) := \int_0^{2\pi} g^2(s,t)\, ds.$$

Finally, we let

$$\bar{\kappa}(t) := \int_0^{2\pi} |\kappa(s,t)| g(s,t)\, ds.$$

denote the total absolute Gaussian curvature.

2.3 Evolution Equations

In this section we will derive the evolution equation for the tangent $\vec{T}$, normal $\vec{N}$, metric g, curvature κ, orientation θ and length L, for families of curves satisfying (2.1).

It is easily established that

$$\begin{cases} \frac{\partial \vec{T}}{\partial s} &= -\kappa g \vec{N} \\ \frac{\partial \vec{N}}{\partial s} &= \kappa g \vec{T}, \end{cases} \tag{2.4}$$

which will be used in the following proofs. Note that these evolution equations are for the general deformation $\{\alpha, \beta\}$.

Moreover, we can compute that the metric g evolves as follows:

$$\begin{aligned} \frac{\partial g^2}{\partial t} &= \frac{\partial}{\partial t} < \frac{\partial C}{\partial s}, \frac{\partial C}{\partial s} > \\ &= 2 < \frac{\partial C}{\partial s}, \frac{\partial}{\partial t}\frac{\partial C}{\partial s} > \\ &= 2 < \frac{\partial C}{\partial s}, \frac{\partial}{\partial s}\frac{\partial C}{\partial t} > \\ &= 2 < g\vec{T}, \frac{\partial}{\partial s}[\alpha \vec{T} + \beta \vec{N}] > \\ &= 2 < g\vec{T}, \frac{\partial \alpha}{\partial s}\vec{T} + \alpha \frac{\partial \vec{T}}{\partial s} + \frac{\partial \beta}{\partial s}\vec{N} + \beta \frac{\partial \vec{N}}{\partial s} > \\ &= 2 < g\vec{T}, \alpha_s \vec{T} - \alpha \kappa g \vec{N} + \beta_s \vec{N} + \beta \kappa g \vec{T} > \\ &= 2g[\alpha_s + \beta \kappa g]. \end{aligned}$$

Hence, we see that

$$\frac{\partial g}{\partial t} = \alpha_s + \beta \kappa g. \tag{2.5}$$

In the special case of $\alpha = 0$,

$$\frac{\partial g}{\partial t} = \beta \kappa g.$$

We will need the following change of partials for computing evolution equations:

$$\frac{\partial}{\partial t}\frac{\partial}{\partial \tilde{s}} = \frac{\partial}{\partial t}[\frac{1}{g}\frac{\partial}{\partial s}]$$

$$
\begin{aligned}
&= \frac{-g_t}{g^2}\frac{\partial}{\partial s} + \frac{1}{g}\frac{\partial}{\partial t}\frac{\partial}{\partial s} \\
&= \frac{-1}{g}[\alpha_s + \beta\kappa g]\frac{\partial}{\partial \tilde{s}} + \frac{\partial}{\partial \tilde{s}}\frac{\partial}{\partial t}.
\end{aligned}
$$

Next we have the following evolution equation for tangent:

$$
\begin{aligned}
\frac{\partial \vec{T}}{\partial t} &= \frac{\partial}{\partial t}\frac{\partial \mathcal{C}}{\partial \tilde{s}} \\
&= \frac{-1}{g}[\alpha_s + \beta\kappa g]\frac{\partial \mathcal{C}}{\partial \tilde{s}} + \frac{\partial}{\partial \tilde{s}}\frac{\partial \mathcal{C}}{\partial t} \\
&= \frac{-1}{g}[\alpha_s + \beta\kappa g]\vec{T} + \frac{\partial}{\partial \tilde{s}}[\alpha\vec{T} + \beta\vec{N}] \\
&= \frac{-1}{g}[\alpha_s + \beta\kappa g]\vec{T} + \alpha_{\tilde{s}}\vec{T} + \alpha\frac{\partial \vec{T}}{\partial \tilde{s}} + \beta_{\tilde{s}}\vec{N} + \beta\frac{\partial \vec{N}}{\partial \tilde{s}} \\
&= \frac{-1}{g}[\alpha_s + \beta\kappa g]\vec{T} + \frac{1}{g}\alpha_s\vec{T} - \alpha\kappa\vec{N} + \frac{1}{g}\beta_s\vec{N} + \beta\kappa\vec{T} \\
&= \frac{1}{g}[\beta_s - \alpha\kappa g]\vec{N}.
\end{aligned}
\tag{2.6}
$$

Similarly, for the normal we see that

$$
\begin{aligned}
\frac{\partial \vec{N}}{\partial t} &= \left< \frac{\partial \vec{N}}{\partial t}, \vec{T} \right> \vec{T} \\
&= -\left< \frac{\partial \vec{T}}{\partial t}, \vec{N} \right> \vec{T} \\
&= -\frac{1}{g}[\beta_s - \alpha\kappa g]\vec{T}.
\end{aligned}
\tag{2.7}
$$

Next we define the orientation of a curve as the angle the tangent makes with the x-axis. Let $\vec{T} = (\cos(\theta), \sin(\theta))$, so that $\vec{N} = (\sin(\theta), -\cos(\theta))$. Then,

$$
\begin{aligned}
\frac{\partial \vec{T}}{\partial t} &= (-\sin(\theta), \cos(\theta))\frac{\partial \theta}{\partial t} \\
&= -\frac{\partial \theta}{\partial t}\vec{N}.
\end{aligned}
$$

Therefore,

$$
\begin{cases}
\frac{\partial \theta}{\partial t} = \frac{-1}{g}[\beta_s - \alpha\kappa g] \\
\frac{\partial \theta}{\partial s} = \kappa g.
\end{cases}
\tag{2.8}
$$

As for curvature, we compute that

$$\begin{aligned}\frac{\partial\kappa}{\partial t} &= \frac{\partial}{\partial t}\frac{\partial\theta}{\partial\tilde{s}} \\ &= \frac{-1}{g}[\alpha_s + \beta\kappa g]\frac{\partial\theta}{\partial\tilde{s}} + \frac{\partial}{\partial\tilde{s}}[-\frac{\partial\beta}{\partial\tilde{s}} + \alpha\kappa] \\ &= \frac{-1}{g}[\alpha_s + \beta\kappa g]\kappa - \frac{\partial^2\beta}{\partial\tilde{s}^2} + \alpha_{\tilde{s}}\kappa + \alpha\frac{\partial\kappa}{\partial\tilde{s}} \\ &= -\frac{\partial^2\beta}{\partial\tilde{s}^2} + \alpha\frac{\partial\kappa}{\partial\tilde{s}} - \beta\kappa^2\end{aligned} \tag{2.9}$$

For the length, we derive

$$\begin{aligned}\frac{\partial L}{\partial t} &= \frac{\partial}{\partial t}\int_0^{2\pi} g(s,t)\,ds \\ &= \int_0^{2\pi}\frac{\partial g(s,t)}{\partial t}\,ds \\ &= \int_0^{2\pi}[\alpha_s + \beta\kappa g]\,ds.\end{aligned} \tag{2.10}$$

and similarly for length-squared,

$$\begin{aligned}\frac{\partial L^{(2)}}{\partial t} &= \frac{\partial}{\partial t}\int_0^{2\pi} g^2(s,t)\,ds \\ &= \int_0^{2\pi}\frac{\partial g^2(s,t)}{\partial t}\,ds \\ &= \int_0^{2\pi} 2g[\alpha_s + \beta\kappa g]\,ds.\end{aligned} \tag{2.11}$$

We now specialize to the case $\beta(\kappa) = 1 - \epsilon\kappa$ which is a common model frequently used in applications such as flame propagation, crystal growth, among others. First, we can easily show in this case that the *metric* evolves according to

$$\frac{\partial g}{\partial t} = (-\epsilon\kappa^2 + \kappa)g.$$

Second, for the *tangent* and *normal* we have

$$\frac{\partial\vec{T}}{\partial t} = -\frac{\epsilon\kappa_s}{g}\vec{N},$$

$$\frac{\partial\vec{N}}{\partial t} = \frac{\epsilon\kappa_s}{g}\vec{T}.$$

Next, the *orientation* evolution is governed by

$$\frac{\partial\theta}{\partial t} = \frac{\epsilon\kappa_s}{g}.$$

Similarly, one can show that the evolution equation for *curvature* is

$$\frac{\partial \kappa}{\partial t} = \epsilon \kappa_{\hat{s}\hat{s}} + \epsilon \kappa^3 - \kappa^2.$$

Finally, length evolves as

$$L_t = 2\pi - \epsilon \int_0^{2\pi} \kappa^2 g \, ds.$$

It is also useful to further constrain the flow and obtain evolution equations for the particular case of $\epsilon = 0$, or $\beta(\kappa) = 1$, for which we have

$$\frac{\partial g}{\partial t} = \kappa g, \tag{2.12}$$

$$\frac{\partial \vec{T}}{\partial t} = 0, \tag{2.13}$$

$$\frac{\partial \vec{N}}{\partial t} = 0, \tag{2.14}$$

$$\frac{\partial \theta}{\partial t} = 0, \tag{2.15}$$

$$\frac{\partial \kappa}{\partial t} = -\kappa^2, \tag{2.16}$$

$$\frac{\partial L}{\partial t} = 2\pi. \tag{2.17}$$

(2.18)

The evolution equation for curvature may be solved explicitly as

$$\kappa(s,t) = \frac{\kappa(s,0)}{1 + \kappa(s,0)t}. \tag{2.19}$$

This implies that the classical solution will fail to exist when

$$t = \frac{-1}{\kappa(s,0)}. \tag{2.20}$$

Hence, if the initial curve to (2.2) is convex, the equation will have a classical solution for all time.

The metric equation may also be solved as

$$\frac{\partial g}{\partial t} = \kappa(s,t) g(s,t)$$

$$
\begin{aligned}
\frac{g_t}{g} &= \frac{\kappa(s,0)}{1+\kappa(s,0)t} \\
\frac{\partial \ln(g)}{\partial t} &= \frac{\kappa(s,0)}{1+\kappa(s,0)t} \\
\frac{\partial \ln(g)}{\partial t} &= \frac{\partial \ln(1+\kappa(s,0)t)}{\partial t} \\
\ln(g(s,t)) - \ln(g(s,0)) &= \ln(1+\kappa(s,0)t) - \ln(1) \\
\ln(g(s,t)) &= \ln(g(s,0)) + \ln(1+\kappa(s,0)t) \\
g(s,t) &= g(s,0)(1+\kappa(s,0)t)
\end{aligned}
$$

Hence, the metric changes linearly in time with a curvature dependent coefficient. In particular,

Lemma 2.1 *Consider a solution of 2.2 when $\beta(\kappa) = 1$. Then, for any point $(s,0)$ with negative curvature $k(s,0)$, curvature will tend to infinity and metric to zero as $t \to \kappa(s,0)$. Furthermore, in any neighborhood of the curve C, the point of negative curvature minimum is the first point whose curvature becomes unbounded.*

2.4 Bounds for Things

In this section we give bounds on the length and total absolute curvature for the family defined in Section 1. As before we are particularly interested in the case $\alpha = 0$ and $\beta(s,t) = 1 - \epsilon\kappa(s,t)$ which is not only of interest in physical applications, but also as we will show in subsequent chapters for the study of shape.

2.4.1 A Bound for Length

Lemma 2.2 *Let $C(s,t)$ be a solution of (2.2) for $t \in [0,t')$ and $\kappa\beta(\kappa) \leq M$ for all $\kappa \in \mathbf{R}$ (regarding β as a function of κ). Then,*

$$L(t) \leq \min(L(0) + 2\pi t, L(0)e^{Mt}).$$

In particular, for $\beta(\kappa) = 1 - \epsilon\kappa$,

$$L(t) \leq \min(L(0) + 2\pi t, L(0)e^{\frac{t}{4\epsilon}}).$$

Proof. We have

$$L_t = 2\pi - \epsilon\int_0^{2\pi} \kappa^2 g\, ds.$$

So,

$$L_t \leq 2\pi,$$

$$L(t) \leq 2\pi t + L(0).$$

Note, the equality holds for $\epsilon = 0$. Alternatively,

$$\frac{\partial L}{\partial t} = \int_0^{2\pi} \beta\kappa g\, ds$$

Since $\kappa\beta(\kappa) \leq M$

$$\begin{aligned} \frac{\partial L}{\partial t} &\leq \int_0^{2\pi} Mg\, ds \\ &\leq ML(t) \end{aligned}$$

Therefore,

$$\frac{L'(t)}{L(t)} \leq M$$

$$(\ln[L(t)])' \leq M$$

that is,

$$\ln[L(t)] \leq Mt + \ln(L(0))$$

$$L(t) \leq L(0)e^{Mt}.$$

In particular for $\beta = 1 - \epsilon\kappa$, $M = \frac{1}{4\epsilon}$, and

$$L(t) \le L(0)e^{\frac{t}{4\epsilon}}.$$

∎

Remarks 1.

(i) For the second estimate, as $\epsilon \to \infty$, $L(t) \le L(0)$. It is interesting to observe that the two estimates complement each other: for small ϵ the second estimate is very large making the first estimate more useful. However, for large ϵ, the first estimate is exaggerated making the second estimate more useful.

(ii) A similar same proof shows that the length-squared

$$L^{(2)}(t) := \int_0^{2\pi} g^2 ds$$

is bounded by

$$L^{(2)}(0)e^{2Mt}).$$

2.4.2 A Bound for Total Absolute Curvature

Lemma 2.3 *Let $C(s,t)$ be a solution of (2.2) for $t \in [0,t')$. Suppose that $\kappa\beta(\kappa) \le M$, and $\beta_\kappa \le 0$ Then,*

$$\bar{\kappa}(t) \le \bar{\kappa}(0).$$

Proof. Define

$$\hat{q}(t) := \int_0^{2\pi} q(\kappa(s,t))g(s,t)\,ds,$$

where q is the piecewise smooth convex approximation of $f(x) = |x|$ given by

$$q(x) = \begin{cases} |x| & \text{if } |x| \ge \frac{1}{n} \\ \frac{1}{2n} + \frac{n}{2}x^2 & \text{if } |x| \le \frac{1}{n} \end{cases}$$

Then

$$
\begin{aligned}
\hat{q}'(t) &= \int_0^{2\pi} q_\kappa(\kappa)\kappa_t g\, ds + \int_0^{2\pi} q(\kappa) g_t\, ds \\
&= -\int_0^{2\pi} q_\kappa(\kappa)(\beta_{\tilde{s}\tilde{s}} + \beta\kappa^2) g\, ds + \int_0^{2\pi} q(\kappa)(\beta\kappa g)\, ds \\
&= -\int_0^{L(t)} q_\kappa(\kappa)\beta_{\tilde{s}\tilde{s}}\, d\tilde{s} + \int_0^{2\pi} [q(\kappa) - \kappa q_\kappa(\kappa)](\beta\kappa g)\, ds. \\
&= -(q_\kappa(\kappa)\beta_{\tilde{s}})\Big|_0^{L(t)} + \int_0^{L(t)} q_{\kappa\kappa}(\kappa)\kappa_{\tilde{s}}\beta_{\tilde{s}}\, d\tilde{s} + \int_0^{2\pi} [q(\kappa) - \kappa q_\kappa(\kappa)](\beta\kappa g)\, ds. \\
&= \int_0^{L(t)} q_{\kappa\kappa}(\kappa)\kappa_{\tilde{s}}\beta_{\tilde{s}}\, d\tilde{s} + \int_0^{2\pi} [q(\kappa) - \kappa q_\kappa(\kappa)](\beta\kappa g)\, ds. \\
&= \int_0^{L(t)} q_{\kappa\kappa}(\kappa)\kappa_{\tilde{s}}^2\beta_\kappa\, d\tilde{s} + \int_0^{2\pi} [q(\kappa) - \kappa q_\kappa(\kappa)](\beta\kappa g)\, ds.
\end{aligned}
$$

Since $\beta_\kappa \leq 0$ and convexity of q requires $q'' \geq 0$, we have

$$
\hat{q}'(t) \quad \leq \int_0^{2\pi} [q(\kappa) - \kappa q_\kappa(\kappa)](\beta\kappa g)\, ds.
$$

Note that

$$
\bar{\kappa}(t) \leq \hat{q}(t),
$$

so that a bound on $\hat{q}$ is a bound on $\bar{\kappa}$. Moreover, we have that

$$
0 \leq q(x) - xq'(x) \leq \begin{cases} 0 & \text{if } x \geq \frac{1}{n} \\ \frac{1}{2n} & \text{if } x \leq \frac{1}{n} \end{cases}
$$

Now since

$$
\beta(\kappa)\kappa \leq M,
$$

and $[q(\kappa) - \kappa q_\kappa(\kappa)] \geq 0$,

$$
\begin{aligned}
\hat{q}'(t) &\leq M \int_0^{2\pi} [q(\kappa) - \kappa q_\kappa(\kappa)] g\, ds \\
&\leq M \frac{1}{2n} \int_0^{2\pi} g\, ds. \\
&\leq \frac{M}{2n} L(t).
\end{aligned}
$$

and so,

$$\bar{\kappa}'(t) \quad \leq \frac{M}{2n} L(t)$$

Since by lemma 2.21 the length is finite, letting $n \to \infty$, we get

$$\bar{\kappa}'(t) \leq 0.$$

or

$$\bar{\kappa}(t) \leq \bar{\kappa}(0) \qquad \blacksquare$$

Remark 2. The conditions of the above lemma holds for $\beta(\kappa(s,t)) = 1 - \epsilon\kappa(s,t)$, for $\epsilon > 0$.

Lemma 2.4 *Let a family of curves satisfy (2.2) with convex initial condition, i.e.* $\kappa(s,0) \geq 0$. *Then,* $\bar{\kappa}(t) = \bar{\kappa}(0) = 2\pi$ *and the curve remains convex for all times.*

Proof. For convex curves,

$$\bar{\kappa}(s,0) = \int_0^{2\pi} \kappa g \, ds = 2\pi.$$

There is some neighborhood of time such that $\kappa(s,t) > 0$ for all s. Therefore,

$$\begin{aligned}
\frac{\partial \bar{\kappa}}{\partial t} &= \frac{\partial}{\partial t} \int_0^{2\pi} \kappa g \, ds \\
&= \int_0^{2\pi} [\kappa_t g + \kappa g_t] \, ds \\
&= \int_0^{2\pi} [(-\beta_{\tilde{s}\tilde{s}} - \beta\kappa^2) g + \kappa\beta\kappa g] \, ds \\
&= -\int_0^{2\pi} \beta_{\tilde{s}\tilde{s}} g \, ds \\
&= -\int_0^{L(t)} \beta_{\tilde{s}\tilde{s}} \, d\tilde{s} \\
&= -\beta_{\tilde{s}} \Big|_0^{L(t)} \\
&= 0.
\end{aligned}$$

Hence,

$$\bar{\kappa}(t) = 2\pi.$$

Since only convex curves can satisfy this condition, the evolved curve must be convex.

∎

Lemma 2.5 *Let a family of curves satisfy (2.2) for which $\beta_\kappa < 0$. Then, if $\kappa_{\hat{s}}(\hat{s}, t) \neq 0$ for all $\hat{s}$ and $0 \leq t < t'$*

$$\bar{\kappa}(t) < \bar{\kappa}(0).$$

For $\beta_\kappa = 0$,

$$\bar{\kappa}(t) = \bar{\kappa}(0).$$

Proof. This proof is due to Sethian [75] and we include it here for completeness with a few changes.

Without loss of generality pick the starting point $\hat{s} = 0$ to be a zero of curvature such that positive curvature begins in the positive direction of the curve. Partition the interval $[0, L(t)]$ into $n+1$ maximal subintervals,

$$\{[\hat{s}_0 = 0, \hat{s}_1], [\hat{s}_1, \hat{s}_2], \cdots, [\hat{s}_i, \hat{s}_{i+1}], \cdots, [\hat{s}_n, \hat{s}_{n+1} = L(t)]\},$$

such that $\kappa(\hat{s})$ is entirely positive, negative, or zero in the interval $(\hat{s}_i, \hat{s}_{i+1})$ for $i = 1, 2, \cdots, n$. Then, $\hat{s}_i$ are zeros of curvature, $\kappa(\hat{s}_i) = 0$. Note further that in general $s_i = s_i(t)$. Also, let

$$\rho(\kappa, [a, b]) := \begin{cases} 1 & \text{if } \kappa(\hat{s}) > 0 \text{ for } \hat{s} \in (a, b) \\ 0 & \text{if } \kappa(\hat{s}) = 0 \text{ for } \hat{s} \in (a, b) \\ -1 & \text{if } \kappa(\hat{s}) < 0 \text{ for } \hat{s} \in (a, b) \end{cases}$$

Then,

$$\frac{\partial \bar{\kappa}}{\partial t} = \frac{\partial}{\partial t} \int_0^{2\pi} |\kappa| g \, ds$$

$$
\begin{aligned}
&= \frac{\partial}{\partial t}\sum_{i=0}^{n}\int_{s_i}^{s_{i+1}} |\kappa| g \, ds \\
&= \sum_{i=0}^{n}\int_{s_i}^{s_{i+1}} \frac{\partial[|\kappa| g]}{\partial t}\, ds + \sum_{i=0}^{n}|\kappa(s_{i+1},t)| g(s_{i+1},t)\frac{\partial s_{i+1}}{\partial t} - \sum_{i=0}^{n}|\kappa(s_i,t)| g(s_i,t)\frac{\partial s_i}{\partial t} \\
&= \sum_{i=0}^{n}\int_{s_i}^{s_{i+1}} [|\kappa|_t g + |\kappa| g_t]\, ds
\end{aligned}
$$

Since intervals for which curvature is uniformly zero do not contribute to the sum, we will discount them. Without loss of generality assume otherwise in the following.

$$
\begin{aligned}
\frac{\partial \bar{\kappa}}{\partial t} &= \sum_{i=0}^{n}\int_{s_i}^{s_{i+1}} [\frac{\kappa\kappa_t}{|\kappa|} g + |\kappa| \beta\kappa g]\, ds \\
&= \sum_{i=0}^{n}\int_{\tilde{s}_i}^{\tilde{s}_{i+1}} [\frac{\kappa}{|\kappa|}(-\beta_{\tilde{s}\tilde{s}} - \beta\kappa^2) + |\kappa|\beta\kappa]\, d\tilde{s} \\
&= \sum_{i=0}^{n}\int_{\tilde{s}_i}^{\tilde{s}_{i+1}} [\frac{\kappa}{|\kappa|}(-\beta_{\tilde{s}\tilde{s}})]\, d\tilde{s} + \sum_{i=0}^{n}\int_{\tilde{s}_i}^{\tilde{s}_{i+1}} [\frac{-\beta\kappa^3}{|\kappa|} + \beta\kappa|\kappa|]\, d\tilde{s} \\
&= -\sum_{i=0}^{n}\int_{\tilde{s}_i}^{\tilde{s}_{i+1}} [\rho(\kappa,[\tilde{s}_i,\tilde{s}_{i+1})])\beta_{\tilde{s}\tilde{s}}]\, d\tilde{s} \\
&= -\sum_{i=0}^{n}\rho(\kappa,[\tilde{s}_i,\tilde{s}_{i+1})])\beta_{\tilde{s}}\Big|_{\tilde{s}_i}^{\tilde{s}_{i+1}} \\
&= -\sum_{i=0}^{n}\rho(\kappa,[\tilde{s}_i,\tilde{s}_{i+1})])[\beta_{\tilde{s}}(\tilde{s}_{i+1}) - \beta_{\tilde{s}}(\tilde{s}_i)]
\end{aligned}
$$

Now, by our original assumption $\rho(\kappa,[\tilde{s}_0,\tilde{s}_1]) = 1$. The next interval, then, has negative curvature and $\rho(\kappa,[\tilde{s}_1,\tilde{s}_2]) = -1$. Since zeros of curvature must pair up, $\rho(\kappa,[\tilde{s}_n,\tilde{s}_{n+1}]) = -1$. In short, $\rho(\kappa,[\tilde{s}_i,\tilde{s}_{i+1}]) = (-1)^i$. Therefore,

$$
\begin{aligned}
\frac{\partial \bar{\kappa}}{\partial t} &= -\sum_{i=0}^{n}(-1)^i[\beta_{\tilde{s}}(\tilde{s}_{i+1}) - \beta_{\tilde{s}}(\tilde{s}_i)] \\
&= -\sum_{i=0}^{n}(-1)^i\beta_{\tilde{s}}(\tilde{s}_{i+1}) + \sum_{i=0}^{n}(-1)^i\beta_{\tilde{s}}(\tilde{s}_i) \\
&= \sum_{j=1}^{n+1}(-1)^j\beta_{\tilde{s}}(\tilde{s}_j) + \sum_{i=0}^{n}(-1)^i\beta_{\tilde{s}}(\tilde{s}_i)
\end{aligned}
$$

$$= \sum_{j=0}^{n}(-1)^j\beta_{\tilde{s}}(\tilde{s}_j) + \sum_{i=0}^{n}(-1)^i\beta_{\tilde{s}}(\tilde{s}_i)$$
$$= 2\sum_{i=0}^{n}(-1)^i\beta_{\tilde{s}}(\tilde{s}_i)$$
$$= 2\sum_{i=0}^{n}(-1)^i\beta_{\kappa}(\tilde{s}_i)\kappa_{\tilde{s}}(\tilde{s}_i)$$

Now, since $\kappa_{\tilde{s}}(\tilde{s}_i)$ has sign $(-1)^i$ if $\beta_\kappa < 0$, then

$$\frac{\partial\bar{\kappa}}{\partial t} < 0$$

so that

$$\bar{\kappa}(t) < \bar{\kappa}(0).$$

However, if $\beta_\kappa = 0$, such as the case with $\beta = 1$,

$$\bar{\kappa}(t) = \bar{\kappa}(0). \qquad \blacksquare$$

Remark 3.

In conclusion, convex curves remain convex and $\bar{\kappa}(t) = 2\pi$ for all deformations. For nonconvex curves and $\beta = 1$, we have $\bar{\kappa}(t) = \bar{\kappa}(0)$. Note therefore that for all curves, the deformation $\beta = 1$ does not alter the total absolute curvature. Finally, for nonconvex curves and deformations for which $\beta_\kappa < 0$, such as $\beta = 1 - \epsilon\kappa$ with $\epsilon > 0$, we have

$$\bar{\kappa}(t) < \bar{\kappa}(0).$$

This describes the important role of ϵ in the deformation as one of reducing the total absolute curvature. Note that for $\beta = -\epsilon\kappa$, the deformation will evolve an embedded curve to a circle [28, 35].

In this section we will address the key issue of how far the evolved curve can be away from the initial curve. First we derive a relationship between the distance of a point from a curve and the curvature of the curve at the nearest point. Second, the rate of change of distance of a point to a curve is related to the speed of the curve at its nearest point. This result holds for nonshock points. Third, the distance of a point from a curve bounds the rate of change of that distance with time. Fourth, we show that a curve can not travel too far pointwise. Fifth, for any time neighbourhood for which the curve does not travel beyond ϵ, we constrain its expansion as a function of time. From these we conclude that two curves close in time are close in their Hausdorff distance. Finally, a theorem shows that the limit of curvature evolution exists, and using the above we can even bound the total Gaussian curvature.

2.4.3 On the Distance Travelled

In what follows we will limit ourselves to the case

$$\beta(\kappa) = 1 - \epsilon\kappa.$$

For a subset $S \subset \mathbf{R}^2$. let $\mathbf{N}_\delta(\mathbf{S})$ denote a closed δ—neightborhood. Define the *signed distance* of a point from a curve (regarded as a point set in $\mathbf{R}^2$) as

$$d(p, C_t) := \begin{cases} \inf\{d(p,q) | q \in C_t\} & \text{if } p \text{ is outside } C_t \\ -\inf\{d(p,q) | q \in C_t\} & \text{otherwise,} \end{cases}$$

where *outside* is the region to the right of the curve as one traverses the curve in the positive orientation. In this section we will consider an arbitrary point in the plane, p, and consider its relation to the curve C_t. Set

$$d(t) := d(p, C_t)$$

.

Lemma 2.6 *Let $p \notin C$ be a point in $\mathbf{R}^2$. Let q be the closest point on the curve to p. (Note that q exists by compactness.) Then,*

$$\begin{cases} \kappa(q) \geq \frac{-1}{d(p,q)} & \text{if } p \text{ is outside } C \\ \kappa(q) \leq \frac{-1}{d(p,q)} & \text{if } p \text{ is inside } C. \end{cases}$$

Proof. Set $d = d(p,q)$. First suppose the point p is outside the curve, so that $d > 0$. Let q be the closest point on the curve C to p. Consider the circle of radius d and center p which is tangent to the curve at q. We have two separate cases: (i) the curve has non-negative curvature at q. In this case, $\kappa(q) \geq \frac{-1}{d}$, trivially. (ii) the curve has negative curvature at q. In this case, the curve C lies entirely outside the circle of radius d and center p. In order to see this suppose to the contrary; then there exist points on C closer to p than d, a contradiction. Therefore, the curvature of the circle $\frac{1}{d}$ is greater than the curvature of the curve at q, i.e. $\frac{1}{d} \geq -\kappa(q)$. Therefore, for both cases when the point p is outside the curve C, we have

$$\kappa(q) \geq \frac{-1}{d}$$

Now, as required suppose the point p is inside the curve C, $d < 0$, and q the closest point of the curve C to it. Again, consider the circle of radius $-d$ and center p which is tangent to the curve at q. Once more we have two cases: (i) the curve has non-positive curvature at q. curvature. Trivially, then $\kappa(q) \leq \frac{-1}{d}$. (i) the curve has positive curvature at q. In this case, the circle again lies entirely within the curve, touching it only at q, so that, the curvature of the circle $\frac{-1}{d}$ is greater than the curvature of the curve $\kappa(q)$. Then,

$$\kappa(q) \leq \frac{-1}{d}$$

∎

Lemma 2.7 *Let p be a point in $\mathbf{R}^2$ where C_t deforms along the normal according to (2.2). If $\frac{\beta_s}{g}$ can be bounded, then*

$$d'(t) = -\frac{\partial C}{\partial t}.$$

Proof. Let $q(s,t)$ be the closest point to p on C_t and $q(s+\delta s, t+\delta t)$ the closest point on $C(.,t+\delta t)$ to p. Since the line (p, q(s,t)) is normal to C_t, the point $q(s,t+\delta t)$ is on this line a distance $\frac{\partial C}{\partial t}\delta t$ from $q(s,t)$. Consider the triangle with vertices $p, q(s,t+\delta t), q(s+\delta s, t+\delta t)$, where the angle at p is denoted by $\delta\theta$. Then,

$$
\begin{aligned}
\frac{d(t+\delta t)-d(t)}{\delta t} &= \frac{1}{\delta t}\left[\frac{(d(t)-\frac{\partial C}{\partial t}\delta t)}{\cos(\delta\theta)} - d(t)\right] \\
&= \frac{1}{\cos(\delta\theta)\delta t}[2d(t)\sin^2(\delta\theta/2) - \frac{\partial C}{\partial t}\delta t] \\
&= -2d(t)\frac{\sin^2(\delta\theta/2)}{\cos(\delta\theta)\delta t} - \frac{\frac{\partial C}{\partial t}}{\cos(\delta\theta)}.
\end{aligned}
$$

In the limit, $\delta t \to 0$, $\delta\theta \to 0$. From the equations for rate of change of orientation with sin Section 2,

$$\frac{\partial\theta}{\partial t} = \frac{-\beta_s}{g}.$$

Since θ_t can be bounded

$$d'(t) = -\frac{\partial C}{\partial t}. \qquad \blacksquare$$

Remark 4. Observe that as t aproaches the time of shock formation, $g(s,t)$ goes to zero, and therefore the condition of Lemma 2.7 does not hold in the limit. -

Lemma 2.8 *Let C_t be a solution of (2.2) where $\beta(\kappa) = 1 - \epsilon\kappa$. Let p be a point in $\mathbf{R}^2$. If $d(t) = d(p, C_t) \le \epsilon$, then,*

$$d'(t)d(t) \ge -2\epsilon.$$

Proof. Let $q(t)$ be the closest point on the curve C_t to p. First, consider the case where the point p is outside the curve C_t. Then, by Lemma 2.6, $\kappa(q(t)) \ge \frac{-1}{d(t)}$. Consequently,

$$d'(t) \quad = \epsilon\kappa - 1$$

$$\begin{aligned} &\geq \frac{-\epsilon}{d(t)} - 1 \\ &\geq \frac{-2\epsilon}{d(t)}, \end{aligned}$$

since $d(t)$ is positive and $d(t) \leq \epsilon$. Hence we can conclude that

$$d'(t)d(t) \geq -2\epsilon.$$

Now, consider the case where the point p is inside the curve which implies $\kappa(q(t)) \leq \frac{-1}{d(t)}$. Then,

$$\begin{aligned} d'(t) &= \epsilon\kappa - 1 \\ &\leq \frac{-\epsilon}{d(t)} - 1 \\ &\leq \frac{-2\epsilon}{d(t)}, \end{aligned}$$

since $d(t)$ is negative and $d(t) \leq \epsilon$. Once again, we can conclude that

$$d'(t)d(t) \geq -2\epsilon. \qquad \blacksquare$$

Lemma 2.9 *Consider a curve C_0 evolving through a function of curvature as in (2.2), with $\beta(\kappa) = 1 - \epsilon\kappa$. Then for each ϵ, there exists $\bar{t} = \bar{t}(\epsilon, C_0) > 0$, such that for each $p \in C_{\hat{t}}$ with $0 \leq \hat{t} < \bar{t}$ we have that*

$$d(t) \leq \epsilon \qquad \forall 0 \leq t < \bar{t}.$$

Proof. Let $p \in C_{\hat{t}}$ for some $0 \leq \hat{t} < \bar{t}$. Note that $1 - \epsilon\kappa(q(t), t)$ is the speed of the point $q(t)$ on C_t in the evolving family. Now since $\kappa(s, t)$ is a periodic solution of a polynomial reaction-diffusion equation with analytic coefficients and smooth initial condition, there exists an interval $[0, t_1]$ such that $\kappa(s, t)$ is uniformly bounded as a function in t say by M. Therefore on $[0, t_1]$

$$|1 - \epsilon\kappa(q(t), t)| \leq 1 + \epsilon M.$$

Thus any point $q(0) \in C_0$ cannot have travelled more than distance ϵ from C_0 in time

$$t_2 := \frac{\epsilon}{1 + \epsilon M}.$$

Set

$$\bar{t} := \min(t_1, t_2).$$

Since $p \in C_{\hat{t}}$ for some $0 \leq \hat{t} < \bar{t}$, the lemma is proven. ∎

Theorem 2.1 *Consider a curve C_0 evolving through a function of curvature as in 2.2 with $\beta(\kappa) = 1 - \epsilon\kappa$. Let $\bar{t} = \bar{t}(\epsilon, C_0)$ be as in the previous lemma. Then*

$$C_t \subset \mathbf{N}_{\sqrt{4\epsilon t}}(C_0).$$

for all $t \in [0, \bar{t}]$.

Proof. From Lemma 2.9, given ϵ there exists $\bar{t}$ such that for all $t \in [0, \bar{t}]$ and for all $p \in C_t$ we have

$$d(t) = d(p(t), C_t) \leq \epsilon.$$

Now, by Lemma 2.8,

$$[\frac{d^2(t)}{2}]' = d'(t)d(t) \geq 2\epsilon.$$

for all $t \in [0, \bar{t}]$. By integration

$$d(t) \leq \sqrt{4\epsilon t}.$$

Hence, we have shown there is $\bar{t}$ such that for $t \in [0, \bar{t}]$ we have

$$C_t \subset \mathbf{N}_{\sqrt{4\epsilon t}}(C_0)$$ ∎

Remark 5. For d_H the Hausdorff metric defined on compact subsets of $\mathbf{R}^2$, from the above theorem we have that

$$d_H(C_t, C_0) \leq \sqrt{4t}.$$

2.4.4 Limits of Classical Solutions

Lemma 2.10 *Let $C_t : S^1 \to \mathbf{R}^2$ be a family of C^2 functions with uniformly bounded length-squared $L^{(2)}(t)$. Then, C_t is uniformly equicontinuous.*

Proof. The lemma is a simple modification of the result for functions with bounded derivatives. Note that

$$C(s,t) - C(s_o,t) = \int_{s_o}^{s} \frac{\partial C}{\partial \sigma} d\sigma.$$

Therefore if L is the uniform bound on the length-squared

$$\|C(s,t) - C(s_o,t)\| \leq$$

$$\int_{s_o}^{s} \|\frac{\partial C}{\partial \sigma}\| d\sigma = \int_{s_o}^{s} \left[\left(\frac{\partial x}{\partial \sigma}\right)^2 + \left(\frac{\partial y}{\partial \sigma}\right)^2\right]^{1/2} d\sigma$$

$$\leq \left[\int_{s_o}^{s} \left(\frac{\partial x}{\partial \sigma}\right)^2 + \left(\frac{\partial y}{\partial \sigma}\right)^2 d\sigma\right]^{1/2} \leq L|s - s_o|^{1/2},$$

that is, the family is equicontinuous with Hölder constant L and exponent $1/2$. ∎

Theorem 2.2 *Consider a curve C_0 evolving through a function of curvature as in (2.2). Then,*

$$\lim_{t \to t'} C_t = C^*,$$

in the Hausdorff metric. The curve C^* regarded as a mapping $C^* : S^1 \to \mathbf{R}^2$ is Hölder continuous with exponent 1/2

Proof. Since the lengths-squared of the curves C_t are uniformly bounded (see Lemma 2.2 and Remark 1(ii)) regarding each $C_t : S^1 \to \mathbf{R}^2$, we can apply the Lemma 2.10 to the family

$$\{C_t\}_{t\in[0,t']}$$

to conclude that it is equicontinuous. Moreover from Theorem 2.1, the curves lie in a compact region. Thus by the Arzela-Ascoli theorem and the proof of Lemma 2.10. there exists a uniformly convergent subsequence $C_{t_n} \to C^*$, where $C^* : S^1 \to \mathbf{R}^2$ is a Hölder continuous function with exponent $1/2$. (The Hölder continuity of the limit follows from the fact that the family is equicontinuous and Hölder continuous. C^* will also denote the corresponding curve.) Thus as compact subsets of the plane. we have that $C_{t_n} \to C^*$ in the Hausdorff metric.

To complete the proof. we need to show that all the $C_t \to C^*$ (in the Hausdorff metric) as $t \to t'$. Let $\delta > 0$. and choose t_n such that

$$C_{t_n} \subset \mathbf{N}_{\delta/2}(C^*)$$

and

$$t_n > t' - \frac{\delta^2}{16\epsilon}.$$

(We choose $\delta > 0$ sufficiently small so that $t' - \frac{\delta^2}{16\epsilon} > 0$.) Note that for all $t \in [t_n, t')$. we have

$$t - t_n < \frac{\delta^2}{16\epsilon}.$$

Therefore, by Theorem 2.1

$$C_t \subset \mathbf{N}_{\sqrt{4\cdot\frac{\delta^2}{16\epsilon}\cdot\epsilon}}(C_{t_n}).$$

$$C_t \subset \mathbf{N}_{\delta/2}(C_{t_n}).$$

$$C_t \subset \mathbf{N}_{\delta}(C^*),$$

as required. ∎

Remarks 6.

(i) Note that since C^* is Hölder continuous, and since the total Gaussian curvature of the family is uniformly bounded (see Lemma 3.2.1), C^* will have finite total Gaussian curvature.

(ii) From the above results, we have a fairly complete picture about the the classical evolution of a family of curves with

$$\beta(\kappa) = 1 - \epsilon\kappa \quad \epsilon \geq 0.$$

Chapter 3

Conservation Laws

We now continue the study of curve deformations, and relate them to conservation laws. In particular, we review an expression of hyperbolic conservation laws as differential equations and we show that orientation and the product curvature-metric satisfy it. First, it is shown that the axiom "slightly deformed shapes appear similar" leads to a qualitative description of arbitrary deformation of shape as a sum of two types of deformations: *constant motion* and *curvature motion.* It is shown that while constant motion leads to a conservation law for orientation, adding curvature motion is tantamount to adding viscosity to the system.

3.1 Hyperbolic Conservation Laws

Conservation laws appear frequently in physical sciences. Examples include conservation of matter, energy, electric charge, and heat, among others. To illustrate, consider the conservation of matter, which can be stated as follows: "the amount of matter that flows into a volume is exactly the amount of increase of matter within that volume." In other words, matter is neither created nor destroyed. In this section, we first review hyperbolic conservation laws, express them as differential equations, and then show that orientation satisfies a similar equation. As such, given a "piece" of orientation. the total change of orientation in that "piece" is equal to the change in the orientation of neighboring curve segments.

To derive an equation expressing the conservation of a quantity u, such as heat, consider the volume G with boundary ∂G. The total quantity of u in the volume is $\int_G u dv$, where dv is the volume element, and the total quantity passing through the boundary is $\int_{\partial G} u dS$, where dS is the surface element, figure 3.1. Then, conservation holds if

$$\frac{\partial}{\partial t}\int\int\int_G u\,dv = -\int\int_{\partial G} H(u)\cdot\vec{n}\,dS, \tag{3.1}$$

where H is the flux. Using the Divergence Theorem, the right hand side is simply $\int\int\int_G \nabla\cdot H(u)\,dv$, so that

$$\int\int\int_G [\frac{\partial u}{\partial t} + \nabla\cdot H(u)]\,dv = 0. \tag{3.2}$$

Since this holds for any volume G,

$$\frac{\partial u}{\partial t} + \nabla\cdot H(u) = 0, \tag{3.3}$$

which is the differential equation representing the above integral equation. Equation 3.3 is called a *hyperbolic conservation law* and is satisfied by heat, mass, energy, momentum, electric charge and some other physical quantities. For functions of one variable x the equation reduces to

$$\frac{\partial u}{\partial t} + H_x(u) = 0. \tag{3.4}$$

For example, $H(u) = -u_x$, yields the heat equation

$$\frac{\partial u}{\partial t} = u_{xx}.$$

At the heart of this thesis is the abstraction of certain properties of shape that also satisfy conservation laws.

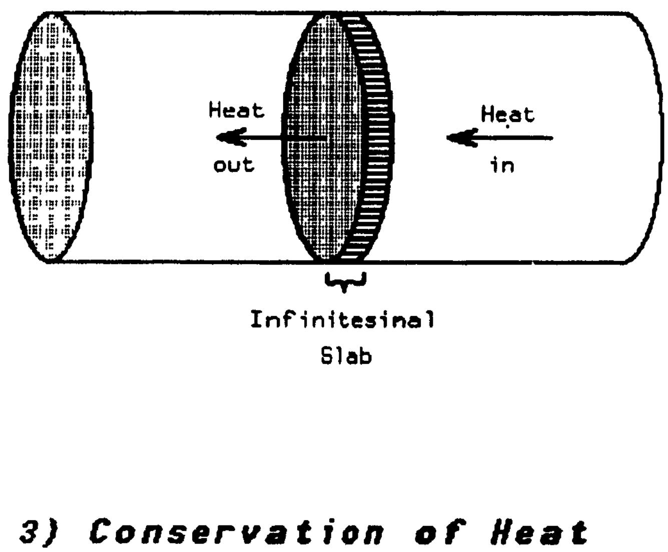

Figure 3.1: This figure illustrates the conservation of heat: the net amount of heat that flows into the volume is exactly the amount of increase of heat in that volume.

3.2 Conservation of Orientation

We now turn to conservation laws for orientation and show that, in an arbitrary deformation of a shape, orientation satisfies a viscous conservation law. Specifically, we show first that when a curve is deformed by constant motion, orientation is conserved. By adding curvature motion, orientation then follows a viscous conservation law, i.e. curvature plays the role of viscosity [75].

Consider a curve $\mathcal{C}(s,t) = (x(s,t), y(s,t))$ satisfying 1.3. Then, for almost any s and for some neighborhood t, we can write

$$y = \gamma(x,t).$$

The metric is

$$\begin{aligned} g &= \sqrt{1+\frac{\partial y}{\partial x}^2} \\ &= \sqrt{1+\gamma_x^2} \end{aligned} \tag{3.5}$$

The tangent and normal are

$$\begin{aligned} \vec{T} &= \frac{1}{\sqrt{1+\gamma_x^2}}(1,\gamma_x) \\ \vec{N} &= \frac{1}{\sqrt{1+\gamma_x^2}}(-\gamma_x,1) \end{aligned} \tag{3.6}$$

Curvature in turn is

$$\kappa = \frac{\frac{\partial^2\gamma}{\partial x^2}}{(1+\gamma_x^2)^{\frac{3}{2}}}. \tag{3.7}$$

Then equation 1.3 translates into

$$\begin{aligned} (\tfrac{\partial y}{\partial t},\tfrac{\partial x}{\partial t}) &= \beta(\kappa)\vec{N} \\ (\tfrac{\partial y}{\partial t},\tfrac{\partial x}{\partial t}) &= \beta(\kappa)\frac{1}{\sqrt{1+\gamma_x^2}}(-\gamma_x,1) \end{aligned} \tag{3.8}$$

Now, $y_t = \gamma_x x_t + \gamma_t$, leading to

$$\begin{aligned} \gamma_t &= y_t - \gamma_x x_t \\ &= \beta(\kappa)\frac{1}{\sqrt{1+\gamma_x^2}} - \beta(\kappa)\gamma_x\frac{1}{\sqrt{1+\gamma_x^2}}(-\gamma_x) \\ &= \beta(\kappa)\sqrt{1+\gamma_x^2} \end{aligned} \tag{3.9}$$

This can also be shown to hold in the weak sense when one removes smoothness assumptions.

Now, let us turn to constant motion, namely $\beta(\kappa) = 1$. The equation $\gamma_t = \sqrt{1+\gamma_x^2}$ is a first order Hamilton-Jacobi equation. Using the transformation $m = \gamma_x$, the equation becomes a conservation law [18]. Specifically, the evolution for orientation γ_x can be found by differentiating

$$(\gamma_x)_t = [\sqrt{1+\gamma_x^2}]_x. \tag{3.10}$$

As such, the slope of the curve $m = \gamma_x$ satisfies

$$m_t + [\mathcal{H}_m(m)]_x = 0, \tag{3.11}$$

where $\mathcal{H}_m(m) = -\sqrt{1+m^2}$, the flux of slope. To translate this equation into one with orientation, θ, observe $\tan(\theta) = m$:

$$\begin{aligned}
[\tan(\theta)]_t &= [(1+\tan^2(\theta))^{\frac{1}{2}}]_x \\
(1+\tan(\theta)^2)\theta_t &= \tfrac{1}{2}(1+\tan^2(\theta))^{\frac{-1}{2}}\cdot 2tan(\theta)(1+\tan^2(\theta))\theta_x \\
\theta_t &= \frac{tan(\theta)}{(1+\tan^2(\theta))^{\frac{1}{2}}]}\theta_x \\
\theta_t &= \sin(\theta)\theta_x.
\end{aligned} \tag{3.12}$$

Hence,

Theorem 3.1 *Orientation of a curve deformed by constant motion satisfies a hyperbolic conservation law for orientation θ:*

$$\frac{\partial\theta}{\partial t} + \mathcal{H}_\theta(\theta)_x = 0, \tag{3.13}$$

where $\mathcal{H}_\theta(\theta) = \cos(\theta)$, $-\pi/2 < \theta \leq \pi/2$.

So far, we have shown that slope and orientation satisfy conservation laws when the deformation is a constant one along the normal. It is natural to ask what happens when the deformation is arbitrary, i.e. when curvature motion is now involved as well.

The role of curvature may be examined by deriving an equation for the combination of constant and curvature motions which is similar to 3.13. Returning to equation 3.9, by letting $\beta(\kappa) = \beta_0 + \beta_1 K$ to include curvature motion, we have:

$$\begin{aligned}\gamma_t &= (\beta_0 + \beta_1 K)\sqrt{1+\gamma_x^2} \\ &= \beta_0\sqrt{1+\gamma_x^2} + \beta_1 \tfrac{\gamma_{xx}}{(1+\gamma_x^2)}\end{aligned} \tag{3.14}$$

Differentiate

$$(\gamma_x)_t - \beta_0[\sqrt{1+\gamma_x^2}]_x = \beta_1[\frac{\gamma_{xx}}{(1+\gamma_x^2)}]_x, \tag{3.15}$$

or

$$m_t + \beta_0[\mathcal{H}_m(m)]_x = \beta_1[\frac{m_x}{(1+m^2)}]_x. \tag{3.16}$$

For orientation $\tan(\theta) = \gamma_x$,

$$\begin{aligned}
[\tan(\theta)]_t - \beta_0[(1+\tan^2(\theta))^{\frac{1}{2}}]_x &= \beta_1[\tfrac{\tan(\theta)_x}{[1+\tan^2(\theta)]}]_x \\
[1+\tan^2(\theta)]\theta_t - \beta_0\tan(\theta)(1+\tan^2(\theta))^{\frac{1}{2}}\theta_x &= \beta_1[\tfrac{(1+\tan^2(\theta))\theta_x}{[1+\tan^2(\theta)]}]_x \\
\theta_t - \beta_0\sin(\theta)\theta_x &= \beta_1\cos^2(\theta)\theta_{xx} \\
\theta_t + \beta_0[\mathcal{H}(\theta)]_x &= \beta_1\cos^2(\theta)\theta_{xx}.
\end{aligned} \tag{3.17}$$

Theorem 3.2 *Orientation of a curve deformed by a combination of constant motion and curvature motion satisfies a viscous hyperbolic conservation law for orientation θ:*

$$\theta_t + \beta_0[\mathcal{H}(\theta)]_x = \beta_1\cos^2(\theta)\theta_{xx}, \tag{3.18}$$

where $\mathcal{H}_\theta(\theta) = \cos(\theta)$.

Note that the latter equation is the original conservation law with a right hand side that contains a second derivative for θ, a diffusive term (recall the heat equation $\theta_t = \theta_{xx}$). In fact, this is a *reaction-diffusion* equation where the term $\beta_0[\mathcal{H}(\theta)]_x$ is the reaction term and $\beta_1\cos^2(\theta)\theta_{xx}$ is the diffusion term. It can be seen from the coefficients of these terms, β_0 and β_1, that the constant motion corresponds to reaction and the curvature motion to diffusion. In the next chapter we continue with this idea and build a reaction-diffusion space where, through the interaction of the two "forces" reaction and diffusion, the various aspects of shape can be characterized.

3.3 Conservation of Curvature-Metric

We end this chapter with a second intriguing conservation law and one on which the remainder of this thesis will not depend. Consider the product of curvature and the metric g defined as in 2.3. Define the *curvature-metric* as $\mathcal{K} = \kappa g$.

Lemma 3.1 *The quantity $\mathcal{K} = \kappa g$ is conserved.*

Proof:

$$\begin{aligned} \frac{\partial \mathcal{K}}{\partial t} &= \kappa_t g + \kappa g_t \\ &= -\kappa^2 g + \kappa \kappa g \\ &= 0. \end{aligned} \tag{3.19}$$

The question naturally arises whether the curvature-metric $\mathcal{K}$ deserves special attention. To answer this, observe that, intuitively curvature is taken to be a measure of how bent a curve is. However, while curvature is formally defined as change in tangent per unit arclength, arclength is not always easy to specify or to measure, an issue often ignored in numerical implementations. Recall that a curve is defined by two coordinate functions. The theorem stating that curvature alone can determine a curve [22], involves an implicit assumption of parameterization by arc-length. However, it seems that our perceptual judgements of bending depend on curvature and on a perceived arc-length as well. [1]. To illustrate, consider figure 3.2, where the curve parametrized as (s^2, s^3) is sketched. A computation reveals that curvature increases in magnitude and is unbounded as we approach the cusp. Note in addition that curvature changes sign as we cross the cusp. Covering half the graph, so that only the right or the left portion is visible, indicates that the curve does not appear to

[1] This point among others in this section was the result of many discussions with Allan Dobbins

be infinitely bent as we approach the cusp. This is in clear contradiction to what a computation of curvature would predict.

The problem appears to be based on several assumptions. First, the curve is assumed to be smooth, when in fact a large number of shapes contain discontinuities. Second, is the issue of representation: A curve may be represented by a pair of functions $\{x(s), y(s)\}$, or it may alternatively be represented by curvature κ. Implicit in this latter representation is that curvature is a function of arc-length $\hat{s}$. However, this is not always possible. We suggest that a perceptually important representation could be the pair of functions (κ, g) leading to the definition of *generalized curvature* as

$$\hat{\kappa}_{\Delta s}(s) = \frac{\int_{s-\Delta s/2}^{s+\Delta s/2} \kappa g \, ds}{\int_{s-\Delta s/2}^{s+\Delta s/2} g \, ds}, \tag{3.20}$$

where $2\Delta s$ is the "stick size" of measurement, κ is curvature, and g is "speed" as before.

To motivate this definition, consider the following physical analogy. Imagine yourself driving along a winding road and observe the speed variation. When the road is relatively straight, one increases speed and, when approaching the bends, one decreases speed. For the very difficult turns, one may even slow down to zero. The limiting factor is friction and lateral acceleration. In analogy, as one's mind's eye traverses a curve, it must limit the "visual acceleration"; i.e. sample greatly when close to higher bending and sample sparsely when the curve is straight. Returning to the definition, the integral $\int_{s-\Delta s/2}^{s+\Delta s/2} G\, ds$ represents an "extent" over which bending is measured. The numerator $\int_{s-\Delta s/2}^{s+\Delta s/2} \kappa g \, ds$ is the change in orientation in that interval. As such our definition takes into account both *extent* of the curve and *speed* of traversal. In the cusp example of figure 3.2 speed approaches zero as we approach the cusp, thereby the extent over which curvature is unbounded is infinitesimal.

When $g(s) = 1$, namely, when the curve is represented by arclength, the generalized curvature $\hat{\kappa}$ reduces to the standard notion of curvature. Also, note that a

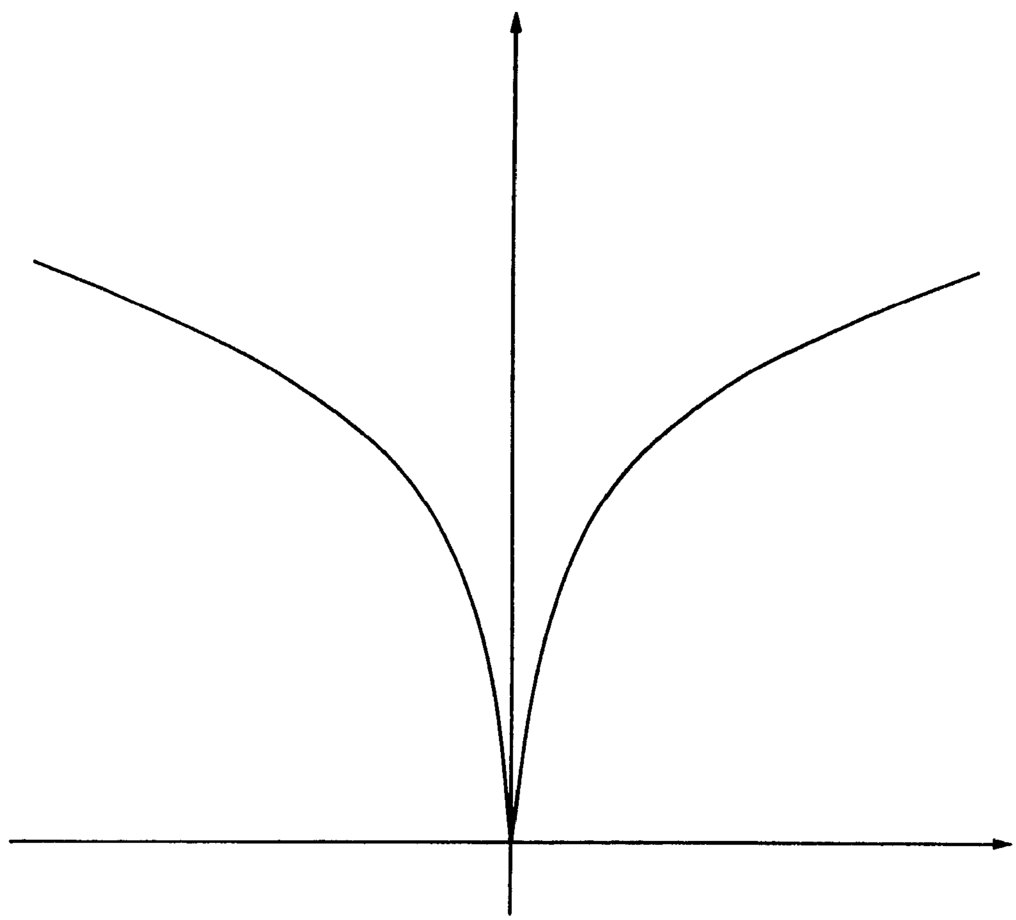

Figure 3.2: This example illustrates that the standard notion of curvature as a function of arc length may not be the ideal mathematical representation of our perceptual representation for "amount of bend". This graph is a sketch of (s^2, s^3) whose curvature at $t = 0$ is unbounded for each side of the cusp. However, covering half the graph, we can not possibly associate infinite bending with the curve. Our proposal is that not curvature, but curvature-metric is involved in a notion of "amount of bending".

notion of scale is built in to the definition. Singularities in this representation are the highest possible change in the smallest possible scale. Now, consider a rectangle. While at the corners curvature is undefined, the generalized curvature gives $\pi/2$, which is perceptually intuitive. This preliminary definition deserves a great deal more development, but is beyond the scope of this thesis.

Chapter 4

Shocks and the Role of Entropy

In the previous chapters it was shown that within a stable representation of shape, slightly deformed shapes ought to look similar. The study of arbitrary deformations lead to their classification as combinations of *constant motion* and ***curvature motion***. This in turn leads to conservation laws for orientation and other quantities when the shape is deformed by constant motion. The more general case, when curvature motion is added to the deformation, leads to viscous conservation laws. Solving these conservations laws, however, is not trivial: the space of differentiable or continuous function is not large enough to accommodate the *shocks* that signal key aspects of shapes. In this chapter, solutions of conservation laws are sought in the much larger space of *generalized functions*. This leads to too many solutions, and a notion of *entropy* is required to pick the physically significant one. Entropy satisfying solutions exist and are the unique solutions of the conservation law. Finally, the role of shocks and entropy for shape is described.

4.1 The Formation of Shocks

Consider a single hyperbolic conservation law

$$\frac{\partial u}{\partial t} + H_x(u) = 0, \tag{4.1}$$

where x is the space variable, t is time, u is the conserved quantity and H is the flux of u. This is a nonlinear partial differential equation and, as such, smooth initial conditions may not (and as will shortly become clear, often will not) remain smooth or even continuous. The lack of a classical solution, however, does not imply the lack of a physical solution. Observe that the differential form of the conservation law in 3.3 is a convenient representation for differentiable functions only and that the original relation is an integral one (3.2). Consequently, given the integral relation, there in no inherent reason for limiting the space to that of continuous functions, especially since in our case of shape representation (as well as other areas of vision), discontinuities are often salient features that play a significant role in the recovery of structure. Consider, then, the much larger space of *generalized functions*, i.e. the space of bounded and measurable functions, which are capable of representing many kinds of discontinuities. The notion of what constitutes a solution, must, however, be reformulated from an integral perspective. This leads to the idea of *weak solutions* of (3.3), with bounded and measurable initial condition $u(x,t) = u_0(x,t)$, as those functions that satisfy the integral relation

$$\int\int_{t\geq 0}[u\phi_t + \mathcal{H}(u)\phi_x]dx\,dt + \int_{t=0} u_0\phi\, dx = 0, \tag{4.2}$$

for all differentiable ϕ with compact support. Notice that a classical solution of 3.3 is also a weak solution of it.

Unfortunately, while the larger space of generalized functions is richer in its representational power, now there are many generalized solutions that satisfy (3.1)[1] Since the physical solution exists and is unique, however, the question arises as how to determine which generalized solution is physically significant. The solution lies in the notion of *entropy* [19, 48, 62] which, in the case of gas dynamics dictates that the "entropy of the particles must increase as they cross a *shock* front". In the domain of generalized functions, it can be shown that an entropy satisfying solution exists and is the unique physical solution.

There are at least five mathematically different approaches to the problems concerned with the solutions of scalar conservation laws, namely: (1) Calculus of variations and the Hamilton-Jacobi theory [18]; (2) the viscosity method [21, 45]; (3) nonlinear semigroup theory [20]; (4) the method of characteristics [23]; and (5) the method of finite differences [47, 32], [78]. In the following illustration of shocks and entropy, we will principally use the method of *characteristics*, with some reference to other methods.

To motivate the idea of shocks and entropy, let us consider the well-studied Burgers' equation [37] as a simple model of turbulence in fluid flow

$$u_t + uu_x = \mu u_{xx}, \tag{4.3}$$

which is a conservation law with $H = 1/2u^2$ when viscosity μ is zero,

$$u_t + uu_x = 0. \tag{4.4}$$

The solution to 4.4 for the initial condition

$$u_0(x) = \begin{cases} 1 & \text{if } x \leq 0 \\ 1 - x & \text{if } 0 \leq x \leq 1 \\ 0 & \text{if } 1 \leq x, \end{cases} \tag{4.5}$$

may be found using the method of *characteristics* [29, 40, 80], where

$$\frac{dx}{dt} = \frac{dH}{du}, \tag{4.6}$$

or $x_t = u$. To interpret this, all points on the negative x-axis will move to the right with speed 1, all points with $0 \leq x < 1$ will move to the right with speeds varying from 1 to 0, and all points with $x \geq 1$ stay put. With time, the point on the left of the slope will get closer to the stationary segment and, consequently, the slope becomes sharper. It is clear from figure 4.1 that for $t < 1$ the function $u(x,t)$ remains single valued. However, for $t \geq 1$, the characteristics clash, and there exists the potential for the formation of a *shock*. Beyond this point, the two characteristics enforce two different values for u, namely, 1 and 0. This is clearly not possible. The dilemma of which of the two values is physically meaningful is solved by enforcing conservation at a traveling shock, leading to the so-called *jump condition* [1] [19].

$$s(u_r - u_l) = \mathcal{H}_r - \mathcal{H}_l, \tag{4.7}$$

where l and r denote left and right, respectively, and s is the speed with which the shock will move. For the case of Burgers' flux, the shock will move with average speed of the two incoming characteristics.

4.2 The Role of Entropy

A second problem arises when we consider diverging characteristics. Consider the initial condition

$$u_0(x) = \begin{cases} 0 & \text{if } x < 0 \\ 1 & \text{if } 0 < x \end{cases} \tag{4.8}$$

Here, the point to the left of the y-axis will stay put, while the points to the right will move to the right with speed 1. As such, there will be points whose value can not be determined as is depicted in figure 4.2. Consider the following functions.

$$u_1(x) = \begin{cases} 0 & \text{if } x < t/2 \\ 1 & \text{if } t/2 < x \end{cases} \tag{4.9}$$

[1] Also known as the Rankine-Hugoniot condition

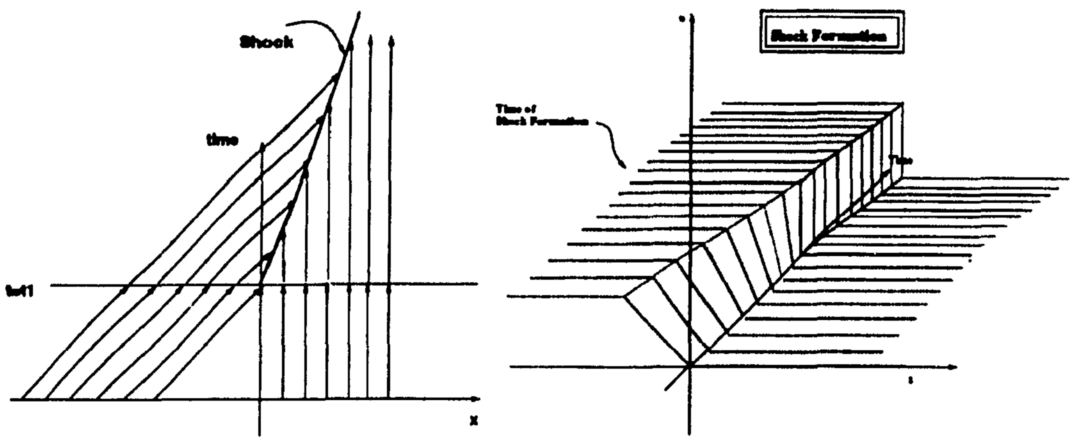

Figure 4.1: This figures illustrates how characteristics clash and shocks form. Note that after the shock forms, it travels with a speed that is determined by the jump condition. To interpret this picture, imagine a pipeline on the x-axis where the particles to the right of the y-axis are stationary; particles to the left of $x = -1$ are moving to the right with velocity 1 and all others with intermediate speeds as the characteristics show (left). On the right the shock forms at the step, and subsequently travels to the right. A significant point is the explicit representation of the singularities in the context of generalized functions.

and u_2.

$$u_2(x) = \begin{cases} 0 & \text{if } x < 0 \\ x/t & \text{if } 0 < x < t \\ 1 & \text{if } t < x \end{cases} \tag{4.10}$$

where u_1 is discontinuous and u_2 is continuous, but which both satisfy 4.4 with initial condition 4.8, see figure 4.2. Since the Rankine-Hugoniot condition (jump condition) admits *rarefaction waves* of the above type, how can one pick the physically significant solution? Observe that the discontinuity of the above solution is such that the characteristics diverge from the discontinuity. In contrast, in the discontinuity of the solution in figure 4.1, the characteristics move into the discontinuity. This is one expression of the notion of *entropy* which forces the shock speed to be intermediate to the speed of its lateral characteristics.

$$\mathcal{H}'(u_l) > \xi > \mathcal{H}'(u_r). \tag{4.11}$$

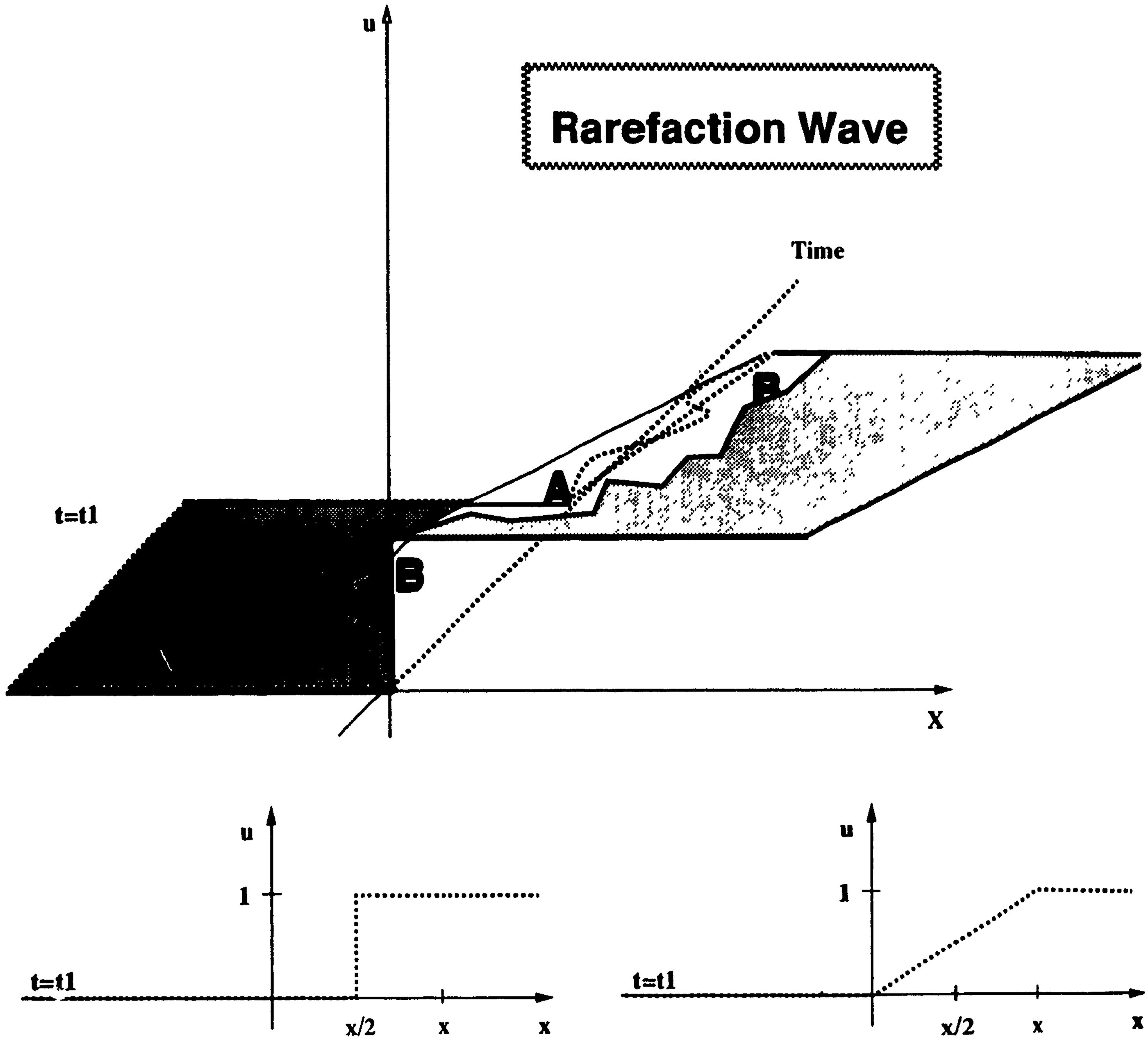

Figure 4.2: This figures illustrates the situation where a gap exists when the characteristics diverge. The jump condition alone does not resolve this situation as the two examples shown above, one continuous and one discontinuous, but which both satisfy 4.4 with initial condition 4.8. The entropy condition rules out the non shock discontinuous solution and picks a unique continuous solution u_2.

where u_l and u_r correspond to the left and right values, respectively, and $\mathcal{H}'(u)$ is the speed of propagation of quantity u, and $\mathcal{H}'' > 0$. Equation 4.11 is referred to as the *entropy inequality*.

A different expression of entropy comes in the form of an *entropy condition*:

$$\frac{u(x + \Delta x, t) - u(x, t)}{\Delta x} \leq E\frac{1}{t}, \qquad \Delta x > 0, t > 0, \tag{4.12}$$

where E is independent of x, t and Δx [62]. Note that for a fixed t increasing x implies that the change in u is always in the same direction across a discontinuity, namely, $u_r > u_r$ when $\mathcal{H}$ is convex ($\mathcal{H}'' > 0$). To reduce this to the entropy inequality, note that, by convexity of $\mathcal{H}$, $\mathcal{H}'(u_l) > \mathcal{H}'(u_r)$. Now consider the speed of the shock as determined by the jump condition

$$\xi = \frac{\mathcal{H}(u_l) - \mathcal{H}(u_r)}{u_l - u_r}.$$

Clearly, $s = \mathcal{H}'(v)$ for some v between u_l and u_r. Now, across a discontinuity, $u_l > v > u_r$ which implies

$$\mathcal{H}'(u_l) > \xi = \mathcal{H}'(v) > \mathcal{H}'(u_r),$$

or the entropy inequality. More generally, Lax introduced the *generalized entropy conditions* [18]:

$$\mathcal{H}(\alpha u_r + (1 - \alpha)u_l) \leq \alpha\mathcal{H}(u_r) + (1 - \alpha)\mathcal{H}(u_l), 0 \leq \alpha \leq 1, \tag{4.13}$$

for $u_l > u_r$.

The usefulness of the entropy inequality 4.11 is in an existence and uniqueness theorem: "Every initial value problem 3.3 has exactly one generalized solution defined for all $t \geq 0$ which has only shocks as discontinuities." [49, 62, 78]. In addition to the entropy inequality and entropy condition, one can define a notion of ***entropy*** through the additional conservation law

$$U_t + [F(U)]_x = 0.$$

[48].

There is also an interesting connection between the notion of entropy and that of viscosity. Consider the following conservation law with viscosity

$$\frac{\partial u}{\partial t} + H_x(u) = \epsilon u_{xx}, \tag{4.11}$$

where ϵ is a measure of viscosity. What happens to the solutions of the viscous conservation law as viscosity vanishes, $\epsilon \to 0$? With viscosity added to the conservation law, the shocks are smoothed out and therefore we are back to the classical situation [84]. As $\epsilon \to 0$, it would be plausible to assume that the limit of the viscous solutions ought to be the solution of the conservation law. In fact, the limit of the viscous solution is precisely the one determined by the entropy condition [62, 45, 7].

4.3 Boundary-Based Shape Entropy

What are the implications of shocks and the notion of entropy for shape? Recall that our goal is to establish a connection between similar shapes by studying deformations that take one to the other. We have already shown that arbitrary deformations of a shape lead to a viscous conservation law for the orientation of the boundary of the shape. The relevant question then is "what happens when, in the process of deformation, a discontinuity develops in orientation?". Our treatment has been one of deforming the curve along the normal and, in the case of a curve with a discontinuity in the orientation, this is clearly no longer in the realm of the classical theory of differential geometry. This situation is illustrated in figure 4.3 where points near a negative curvature minimum bunch up together. In time, these points are destined for collision as lemma 2.1 shows. To continue our deformations separately for each segment of the curve would lead to portions of the curve crossing over each other, figure 4.4. This is clearly not desirable as the crossed-over boundary does not correspond to an object.

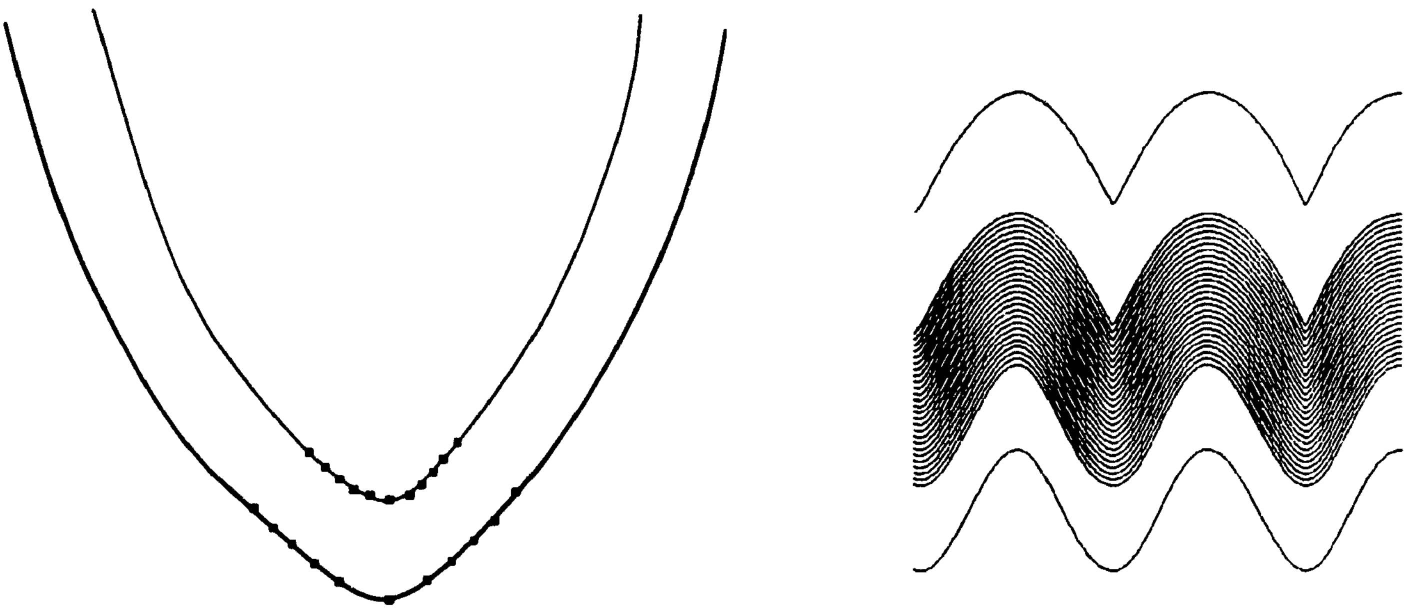

Figure 4.3: (Left) Points near a negative curvature minimum bunch up together. In time, these points are headed for collision and the formation of a shock. (Right) Negative curvature minima give rise to discontinuities.

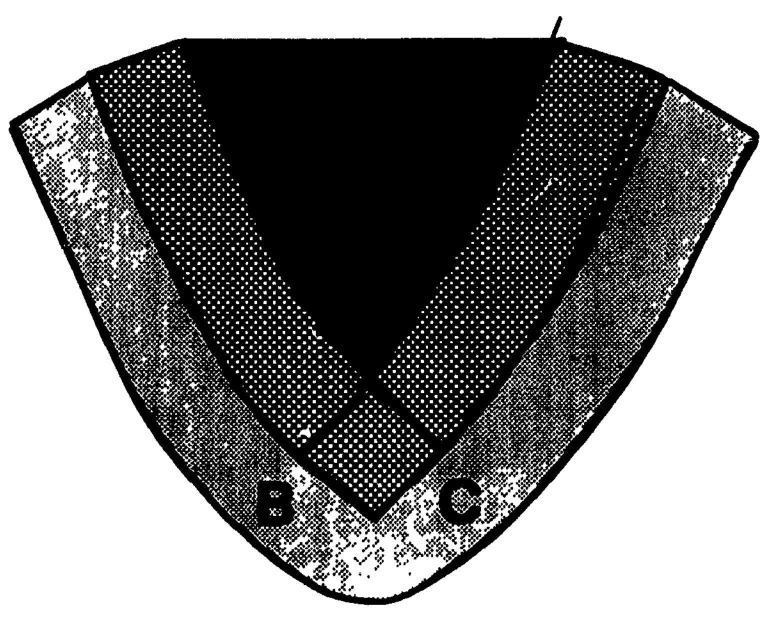

Figure 4.4: Beyond a discontinuity, deformations by following along the normal to each segment procedure boundaries that do not correspond to a shape representing an object.

To answer this question, recall that our initial motivation for studying deformations was to connect shapes through some process; to somehow distinguish "close" shapes from "distant" ones. Now, in the process of deforming the shape, it is possible that non-neighboring portions of the boundary touch each other. To continue the process beyond this point, we are guided by the basic principle that we are *deforming an object to another*. Since boundaries of objects do not cross over (simple curves), we demand

Axiom 4.1 *In the process of deformation the boundary of the shape must not cross over itself.*

Also, at no time should the boundary evolve to an open curve:

Axiom 4.2 *In the process of deformation the boundary of the shape must remain closed.*

Our axioms are in correspondence with the notions of shock and entropy for conservation laws. To illustrate, consider figure 4.5 where the shape and the orientation of its boundary are displayed in corresponding columns. In (i) the shape boundary is a pair of line segments tangent to a circular arc. (ii) is the result of deforming the shape for some time. Here, the points of the circular arc bunch up together, while the points on the line segments simply translate. Eventually, the points on the circular arc collide into one point (shock) resulting in a tangent discontinuity for the curve (iii). Up to the shock formation, the deformation of the boundary along the normal by a constant amount is exactly equivalent to the evolution of orientation according to the conservation law. However, past the formation of the shock, the normal along the boundary is multi-valued and the deformation becomes ill-defined at that point. The evolution in the conservation law domain, however, is still well-defined in the weak sense, where the shock travels with a speed determined by the jump condition.

$\frac{\cos(\theta_1)-\cos(\theta_2)}{\theta_1-\theta_2}$. The orientation and its corresponding shape is shown in (iv). Note that evolving the boundary to the left and the right side of the singularity separately, would produce a cross-over in the boundary of the shape violating axiom 4.1. In contrast, evolution in the conservation law domain satisfies this axiom because shocks form and travel in time, avoiding the formation of a tail, figure 4.4. We will shortly see that this axiom is part of an *entropy condition* for shape.

To summarize, one can view the constant deformation of a shape as a flow of orientation from high curvature points to low curvature points. Figure 4.3 depicts this flow where namely points of higher magnitude negative curvature gain in magnitude and eventually tend to infinity forming a shock. In contrast, positive curvature points decrease in magnitude. As the first shock point is created, it becomes a "black hole of orientation": orientation pours into it locally, never to be recovered. This is the basis of a scale-space of approximation and significance for shape, the *entropy scale space*, which is described in chapter 7.

What does the rarefaction wave of figure 4.2 correspond to in the domain of shape? As before, the entropy condition requires that the only discontinuities of shape be shocks. Recall that for the Burgers equation 4.4 with initial condition 4.8, the discontinuous function u_1 can not be a solution. Similarly, this is also the case with the orientation conservation law and initial condition of figure 4.6. Here, the rarefaction wave evolves to the continuous solution which satisfies $\mathcal{H}'(u(\xi)) = \xi$ with $\xi = x/t$. In our case, it is easy to see that $x = \sin(\theta)t$ and $y = -\cos(\theta)t$. Consequently, the rarefaction solution following a shock yields a circular arc.

4.4 Region-Based Shape Entropy

So far, we have represented the shape *locally* by the orientation of it *boundary*. Using notions of shocks, entropy, and weak solutions of conservation laws for orientation

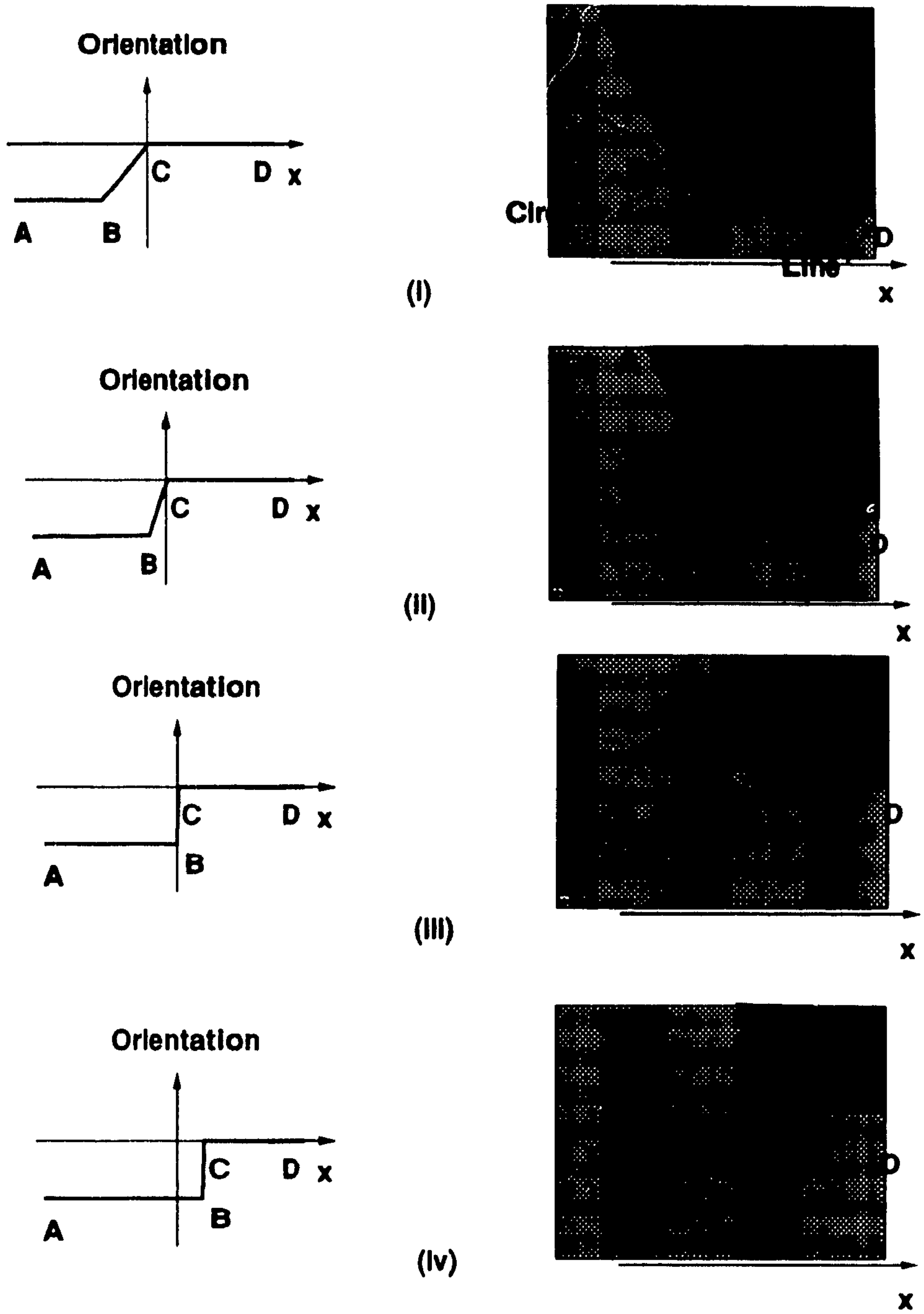

Figure 4.5: The shock as depicted for the Burgers' equation in figure 4.1 is now applied to shape. Recall that orientation satisfies a conservation law which produces a similar shock (left column). On the other hand, the deformation in the shape domain is constant motion along the normal. Note that with time, the circular arc will dissolve into one point, leaving the orientation of the boundary discontinuous. How does one continue the deformation beyond this point?

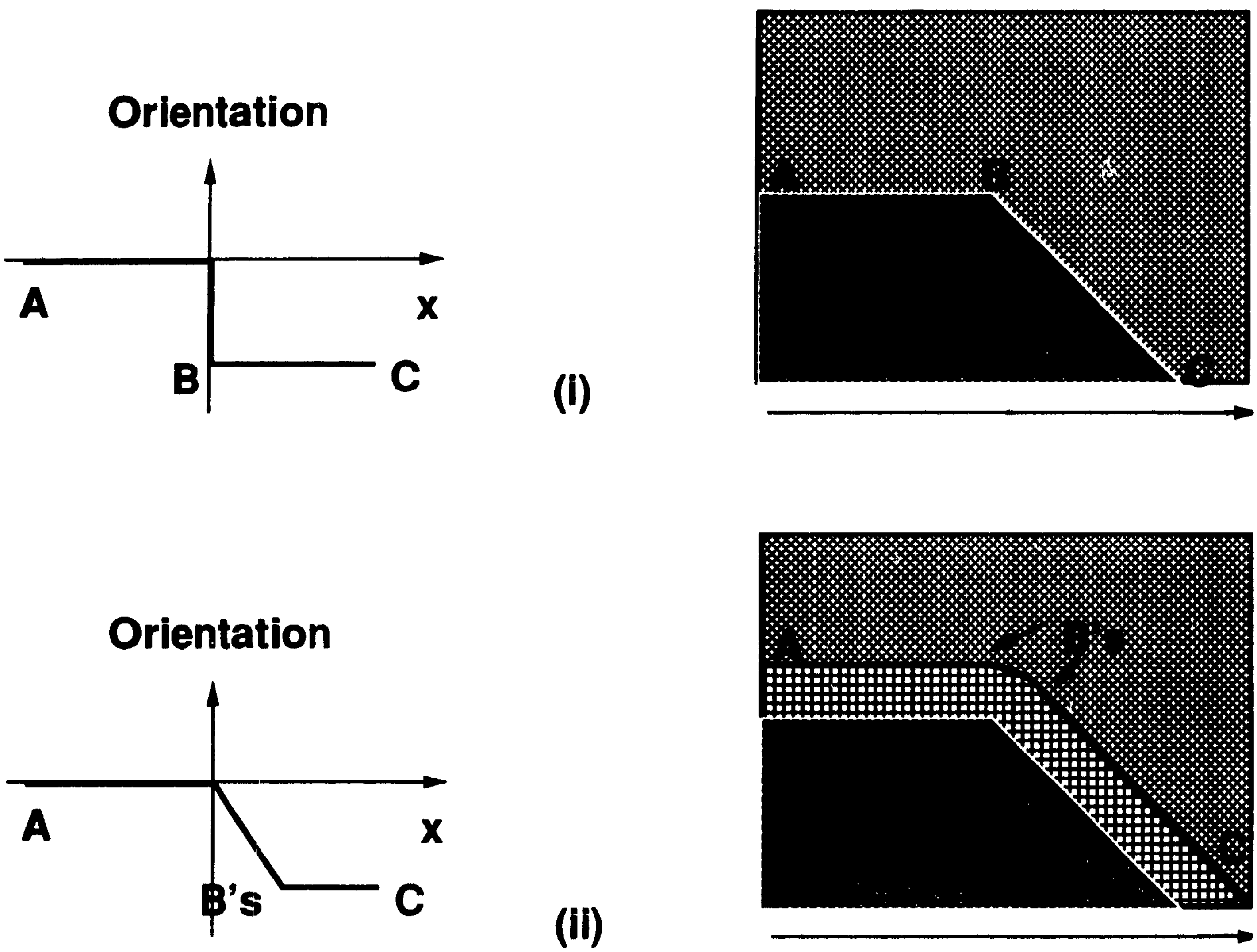

Figure 4.6: How should the shape in (i) deform in time? Again, while the normal is defined elsewhere, at B, it is not clear how to deform the shape. Axiom 4.2 rules out evolving each segment separately. In the conservation law domain this corresponds to a rarefaction wave, figure 4.2. The evolution of orientation is shown in figure (ii) where in the corresponding shape, point B evolves into a circular arc.

we have been able to extend deformations beyond the realm of classical differential geometry using simple shape axioms. However, we have argued that shape is multidimensional in nature: both local/global and boundary/region properties must be taken into account. To motivate, consider figure 4.7 where in the process of deforming the shape, two distant portions of the boundary touch each other. Following the deformation locally and based on the boundary would produce the dashed lines, violating axiom 4.1. Clearly, a richer representation embedding global and regional properties is required.

To motivate our approach, let us consider the field of fluid dynamics and the two formulations capturing flow of fluids, a problem not unlike ours. In the *Lagrangian Formulation*, equations of motion are based on the flow of particles, whereas the *Eulerian Formulation* constrains the physical quantities as a function of their position. One may view the first framework as local and boundary-based, and the latter as global and region-based. To accommodate the regional and global attributes, points distant along the boundary but close through the region may have to be connected. Consider, then, the shape as the level set of some function $z = \psi(x, y, t)$. Here ψ is an imaginary quantity reminiscent of some physical quantity e.g. density, which indicates where the region of interest, e.g. shape, is located The simplest scheme is to consider all points for which $\psi(x, y, t) \geq 0$ as belonging to the region. In shape representation, Koenderink has utilized the characteristic function of some region as an indicator of the shape [42, 44]. Similar representations have been proposed for the propagation of flame fronts [74, 7].

What are the equations governing the evolution of the surface $z = \psi(x, y, t)$? Note that the surface is initially only constrained by its zero level set. Similarly its evolution is only constrained by the evolution of the zero level set. As such, let us impose the same deformation on all level sets. The degree of freedom unconstrained in the initial level set may later be utilized to represent grey level (or other) information

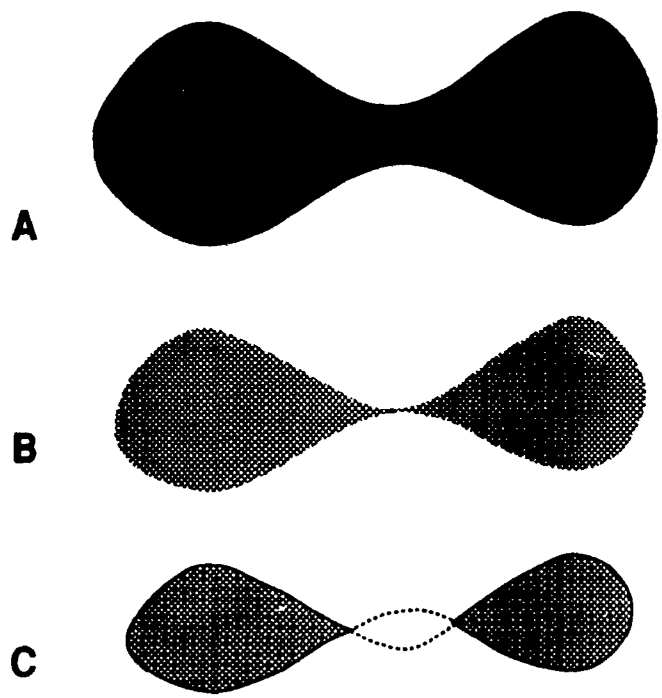

Figure 4.7: This figure depict the case when two points of a shape (A) that are distant along its boundary come together during an arbitrary deformation (B). How should the deformation proceed beyond this point? A pointwise deformation along the normal would produce the dashed-lines, which clearly violate axiom 4.1 since they do not correspond to an actual object.

A level set is defined by $\psi(x, y, t) = C$, which may be solved as $t = f(x, y)$ describing the level set curve implicitly. Now, let the level sets deform according to 2.2. Then,

$$\beta^2[f_x^2 + f_y^2] = 1, \tag{4.15}$$

where f_x, f_y are partial derivatives of f with respect to x and y, respectively and as shown in [63]. To relate this to the surface function ψ, observe from $\psi(x, y, t) = C$ that

$$\begin{cases} \psi_x + \psi_t f_x & = 0 \\ \psi_y + \psi_t f_y & = 0. \end{cases} \tag{4.16}$$

Solving for fx and fy using 4.15,

$$\beta^2[\psi_x^2 + \psi_y^2] = \psi_t^2 \tag{4.17}$$

Or,

$$\psi_t - \beta(\kappa)[\psi_x^2 + \psi_y^2]^{1/2} = 0 \tag{4.18}$$

Now, we are in a position to consider the case of figure 4.7. To restate, the question is how to continue the deformation beyond the point where two remote points of the boundary collide. The straightforward motion in the normal direction along each individual piece of the boundary would produce the dashed lines that violate Axiom 4.1. On the other hand, if one properly identifies the two points that have come together (at the moment the boundaries touch) as one, then it is not clear what the normal should be. The proper identification is formed by returning to the world of objects and visualizing the boundary as encapsulating the material of which objects are made. Then, when such a pinching of the shape takes place, the object should be segregated into two sub-objects, since the pinching has left the point of touch with no material to connect the two. This suggests

Axiom 4.3 *When in the process of deforming shape, two distinct points of the boundary of the evolved shape touch each other, the evolved shape segregates into two (sub)shapes which represent two separate objects.*

With the help of this axiom, the evolution of the region-based surface function ψ is now unambiguous. Since the surface function may correspond to many connected shapes, the transition from one shape to two is not inconceivable. The two points that come together will transform to the two cusp point that belong to separate shapes, figure 4.7

There is a connection between conservation laws and Hamilton-Jacobi theory that is relevant here. A first order Hamilton-Jacobi equation is of the form

$$J_t + \mathcal{H}(t, x, J_x) = 0, \tag{4.19}$$

where J is a function of x and t. Note that with constant motion equation 4.18 becomes first order Hamilton-Jacobi of the above type. Barles studied this equation and contrasted it with its other applications of geometric optics and optimal control [7]

There are several advantages for using a formulation of this kind. While boundary methods do not easily lend to a split or a merge in objects, a regional representation of this kind is suited for it. Furthermore, in cases where points bunch together (see figure 4.3), a segment of the curve with finite arc length eventually disappears into one point. While such a reparametrization is difficult in a boundary representation, it is easily handled by a region-based method. There are also issues of numerical stability extensively discussed in [74, 63] in favor of the latter scheme.

4.5 Shape Entropy

In the previous sections, several axioms defined the deformation of shape beyond the case were the boundary develops a singularity and where two remote points of the boundary come together. These axioms can be brought together by using an *entropy condition* for shape. The use of intuitive language helps, and we need the following terms. Think of the ***boundary*** of the shape as engulfing material ***points*** that define its interior:

Definition 4.1 Entropy Condition: *In the process of inward deformation, once a point is dislodged from a shape, it remains disjoint from it forever. Similarly, in the process of outward deformation, once a point becomes part of a shape, it remains part of it forever.*

The entropy condition relates to Huygens' principle of geometric optics for wave fronts moving outward. Huygens' principle states that the motion of the front along the normal is obtained by the envelope of circular waves issuing from the original wavefront [10]. The "grass fire" analogy for the construction of the medial axis transform is also intimately connected to the entropy condition. The analogy supposes simultaneously lighting fires along the boundary of a shape. Each point of fire would then spread uniformly by consuming grass (interior of the shape). When two fire fronts collide, the fire is subsequently extinguished at that point [12]. The quench points of fire are precisely the shock points, see chapter 9. The grassfire analogy is also presented in [74] in the context of flame propagation.

A more formal justification of the entropy condition is through its equivalence with the viscosity solution [21]. Consider

$$\psi_t - \beta(\kappa)[\psi_x^2 + \psi_y^2]^{1/2} = \epsilon \Delta \psi \tag{4.20}$$

which is the equation of motion 4.18 with added viscosity. Now as $\epsilon \to 0$ it is reasonable to demand that the solution to 4.18 (the entropy solution) and 4.20 (the so-called viscosity solution) be the same. Barles has shown that this is in fact the case [7].

Chapter 5

The Reaction-Diffusion Space

In the previous chapters, it was shown that orientation of arbitrarily deformed curves satisfies a conservation law. Since the goal of this thesis is to use arbitrary deformations as a link between shapes, our representation must capture these deformations even when and after singularities form. Entropy satisfying generalized solutions form *shocks* on which we shall concentrate in this chapter. Our goal is to show how shocks relate to shape. Specifically, *first-order* shocks signal *protrusions* or indentations, isolated *second-order* shocks correspond to *parts* and *third-order* shocks are related to *bends*. Moreover, a degree of *significance* is associated with shocks in a *reaction-diffusion space*. This is a two-dimensional space in which one axis spans the ratio of reaction to diffusion, and the other axis represents deformation time.

5.1 Shocks as Determinants of Shape

In this section we investigate the relationship between shape and shocks. In this regard, we are guided by the processes that create and modify shape. The basic assumption is that "similarity" between two shapes is directly related to the number and simplicity of processes involved in taking one into the other. In this way, one can create a range of simple to complex shapes by taking a simple shape, such as a circle, and deforming it in various ways in increasing magnitudes. For example, one might stretch and squeeze, dent and pull out, split and merge, bend and straighten the shape. We propose that three types of shape processes capture all others, forming a *basis* for shape; see chapter 8 for a more abstract view. More specifically, we now consider three processes: the ***protrusion*** process (***indentation***), a transformation that pushes and pulls parts of shape; the ***part*** process, a process that composes two objects or splits objects into components; and the ***bend*** process which bends or straightens objects. Our goal is to study the effect of these processes on the formation of shocks. We have found a direct correlation between shapes and shocks forming the basis of the ***reaction-diffusion*** space. We begin by considering each shape process in turn and its effect on shocks. Until section 5.6, we concentrate on ***constant motion***.

5.2 First-Order Shocks

Consider the shape in figure 5.1 which is formed by pushing a portion of a circle outwards. It would not be uncommon to describe this shape as a "circle with a protrusion". While other descriptions, e.g. a half circle glued on a half deformed rectangle, are possible, nevertheless our perception is clear (unless we have been primed to another category previously). Now, let us consider the effect of a ***constant motion*** type of deformation on this shape. Recall that in figures 4.5 and 4.3, the ***constant motion*** produces a single isolated orientation discontinuity from a negative curvature minimum. Adhering closely to the terminology of classical conservation laws, then, let us preserve the term shock and define

Definition 5.1 A First-Order Shock ***is a discontinuity in orientation of the boundary of a shape.***

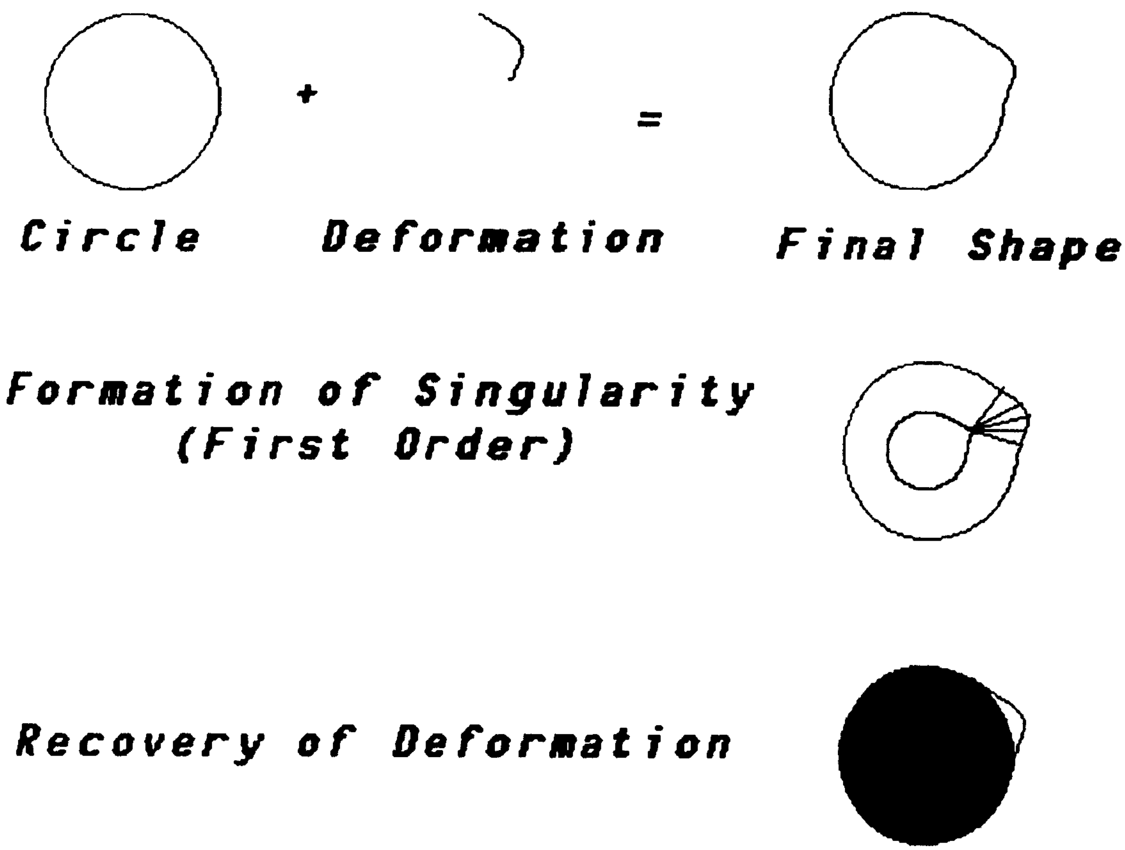

Figure 5.1: The shape on the right is perceived as a circle with a deformation. While a number of other interpretations are possible, this interpretation seems to be favored naturally. How can this deformation be recovered?

Lemma 2.1 shows that this is always true: Every negative curvature minimum will produce a single isolated first-order shock in time, provided there is no interaction from nonlocal portions of the boundary(see the following sections). Figure 5.1 illustrates the process by which the information flows into a propagating first-order shock. The remaining information is the approximated shape, in this case a circle. On the other hand, the lost information is the deformation.

To illustrate this situation in detail, consider the formation of a shock in an ellipse, figure 5.2, represented as,

$$\begin{cases} x(\theta) & = a\cos(\theta) \\ y(\theta) & = b\sin(\theta), \end{cases} \tag{5.1}$$

where $2a, 2b$ are the major and minor axes. Without loss of generality assume $a > b$ Then,

$$\begin{cases} \vec{T}(\theta) & = (-a\sin(\theta), b\cos(\theta)) \\ \vec{N}(\theta) & = (b\cos(\theta), a\sin(\theta)), \end{cases} \tag{5.2}$$

following the convention that the normal points outwards. Curvature is

$$\kappa(\theta) = \frac{-ab}{[a^2\sin^2(\theta) + b^2\cos^2(\theta)]^{3/2}} \tag{5.3}$$

It can be seen from Lemma 2.1 that the time to shock formation is

$$t_{\text{shock}} = \frac{-1}{\kappa(0)} = \frac{b^2}{a} \tag{5.4}$$

All points follow their normals so that the point $B(\theta)$ moves into the x-axis at point C:

$$C(a - \frac{b^2}{a}\cos(\theta), 0)$$

where it annihilates into the shock. The elapsed time for B to move into C is

$$b\sqrt{1 - (1 - \frac{b^2}{a^2})\cos^2(\theta)}$$

Suppose now $a = 2$ and $b = 1$ as is the case in figure 5.2 Then, the shock first forms at $C(1.5, 0)$ after 0.5 units of time. Afterwards, the shock propagates, annihilating increasingly larger portions of the boundary, until after 2.0 units of time the whole shape is consumed. Notice that the locus of shocks, the thick line in the figure, is the Symmetric Axis [11]. It is interesting that the locus of of first-order shocks for piecewise circular boundaries is a piecewise conic section.

Finally, the shape can be deformed both inwards and outwards, corresponding to the sign of β_0. Therefore, both indentations and protrusions can be recovered since both curvature minima and maxima give rise to shocks. To summarize then:

Result 5.1 *In absence of global interaction, every indentation or protrusion (henceforth referred to as protrusion) produces an isolated single first-order shock.*

5.3 Second-Order Shocks

A second kind of shock forms, not due to curvature build-up as in the first type of shock, but due to a collision of boundaries. Consider the shape in figure 5.3. As the shape (A) evolves in time due to a *constant motion* deformation, portions of the boundary collide and give rise to two cusps (B). These cusps are discontinuities, not in tangent, but in curvature. We call these *second-order shocks.* Note the change of connectivity at this instant. Beyond this instant, portions of the boundaries cross each other (the dashed lines). The role of entropy in this case is to remove portions of the boundary that have reached a previously visited point (C). Formally,

Definition 5.2 *When in the process of deformation two distinct non-neighboring boundary points join and not all the other neighboring boundary points have collapsed together, a* Second-Order Shock *is formed.*

In the case of figure 5.3, at the point of shock formation the top and bottom boundaries seem to be tangent.

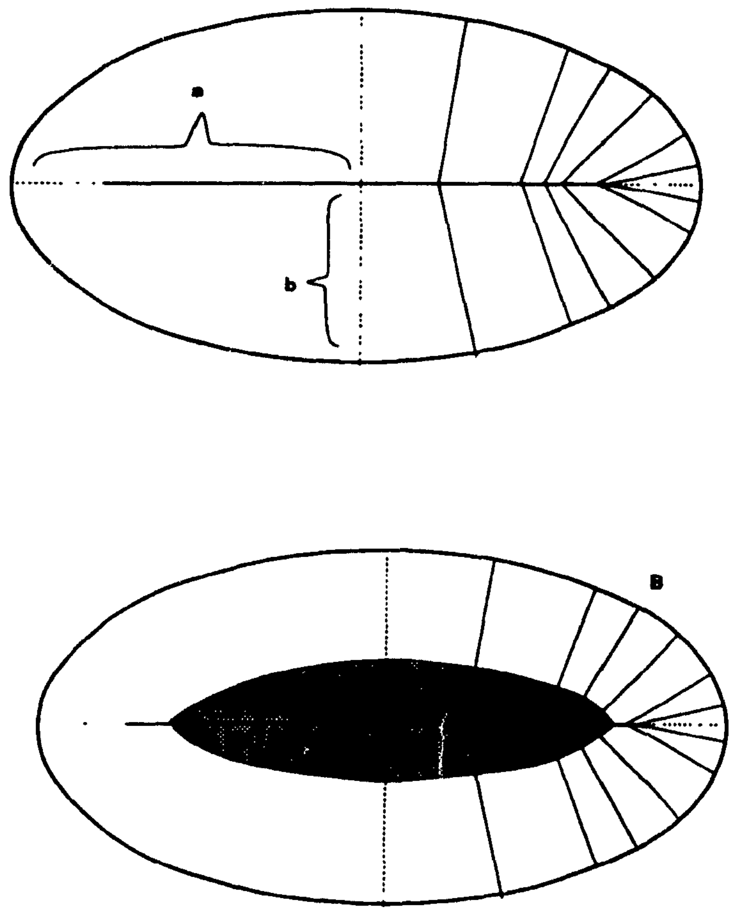

Figure 5.2: The ellipse deforms to form a shock after b^2/a units of time, where a, b are the major and minor axes, respectively. While before this time, the ellipse can be reconstructed completely (each point maps to a point), after this time an arc of the ellipse maps into one point (shock). As a consequence, the process is no longer reversible. A reconstruction yields an arc of a circle. This basis of shape approximation is utilized in chapter 7.

A

B

C

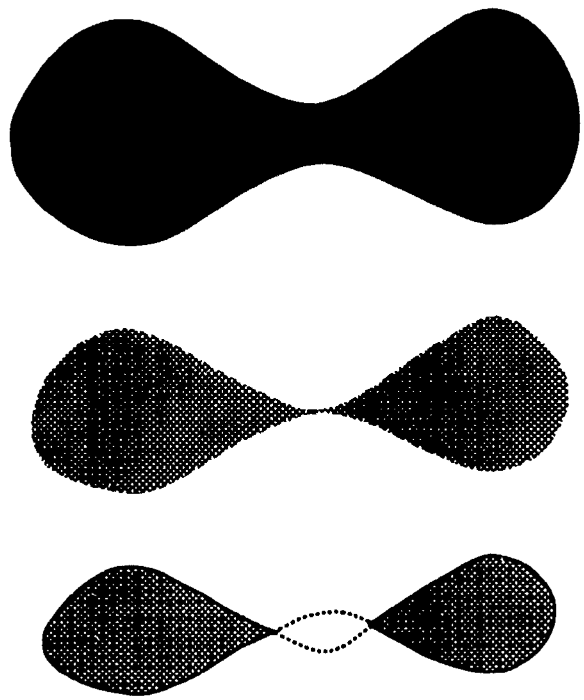

Figure 5.3: This figure illustrate the formation of the second-order shocks. In the process of deformation, distant portions of the boundary of the shape (A) approach each other and finally touch (B). The result is that the shape splits into two *parts* as illustrated in (C). Note that two shocks have formed as a result of two points coming together. The shocks are discontinuities in the curvature of the boundary, in contrast to the tangent discontinuity of the first order shock.

Theorem 5.1 *When two distinct non-neighboring points of the boundary first come together, if boundary tangents exist at the collision point, then the tangents must be parallel*

Proof The proof is by showing that the contrary assertion contradicts the entropy condition Suppose the contrary, namely, that the tangents have different orientations θ_1 and θ_2 at point A, the first collision point at time t_0, figure 5.1 Let us represent the portions of the boundary represented by tangents θ_1 and θ_2 by B_1 and B_2, respectively. Then, since θ_2 is not tangent to B_1, it crosses the shape around B_1, S_1, on both sides. By continuity of tangents, it is not difficult to see that there exists B on B_2 such that a ball of radius ϵ around B, $\mathcal{B}_B(\epsilon)$, is entirely within the shape portion of B_1 for some $\epsilon > 0$ This clearly violates the entropy condition since B could not have belonged both to the boundary B_2 and have been part of the region S_1. Hence, the tangents are parallel. ∎

Is it necessary to assume the existence of tangents at the point of collision? Could the boundary somehow evolve if a discontinuity forms exactly at the same time as colliding with a distant portion of the boundary? The following theorem shows this can not happen

Theorem 5.2 *When two distinct non-neighboring points of the boundary come together, the tangents must be parallel.*

Proof. Consider the shape some Δt units of time earlier. The boundary of this shape has only one point in common (tangent if smooth) A and B, with the ball of radius $\Delta t|\beta_0|$ around P, the point of collision P, $\mathcal{B}_P(\Delta t|\beta_0|)$, by assumption Note that AP is perpendicular to the present boundary at that point, and similarly for BP. Now, balls $\mathcal{B}_A(\Delta t|\beta_0|)$, $\mathcal{B}_B(\Delta t|\beta_0|)$ both include P. In fact, P must be the only point they have in common. Therefore, since the balls are both entirely within the shape (Huygens' principle), they must be tangent to the present boundary This

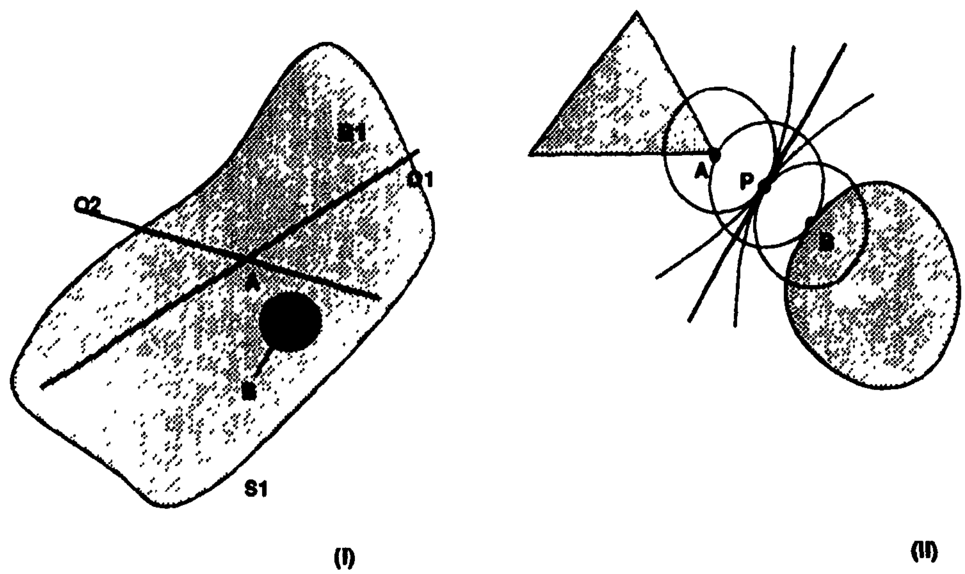

Figure 5.1. The tangents at a second-order shock are parallel. (i) The crossing of tangents is non-intuitive and can not happen as theorem 5.1 shows. (ii) The tangents of the boundary must be parallel even if there closely follow a shock (A), theorem 5.2.

implies that AP and BP are co-linear. Therefore, AB which is orthogonal to the shape boundaries δt units of time earlier, is also orthogonal to the shape boundary now. ∎

It is likely however that two shock points join to form another shock, e.g. a rectangle. The following lemma follows from the previous theorem:

Lemma 5.1 *When three distinct non-neighboring points of a shape collide, immediately past the collision, there is some neighborhood around the point of collision that will contain no point of the shape, in some time neighborhood past collision.*

In other words, three points can not come together, unless part of the shape will annihilate itself entirely, e.g. a circle collapsing to a point.

While theorem 5.2 asserts that tangents at a second-order shock are parallel, curvature (or at times some higher order derivative) need not be equal on both sides

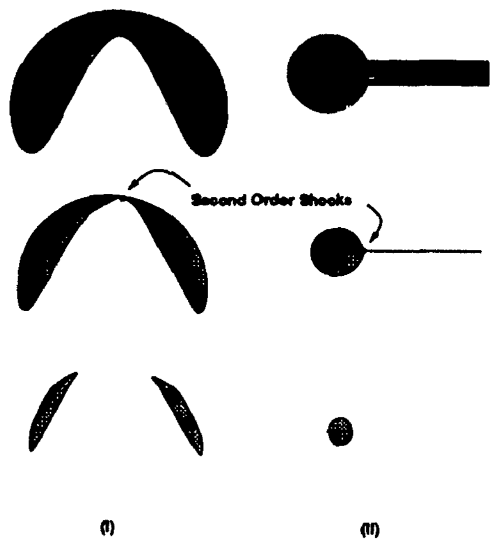

Figure 5.5: Other examples of second-order shocks. (i) the shock forms at the narrowest region of the shape and leads to a change in the connectivity of the shape. (ii) The second order shock form from points where the bar and circle come together, but do not lead to a change of connectivity. This is a case where there is a simultaneous annihilation of the new region with the change in connectivity. Note that other points of the bar are not second-order shocks, but third order ones as we shall see in the next section.

(by definition). Hence, a second-order shock is a discontinuity in curvature, in contrast to the first-order shock which is a discontinuity in the tangent of the boundary of the shape.

Other examples of second-order shocks are displayed in figure 5.5, where the curvature at the second-order shock is different from the previous example. Note that both in the example of figure 5.3 and (i) there is a topological change in the connectivity of the figure. Case (ii) is a degenerate case, in that topological change in connectivity is simultaneously accompanied with an annihilation of the new region. We shall demonstrate that these ideas are essential in a definition of "neck" and its effect on "parts" in chapter 8.

5.4 Third-Order Shocks

A third type of shock point is generated when distinct boundary points are brought together as in second-order shocks, but unlike the second-order shock, the neighboring boundary points on each side have also joined with other distant boundary points. Formally,

Definition 5.3 *When in the process of deformation two distinct non-neighboring boundary points join, so that neighboring boundaries of each point also collapse together, a* Third-Order Shock *is formed*

As defined above, third-order shocks can not possibly change the topological connectivity of the shape. Rather, they indicate a symmetric axis, as in the case of an ellipse. However, this axis is not composed of first-order shocks where portions of the boundary collapse into a single point. Rather, this axis is the result of a region collapsing into points, figure 5.6 Therefore, the locus of these points indicates a *bending* of the region, rather than a protrusion of the boundary.

5.5 Fourth-Order Shocks

In the process of inward evolution of shape, regions shrink and form shocks In time, remining regions finally shrink to a point and disappear due to the entropy condition All parts of a shape must eventually annihilate to a point, since the shape may be entirely embedded inside some circle of radius R which will, in $1/R$ units of time disappear. These are the fourth-order shocks and are the *seeds* for shape

Definition 5.4 *When in the process of deformation a closed boundary collapses to a single point, a* Fourth-Order Shock *is formed*

Figure 5.7 depicts the process of deformation for a "dumbbell".

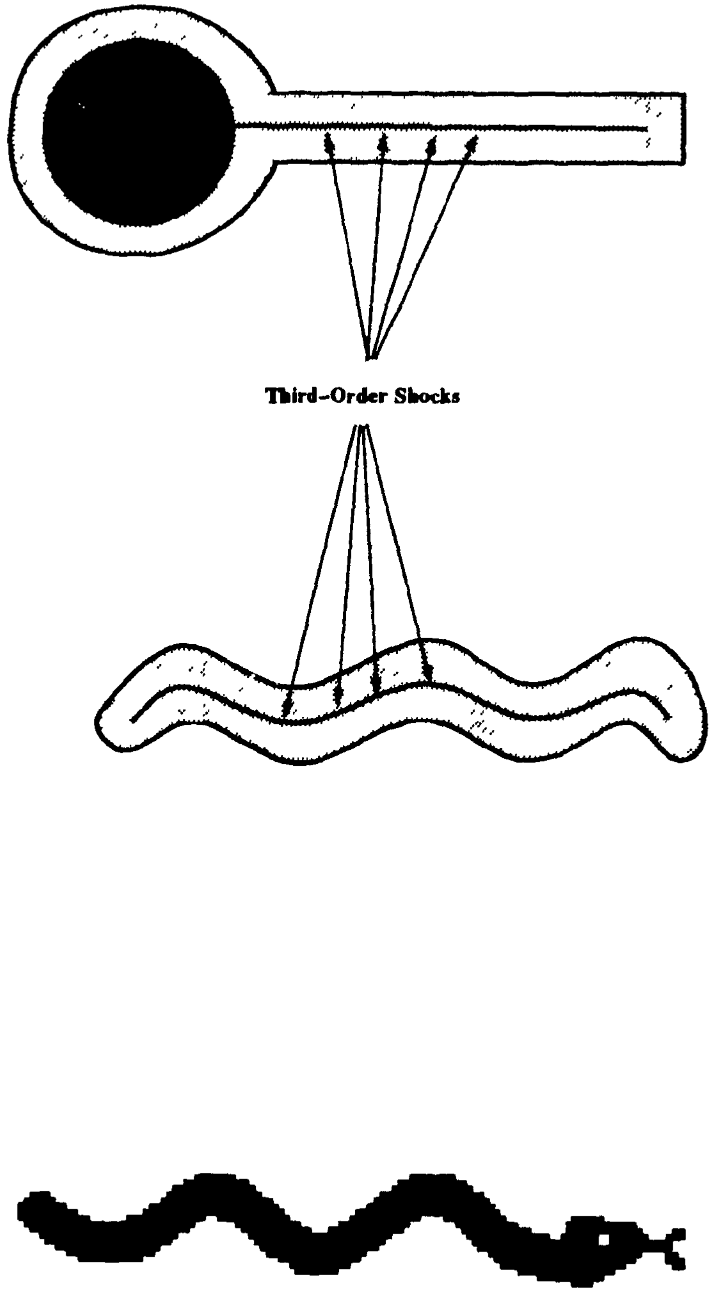

Figure 5.6 The snake shape forms third-order shocks when distant points of the boundary come together not in isolation, but rather in conjunction with neighbors. Third-order shocks indicate the "bending" of an object. The interpretation of the

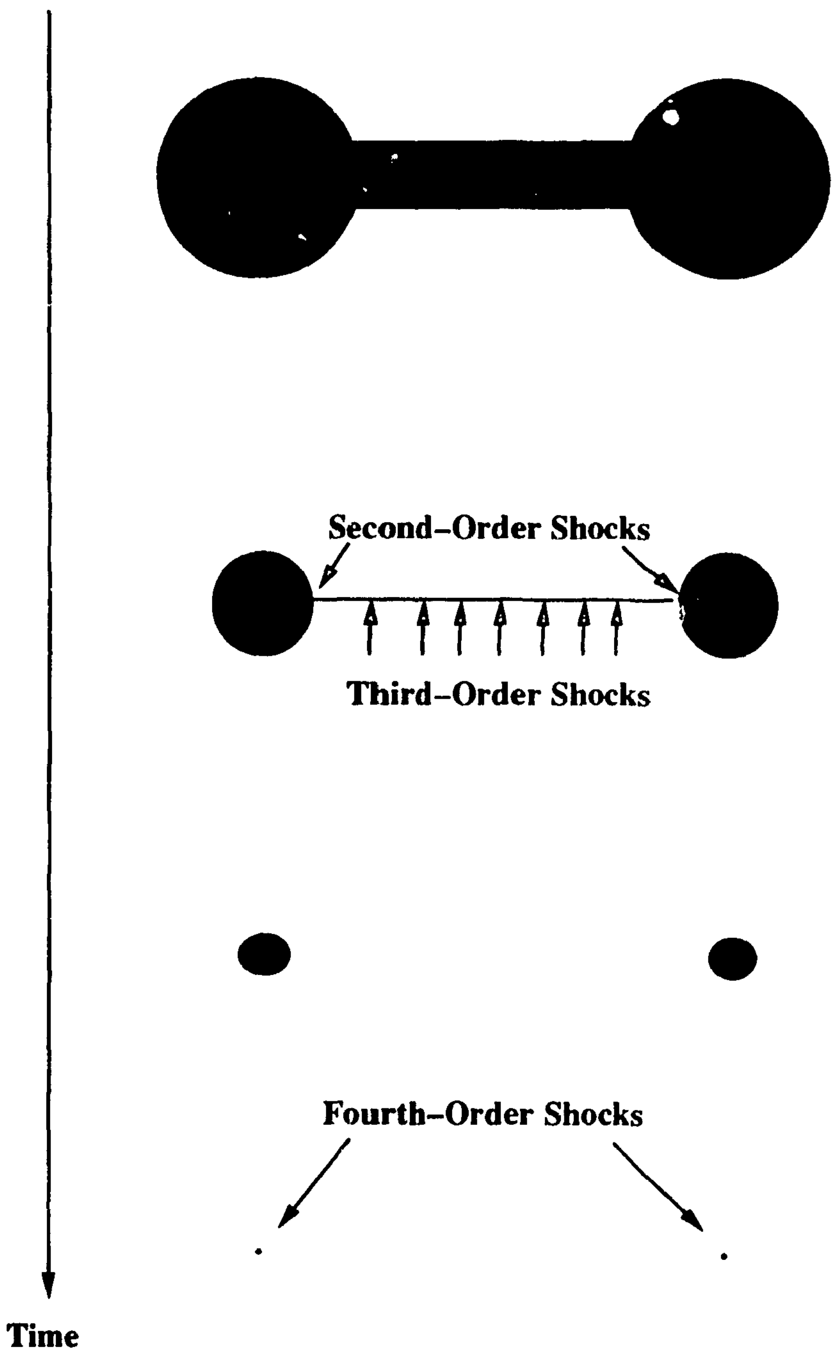

Figure 5.7: In the deformation of a dumbbell, the bar collapses to a single line segment. While, the two end points are second-order shocks, the rest of the line segment consists of third-order shocks. The single circles then collapse to a point each, the forth order shocks.

5.6 Physical Analogy

A number of physical applications are modelled by reaction-diffusion equations, e.g. crystal growth [16], flame propagation [76, 75], predator-prey population dynamics [78], the oil-water boundary problem, and the deterioration of the shapes of stones [25]. Typically, in these models, a reactive term is in conflict with a diffusive term. To illustrate consider the case of crystal growth where the growth pattern of a solidification front is determined by the interaction of two forces, the driving force of the instability due to heat diffusion and the restabilizing force due to surface tension [77]. Common to these models is a reactive force which corresponds to our constant motion and a diffusive force depending on surface curvature which corresponds to our curvature motion.

From a different perspective, Courant and Friedrichs classify events in nature to two classes: the *linear* group of phenomena, e.g. sound, light, and electromagnetic events and the *non-linear* group, e.g. detonation of explosives, supersonic flights, and impact of solids [19]. While the linear group is smoothness preserving, the nonlinear group can lead to singularities. Returning to reaction-diffusion equations, diffusion belongs to the linear group while reaction is a nonlinear phenomenon.

It is not surprising that for shape, as well, the forces of reaction and diffusion capture complementary aspects of shape, figure 1.8. In the next section, then, we study the effect of adding curvature motion, or diffusion, to the deformations.

5.7 Arbitrary Deformations

We have seen how various shape features give rise to shocks under the constant motion deformation. We now consider general deformations of shape, namely when curvature motion deformation (diffusion) is combined with constant motion deformation (reaction). Figure 5.8 illustrates a role for diffusion. Since reaction is region-based, it

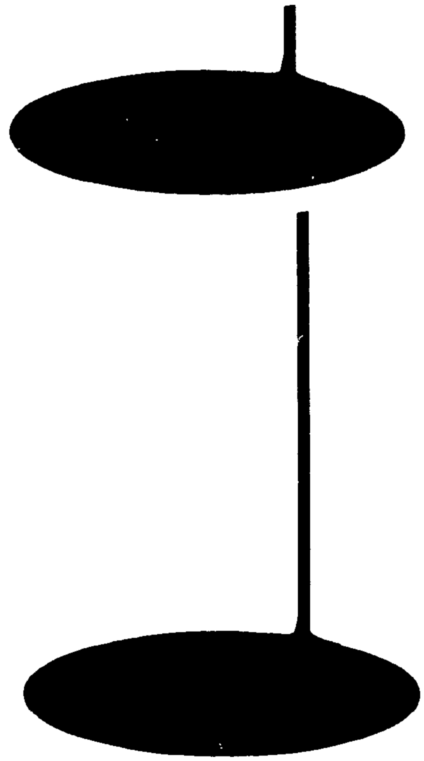

Figure 5.8: Long sticks or short ones?

takes into account the "area" features, rather than the 'length" aspects of the feature. Adding diffusion to the deformation captures the length properties of the features.

Another role for diffusion is the increased connectivity between shapes. Consider figure 5.9 where the top and bottom shapes are differentiated by the reaction process. Diffusion, however, makes the two shape appear "close" in the reaction-diffusion space.

5.8 The Reaction-Diffusion Space

We are in a position now to define the reaction-diffusion space. Recall that in order to associate nearby shapes to each other, we have used deformations which in turn can be captured by a linear combination of *constant motion* and *curvature motion*

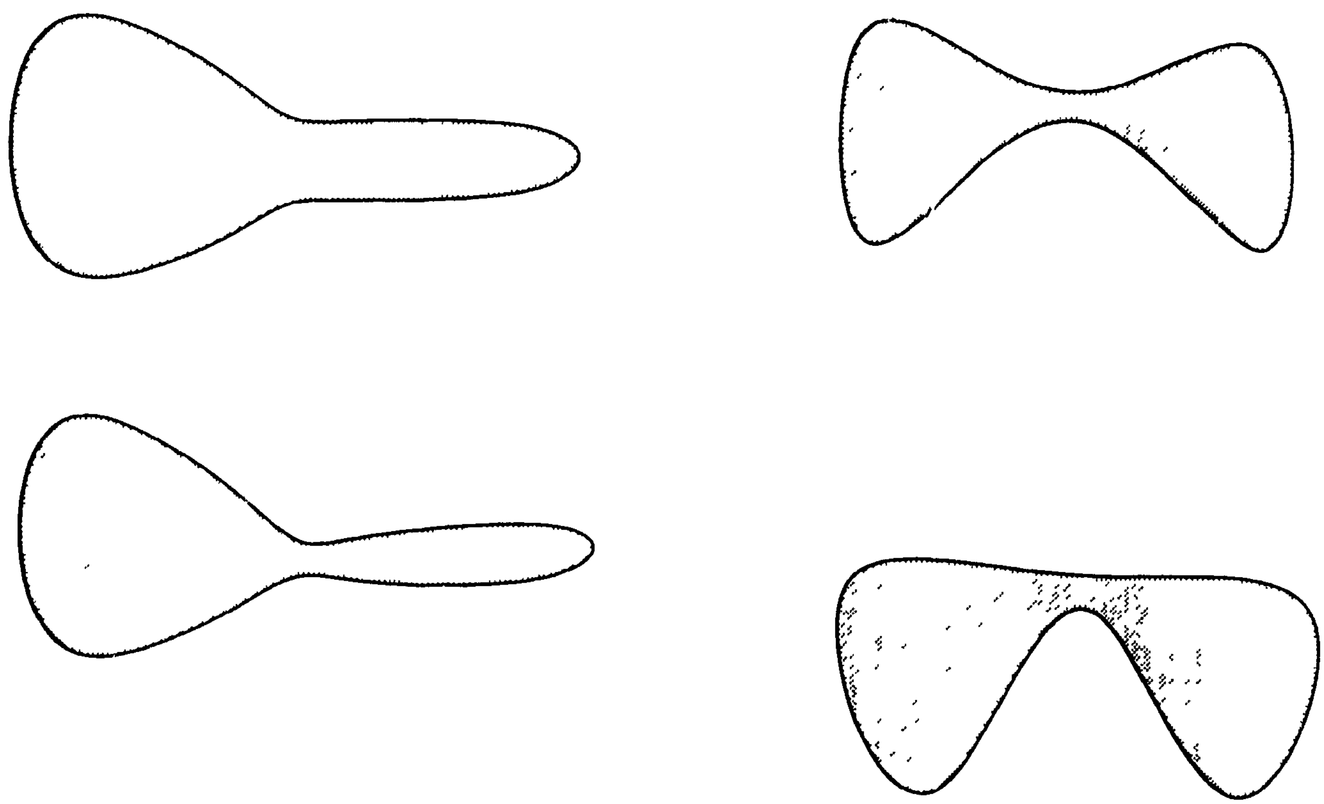

Figure 5.9 Diffusion brings more and a different sort of connectivity to shapes.

deformations. We view these two deformations to have drastically different and complementary properties. Viewed in the reaction-diffusion model of physical systems, these are two forces competing to describe shape. Note that in the viscous conservation law 3.18 two parameters β_0, β_1 that embed the extent of constant motion and curvature motion of the general deformation equation 1.5. It appears then that we should attempt to represent shape by deforming it for all possible combinations (β_0, β_1) and all time. However, note that a scaling of (β_0, β_1) can be reflected in a scaling of time t. Hence, the only relevant parameters are t and the ratio β_0/β_1.

Definition 5.5 *The representation of shape in all possible time and all possible ratios β_0/β_1 is called the* Reaction-Diffusion Space.

Note that while β_1 can not be negative for stability reasons [1], β_0 can be negative or positive corresponding to inward and outward motion. Time can only be positive unless there is no diffusion $\beta_1 = 0$. Since diffusion is always present in the least in some minute form, and since for pure reaction ($\beta_1 = 0$) negative time corresponds to inverting the sign of β_0, negative time need not be represented. As such the reaction-diffusion space may be represented by the x-axis as representing all combinations of (β_0, β_1) and the positive y-axis representing time and where each point in this space represents a shape. Points on the x-axis correspond to the original shape, and any other point $(\beta_0/\beta_1, t)$ is the original shape deformed by equation 3.18 with parameters (β_0, β_1) for duration $\beta_1 t$ units of time.

5.9 Examples

In the following pages, samples of the reaction-diffusion space is displayed for several images. Note that both axes are samples in a nonlinear logarithmic fashion. Also for the moment we have concentrated only on inward motion.

[1]Running the heat equation backwards is ill-conditioned [38].

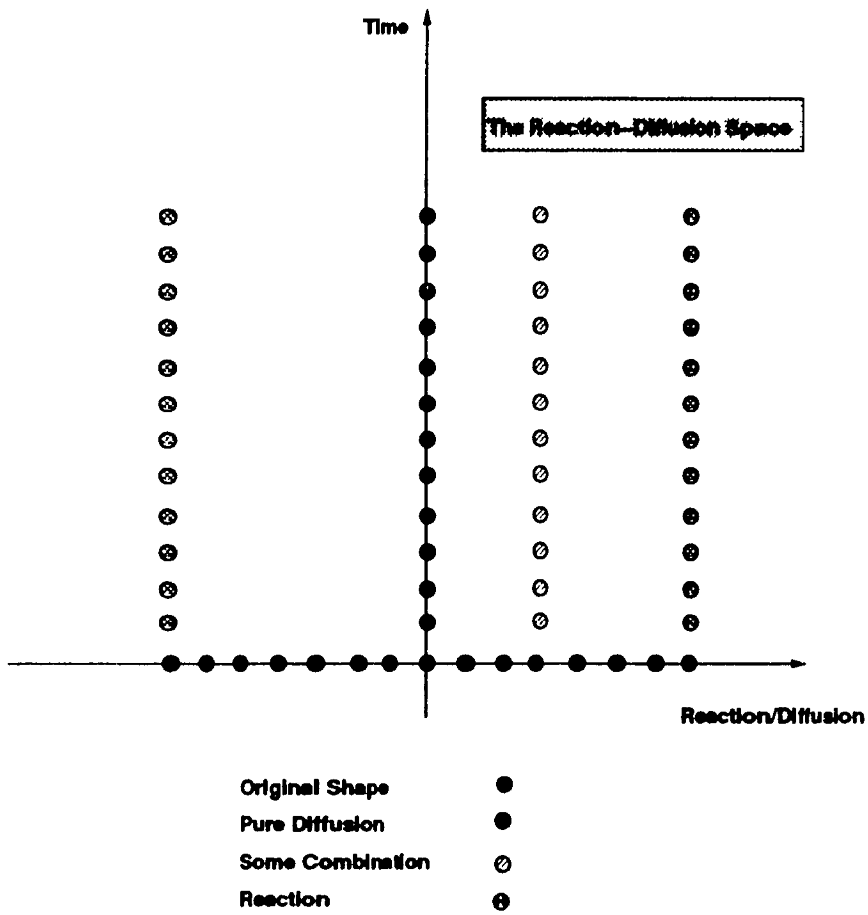

Figure 5.10: The Reaction-Diffusion Space is the representation of all possible deformations of shape. The x-axis represents the relative proportion of reaction to diffusion and the y axis is time. Bote that the absolute magnitude of reaction and diffusion is absorbed in time t.

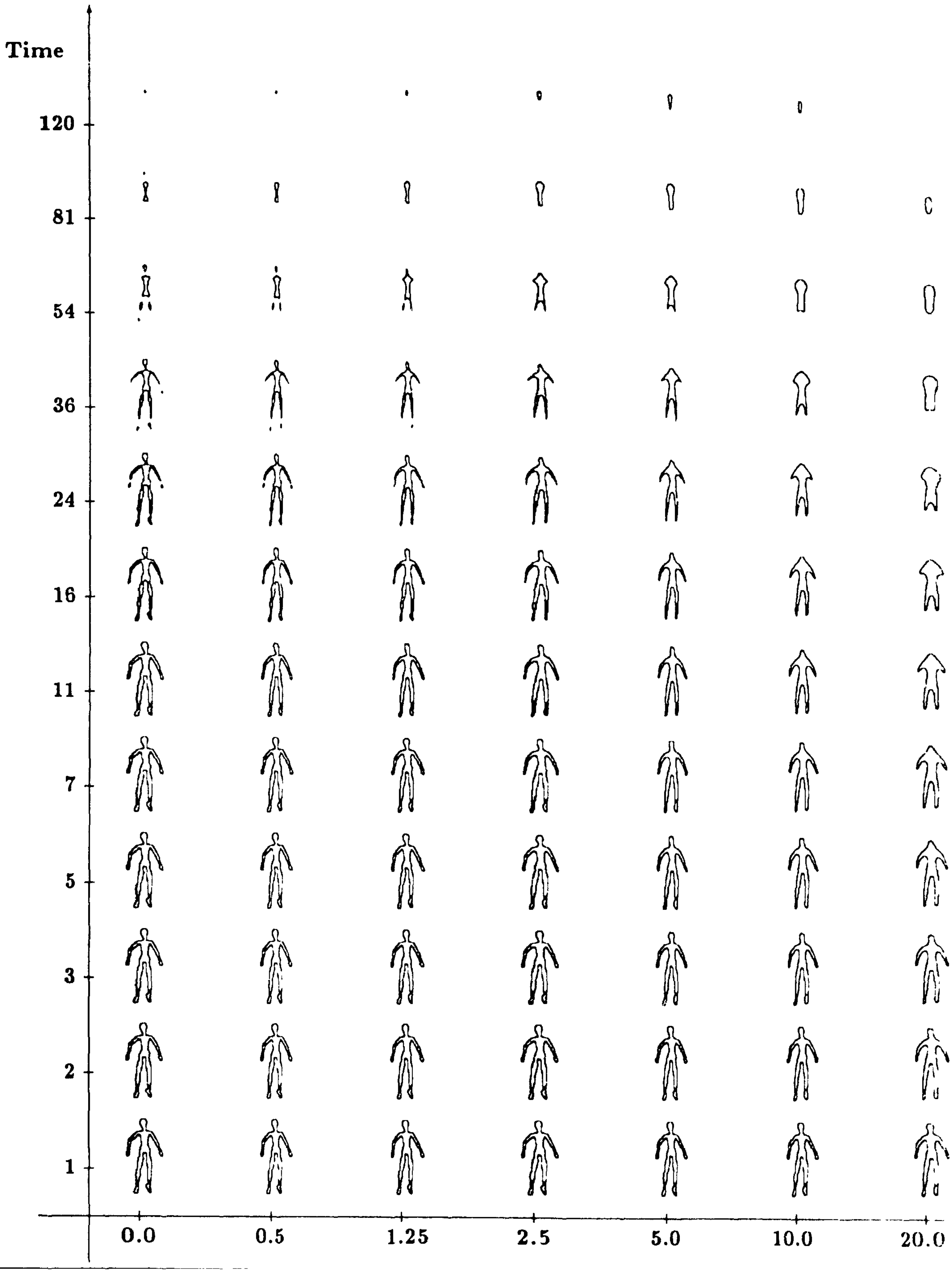
Time
120
81
54
36
24
16
11
7
5
3
2
1
0.0
0.5
1.25
2.5
5.0
10.0
20.0

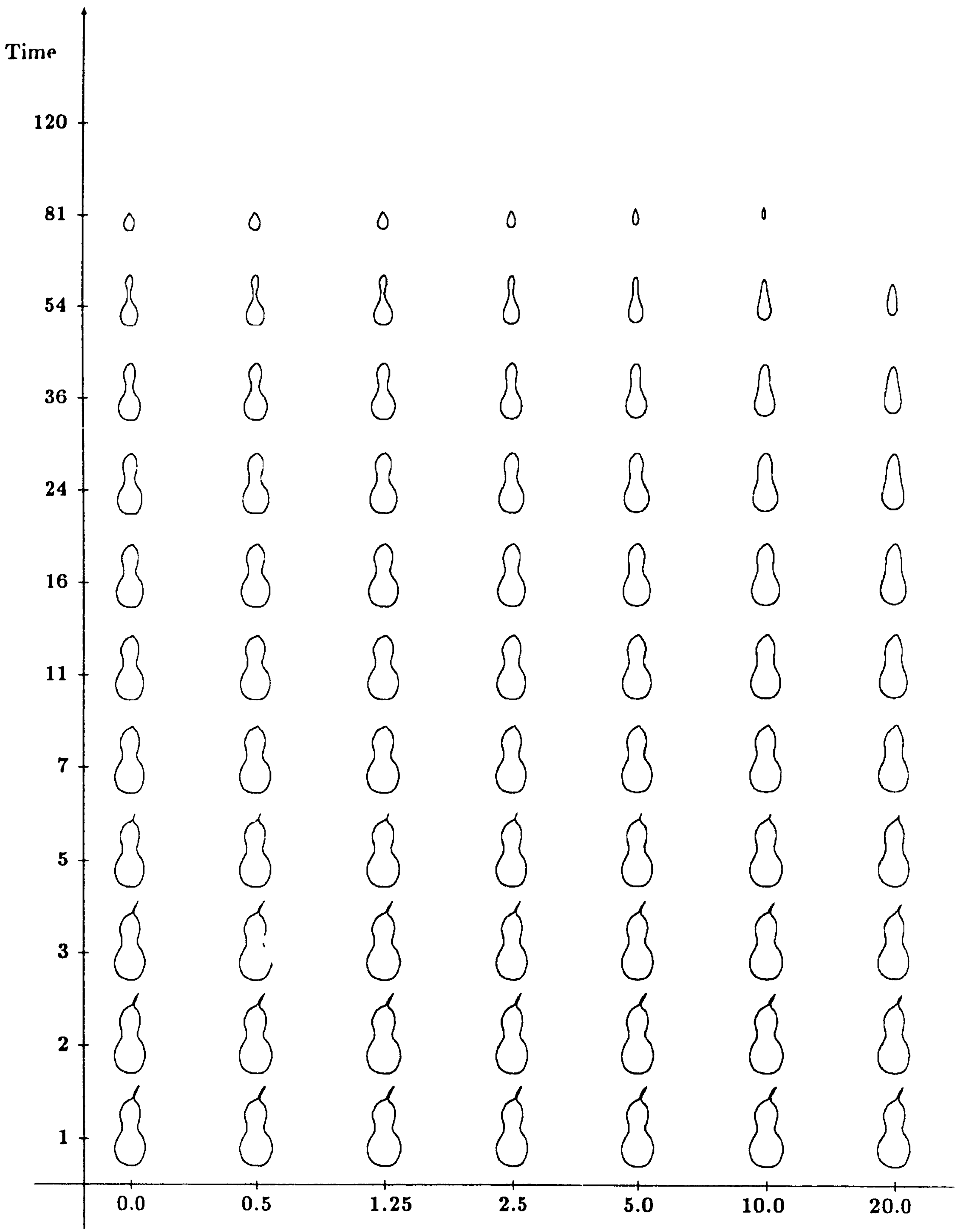
Time
120
81
54
36
24
16
11
7
5
3
2
1
0.0
0.5
1.25
2.5
5.0
10.0
20.0

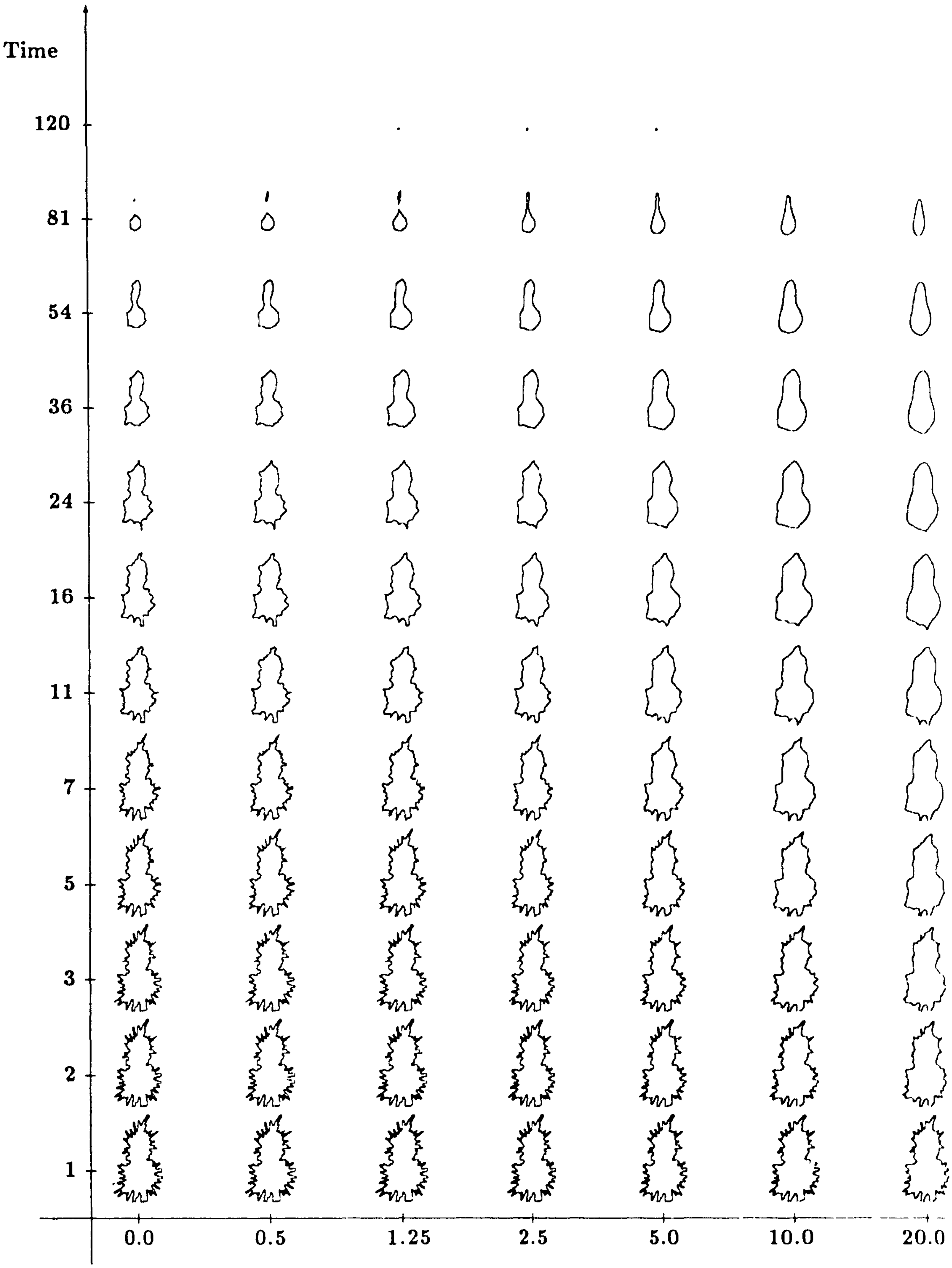
Time
120
81
54
36
24
16
11
7
5
3
2
1
0.0
0.5
1.25
2.5
5.0
10.0
20.0

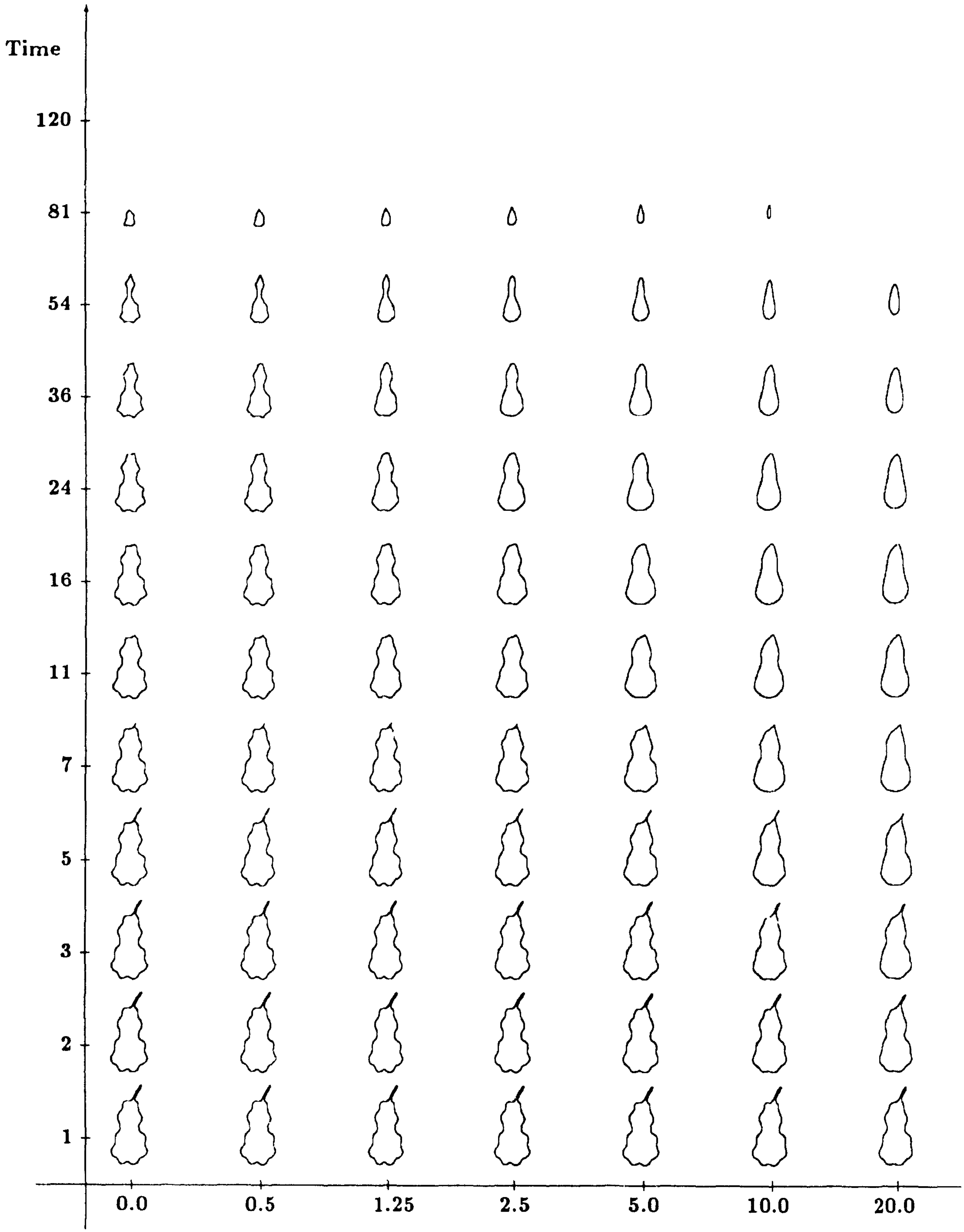

Time
120
81
54
36
24
16
11
7
5
3
2
1
0.0
0.5
1.25
2.5
5.0
10.0
20.0

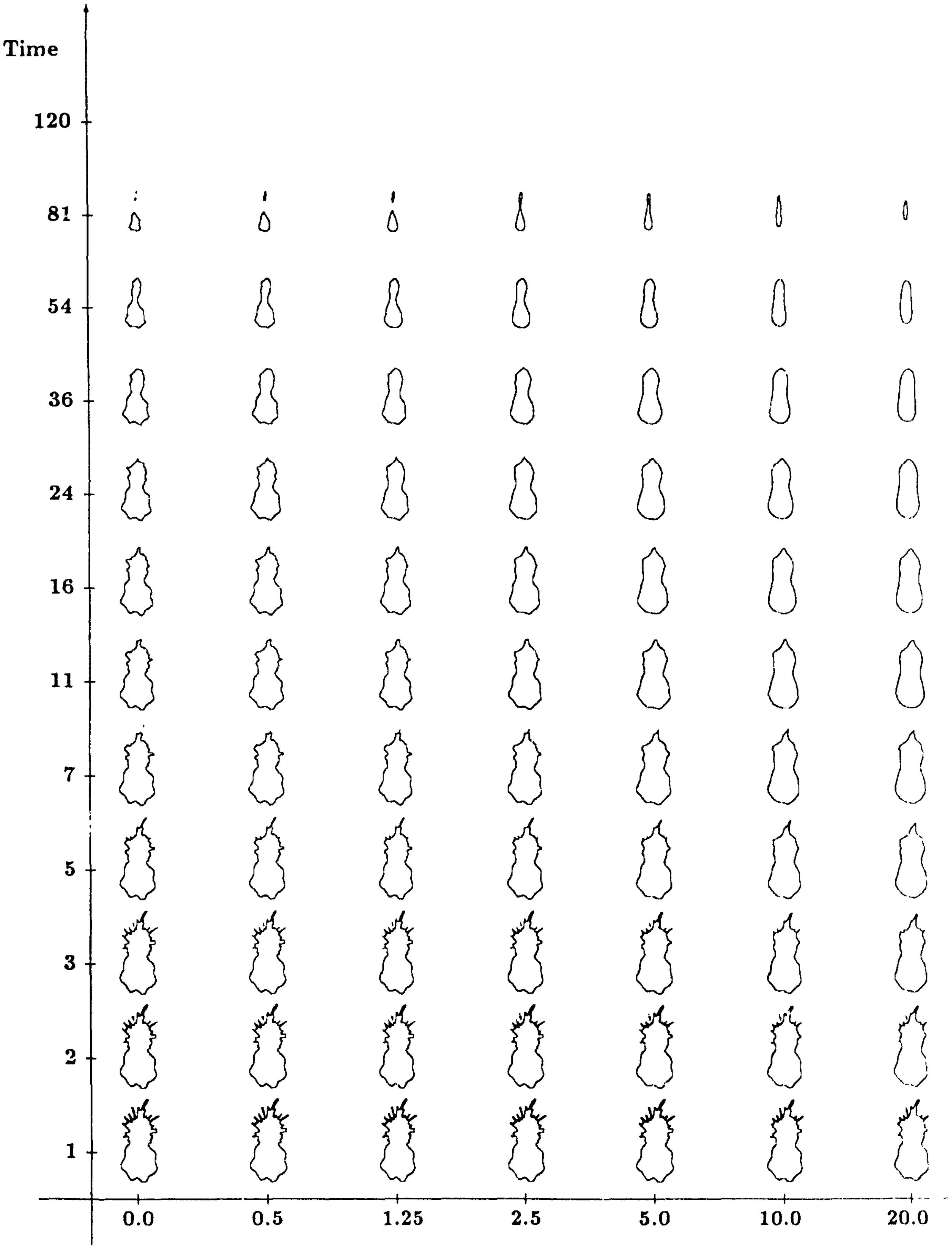

Time
120
81
54
36
24
16
11
7
5
3
2
1
0.0
0.5
1.25
2.5
5.0
10.0
20.0

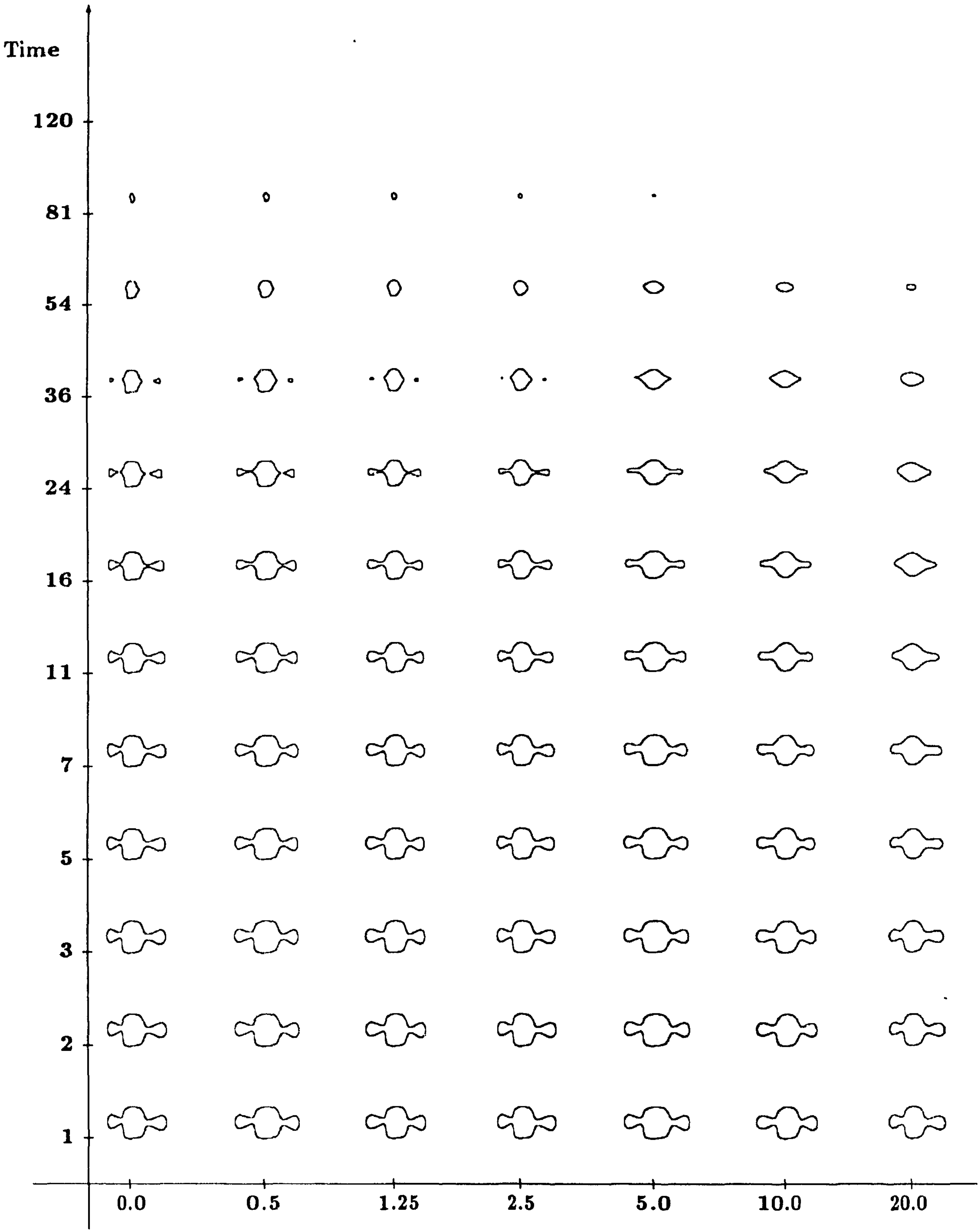
Time
120
81
54
36
24
16
11
7
5
3
2
1
0.0
0.5
1.25
2.5
5.0
10.0
20.0

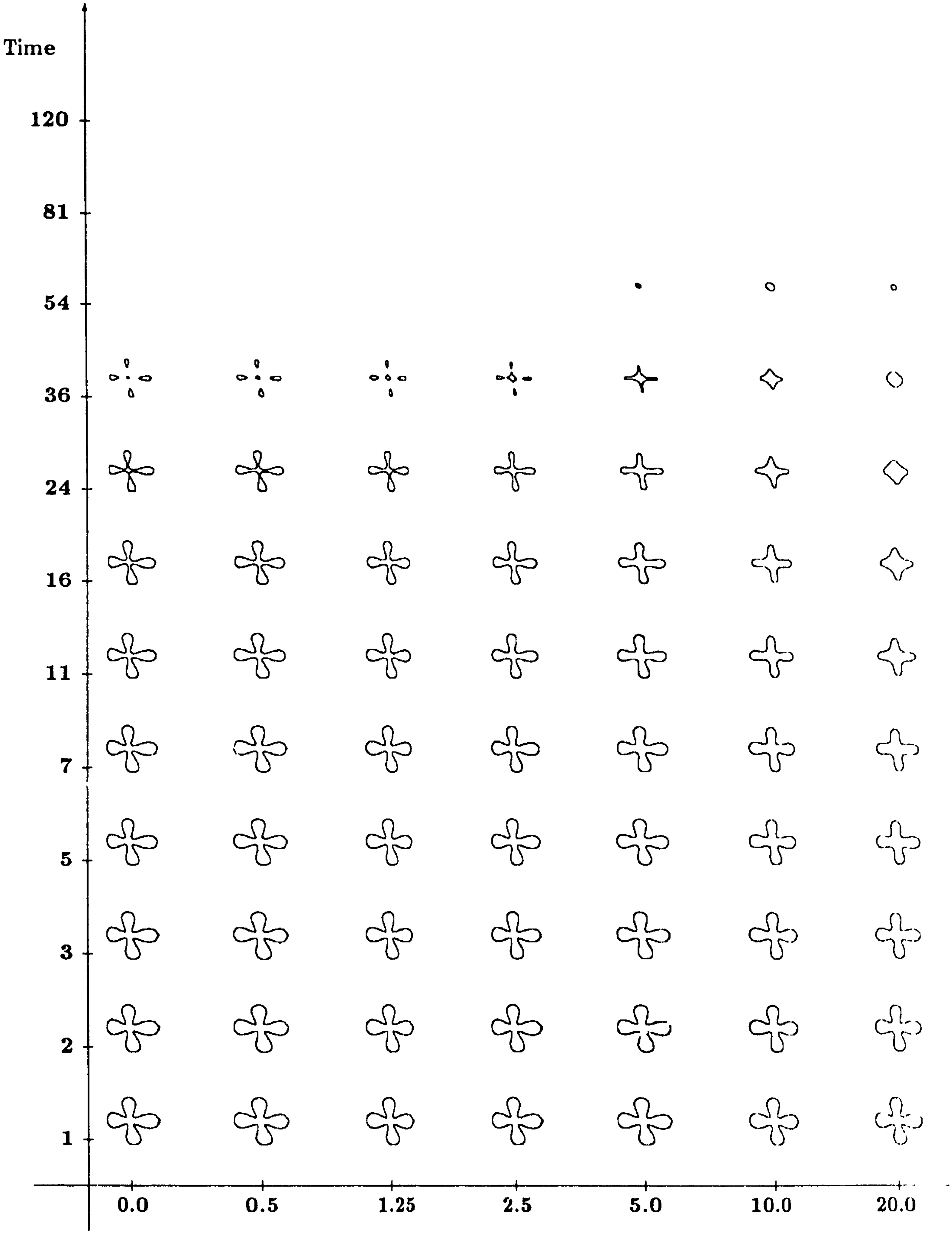
Time
120
81
54
36
24
16
11
7
5
3
2
1
0.0
0.5
1.25
2.5
5.0
10.0
20.0

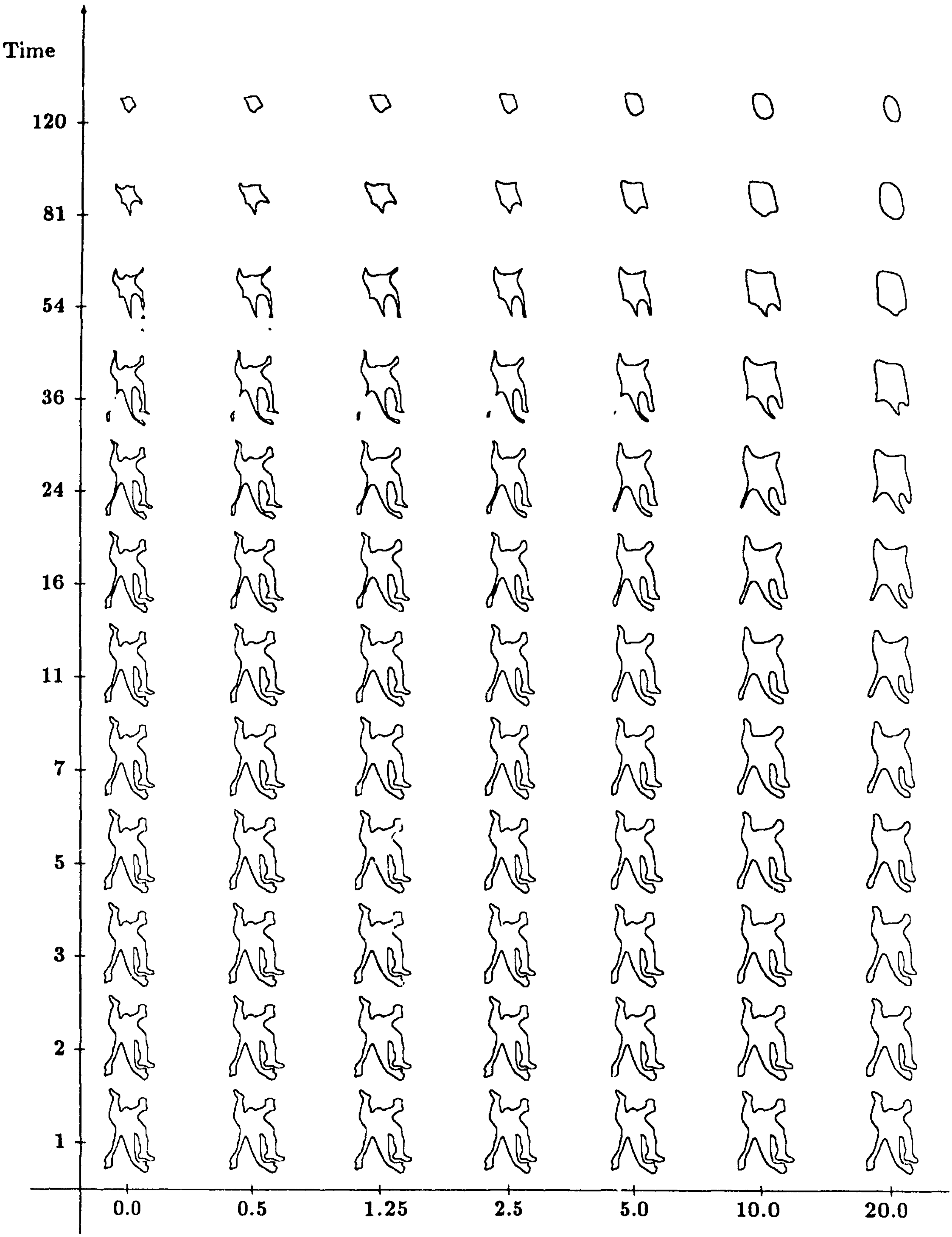
Time
120
81
54
36
24
16
11
7
5
3
2
1
0.0
0.5
1.25
2.5
5.0
10.0
20.0

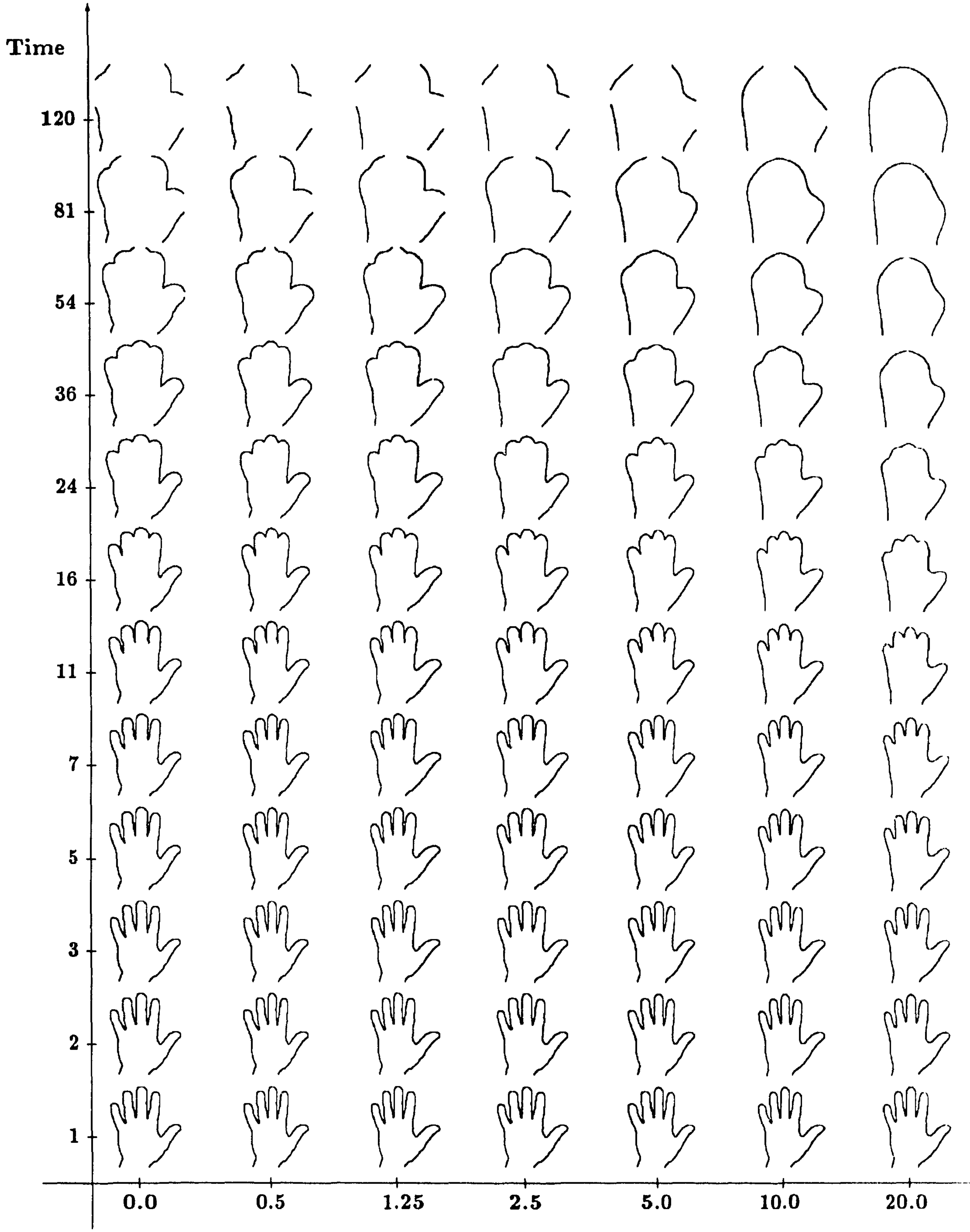

Time
120
81
54
36
24
16
11
7
5
3
2
1
0.0
0.5
1.25
2.5
5.0
10.0
20.0

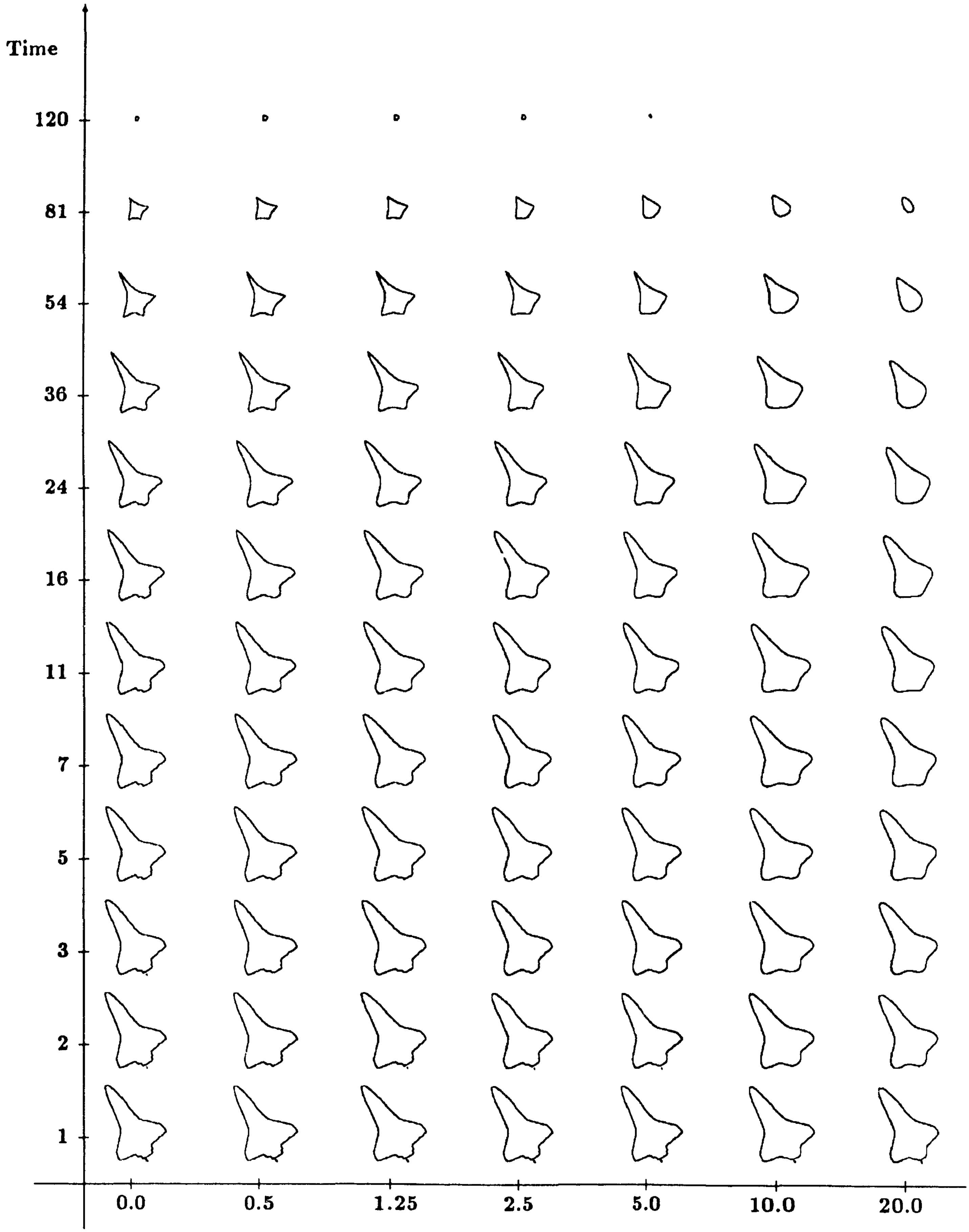

Time
120
81
54
36
24
16
11
7
5
3
2
1
0.0
0.5
1.25
2.5
5.0
10.0
20.0

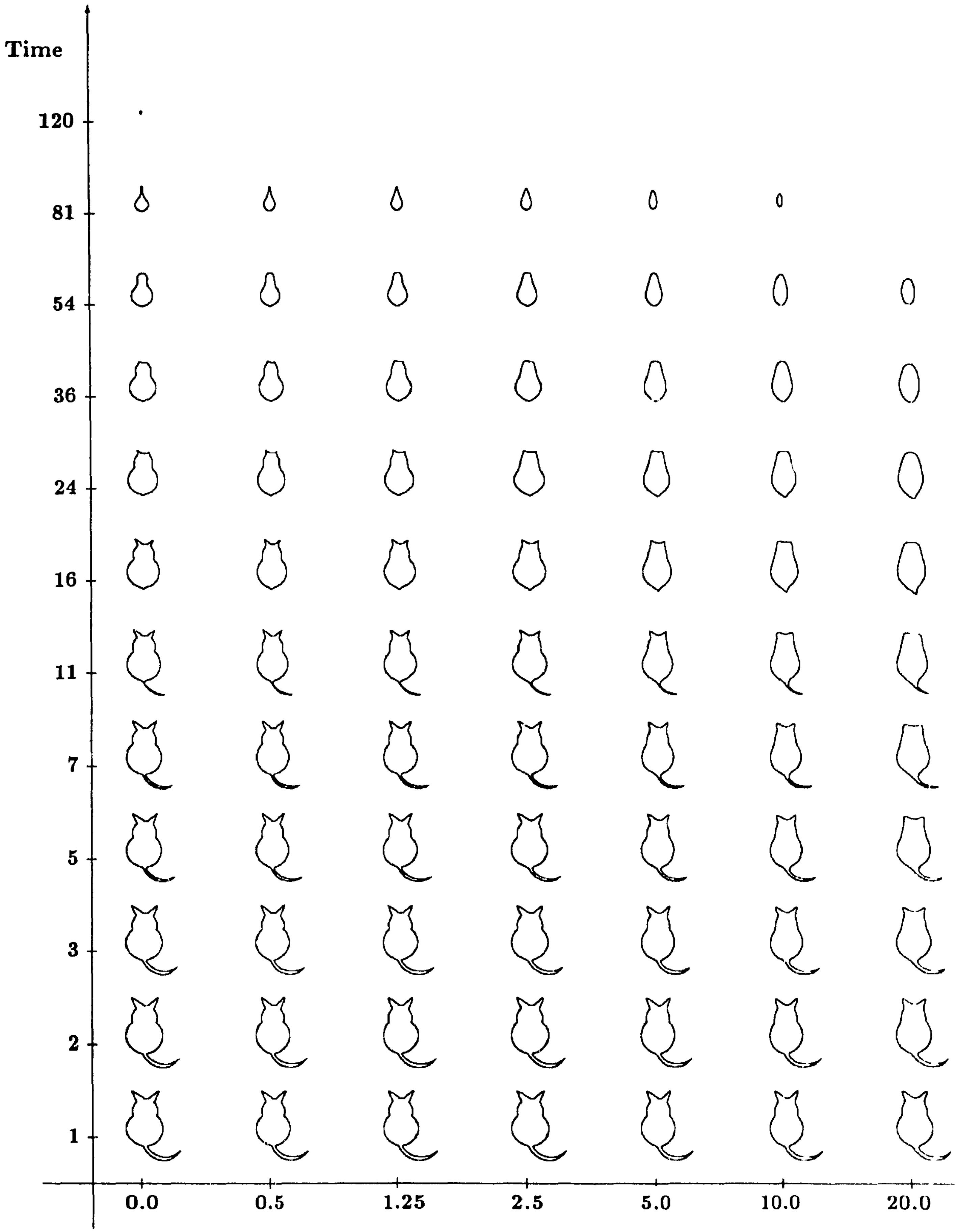
Time
120
81
54
36
24
16
11
7
5
3
2
1
0.0
0.5
1.25
2.5
5.0
10.0
20.0

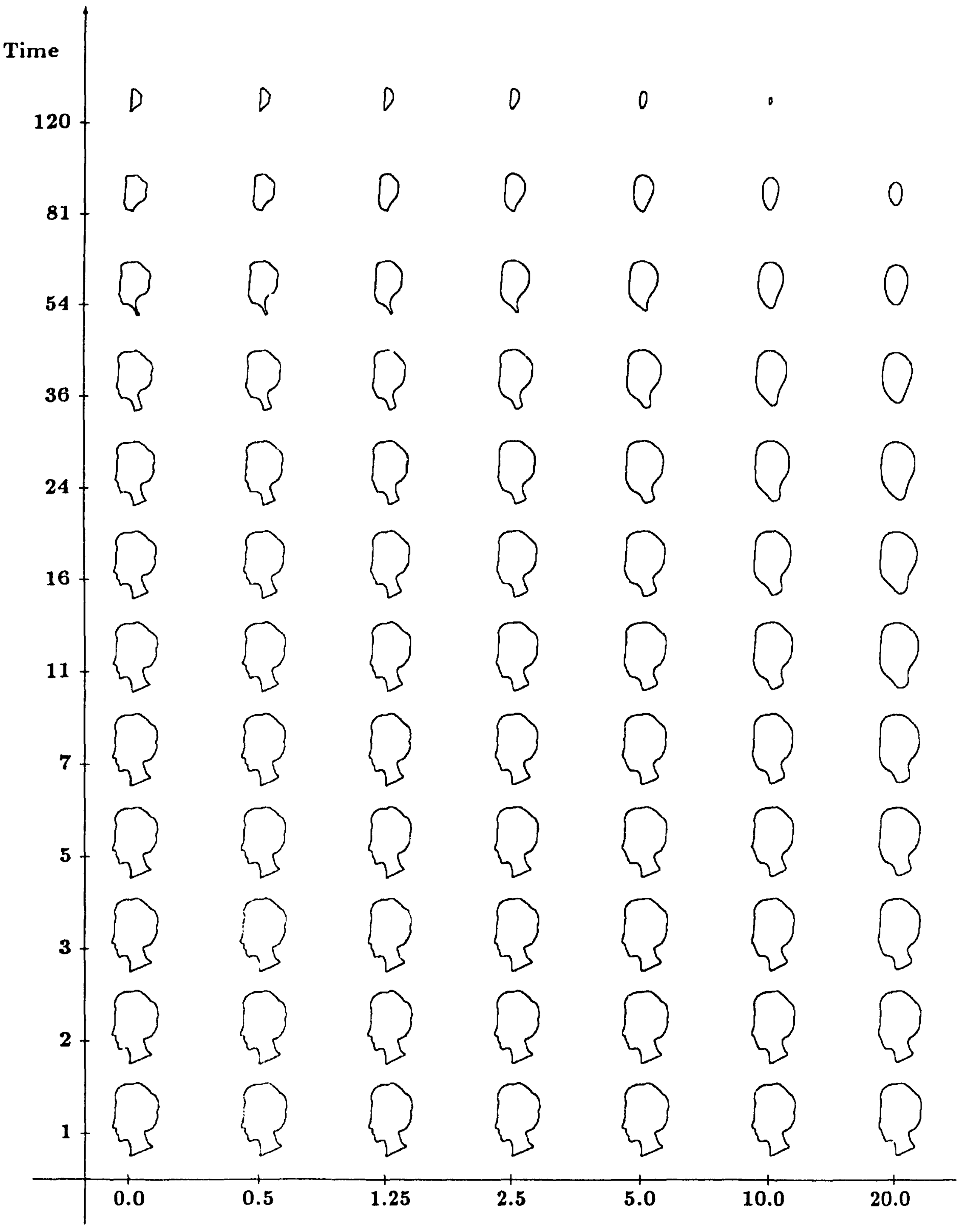

Time
120
81
54
36
24
16
11
7
5
3
2
1
0.0
0.5
1.25
2.5
5.0
10.0
20.0

Chapter 6

The Computational Elements of Shape

In the last chapter we considered shape as represented in the reaction-diffusion space where various types of shocks form. In this chapter, we propose three computational elements for shape: *parts*, *protrusions* to stand for both protrusions and indentations of the boundary, and *bends* to stand for bending, stretching and squishing the shape. We then connect each of these elements to the order (type) of shock that forms in the reaction-diffusion space.

6.1 Necks as Determinants of Parts

Why should a shape be parsed into components? If shapes are to be effectively recognized, it should be more efficient to represent the shape as a composition of parts, each of which is represented in memory rather than an exhaustive representation of all combinations. In this way, recognition can take place in the presence of occlusions while not all of the object is in view, some parts of it are likely to be, each of which can be independently recognized. Furthermore, part-based representations support nonrigid objects with moving parts.

The essential question is how to break an object into parts. One approach has been based on *primitives*, e.g. generalized cylinders [10, 15, 58]. These primitives then impose part boundaries between two primitives and the notion of parts becomes intimately tied to the selection of primitives. Hoffman and Richards [36] differentiate between *primitive-based* and *boundary-based* differentiation of parts and argue against primitive-based representations based on a *versatility* argument: primitives are limited in the range of their applicability, e.g. generalized cylinders are good for animal limbs, but not as good for faces. Rather, they propose a boundary-based representation of parts based on the transversality principle. "When two arbitrarily shaped surfaces are made to interpenetrate, they (almost) always meet in a contour of concave discontinuity of their tangent planes." This in turn leads to the minima rule "divide a surface into parts at loci of negative minima of each principal curvature along its associated family of curvature lines". Another boundary-based partitioning scheme emphasizes inflection points [14] arguing that curvature extrema are not invariant to affine transformation. Motivated by ideas from information theory, Attneave showed that curvature extrema are points of high information. As such, contours replaced by polygons with vertices at curvature extrema approximate the shape well as in the sleeping cat [2]. Lowe proposed that the same principle holds for inflection points. However, while this is valid for complicated shapes, it is not true for simple ones, e.g. a peanut. To explain this, note that in complicated shapes inflection points are close to curvature extrema. Therefore, inflection points approximate a shape since curvature extrema do. When inflection points are not close to curvature extrema, inflection points do not approximate a shape. Furthermore, Leyton showed that curvature extrema are related to symmetry [53, 54]. Biederman showed that midsegment contour deletion is less destructive to our recognition abilities than corner deletions of the contour [9].

In the previous chapters we have argued for a simultaneous representation of shape based on both the boundary and the region of the shape. A purely boundary-based definition of parts renders the regional information unnecessary For example consider shapes in figure 6.1. The shape on the left is seen to have four (or sometimes five) parts, while the shape on the right is seen to have three parts. A purely boundary-based approach is incapable of differentiating between these two shapes Rather, it is also essential to include the pairing of curvature extrema through distance Figure 6.2 depicts a snake's body which will be partitioned into many parts by the boundary-based schemes. However, taking region effects into account, by pairing curvature extrema through the region allows the snake to be perceived as a "bent stick"

One would like to recover from a shape the components from which it was composed. However, there are a large number of ways a shape can be broken into segments. Our motivation for parts comes once again from the world of objects Consider the objects in figure 6.3 and ask whether objects can be broken into components at obvious places These shapes lead us to define a *Neck* of a shape as the strictly shortest line segment whose two distinct end points are on the boundary of the shape

To motivate this notion of necks, observe that when two objects are connected, their interconnection is often playing the role of attaching the two objects only, and as such, need not require a great deal of "material" If this is not the case, then often there is no clue from shape to determine whether the object is indeed composed of two (sub)objects For example, this narrowing of the shape is true of the neck connecting the head and the body of animals, the stem the connects the top and the bottom of a wine glass, the bottle neck, the stem that connects a leaf to a tree, and so on. This is also seen in the interconnection between moving parts, as it allows space for the motion of either part. The proposed narrowing at the point of attachment is also significant for manipulation purposes, necks offer a hold-site since they are stable a slight motion to either side will meet greater width, e.g a dog likely holds a bone at

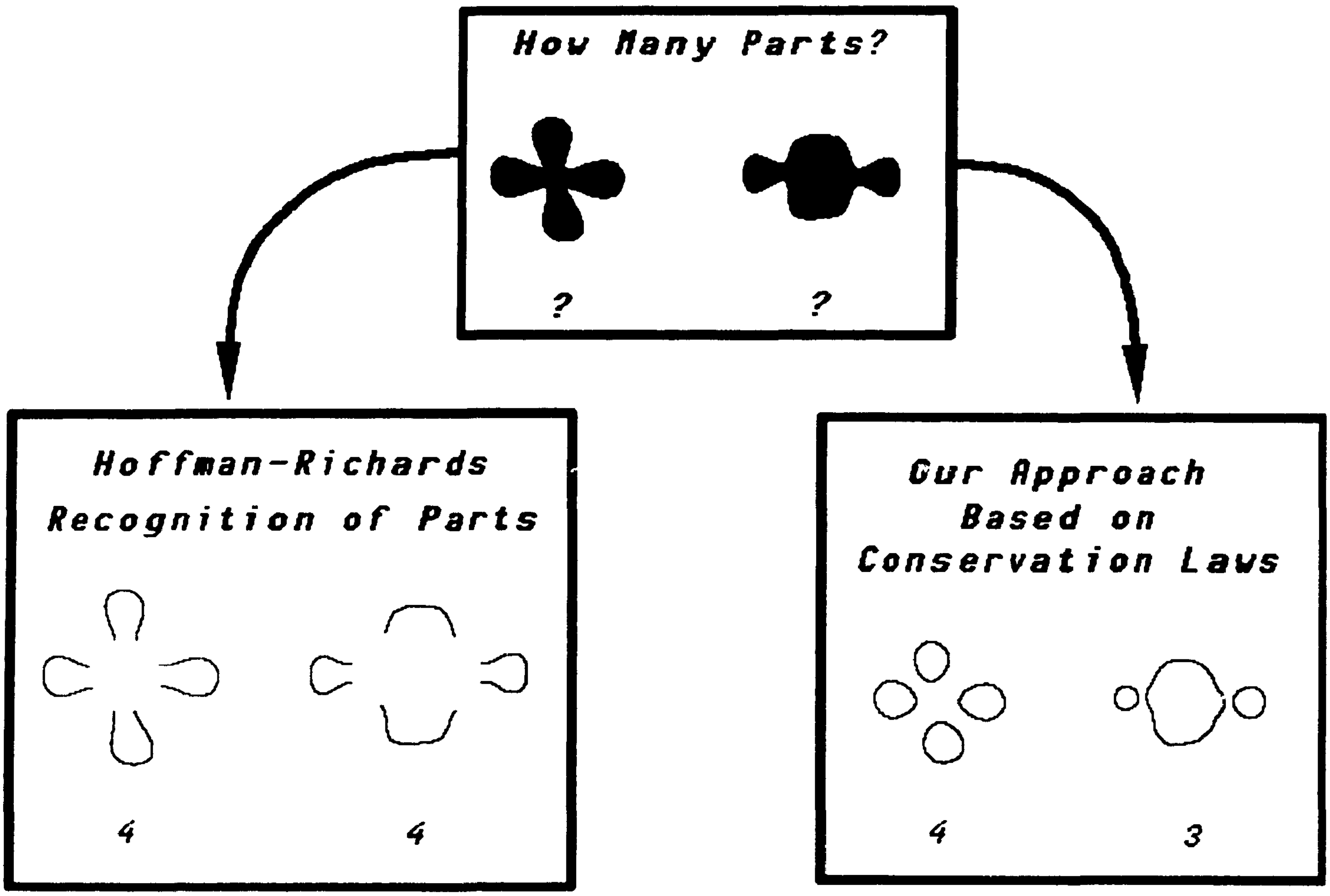

Figure 6.1 A pure boundary-based approach obviates the role of region. The two shape have precisely the same number of curvature extrema of the same type in the right order. Yet the shape on the left is seen to have four (sometimes five) parts, while the shape on the right is seen to have three parts. The difference is the effect of the region: distance between the curvature extrema is varied as one shape is stretched into another. While the curvature extrema of the boundary do indeed play an essential role in determination of parts, the role of region in pairing these extrema must be taken into account, see the definition of a "neck".

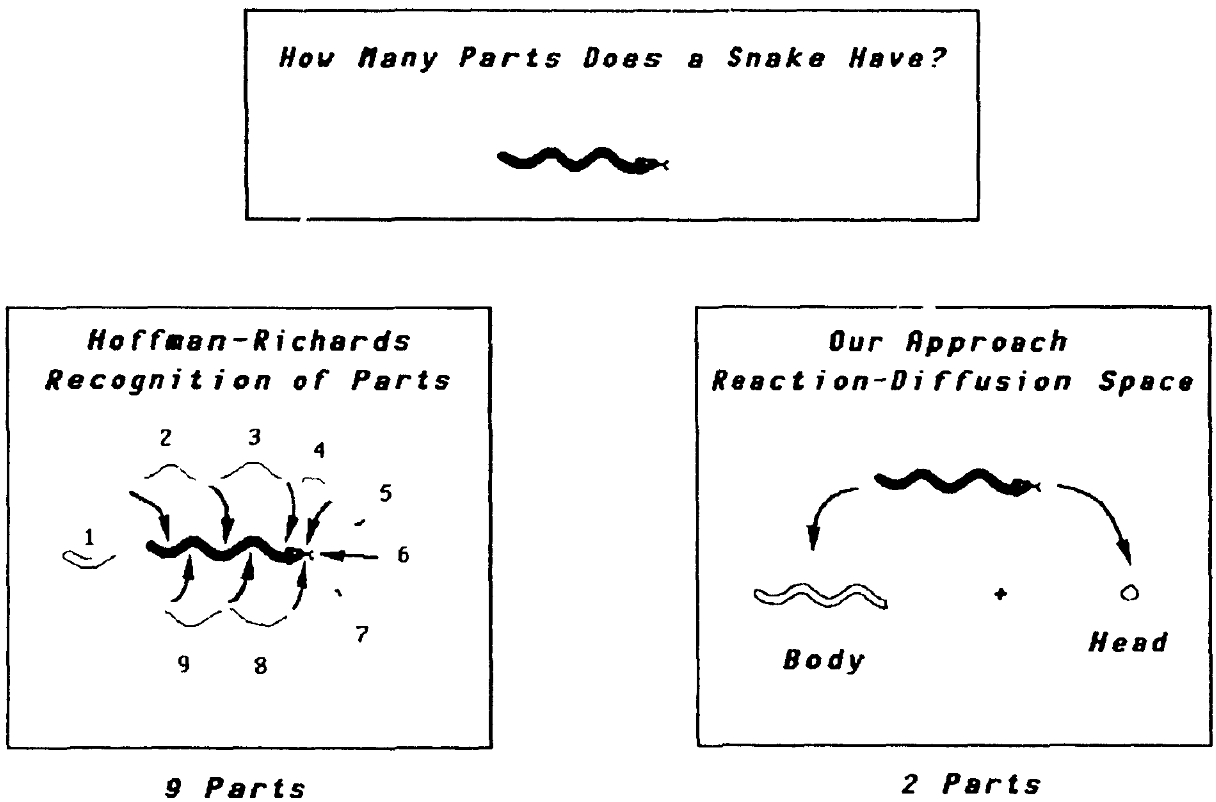

Figure 6.2. This figure illustrates the contrast between a boundary-based scheme and one that takes regional information into account as well. Viewed purely along the boundary the indentations and protrusions are seens as parts. However, viewed along the region, the body is seen to be an undulating stick.

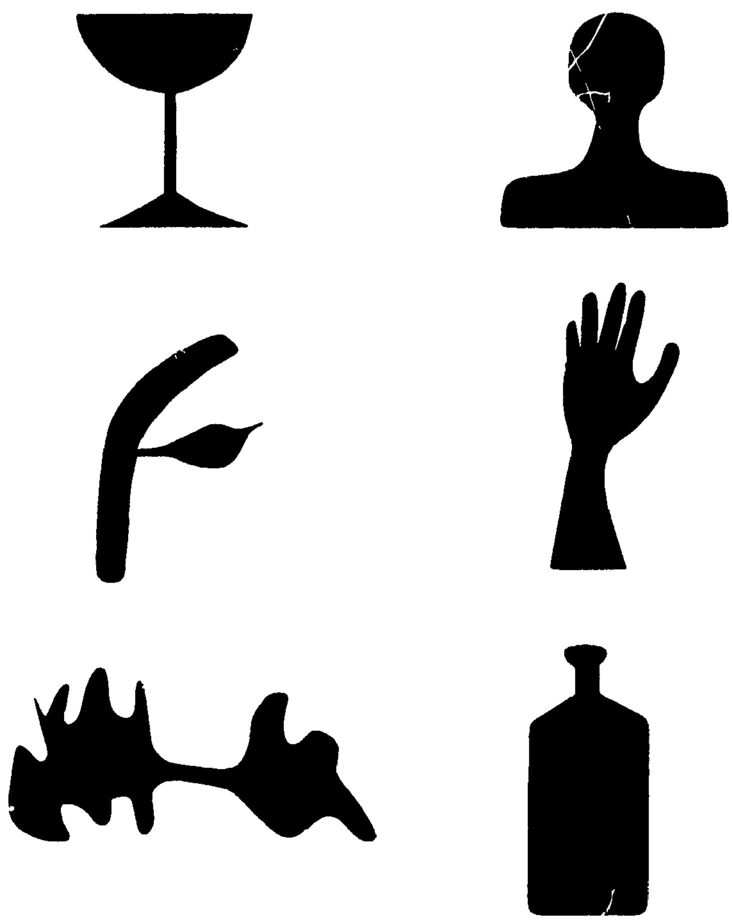

Figure 6.3. Can you easily partition these shape into components? Does this partition correspond to a "neck"?

the center not at the sides. Also, if our goal is to break an object into two, the necks often offer least resistance. Hence, let us summarize our assumptions as: When two shapes are made to interpenetrate, often the point of attachment is not wider than the width of the object on either side.

Can necks be determinants of parts? Observe that a neck is a region-based concept, at least as it is normally described. However, we have been advocating the integration of boundary-based and region-based information. To apply this idea to necks, note that the boomerang-like shape of figure 6.4 has a neck, although the narrowing is often not seen as the interconnection between two parts. As a second example, consider the pipe-like shape where again most often the shape is seen as a single object. This is illustrated more systematically in figure 6.5 where shape (i) is progressively deformed. Note that, in this sequence there is increasing displacement between the neck and the curvature extrema. This is in correspondence with our perception: while object (i) is most often seen as having two parts, object (vi) is most often judged to be a single object that is deformed (this question was put informally to a number of McGill graduate students).

Therefore, problems illustrated with necks as sole determinants of parts are two-fold: one associated with the boomerang and the second with the pipe-like figure. Both can be explained by observing the curvature disparity at the two ends of the neck. In the case of the boomerang, the two boundaries are not bending very differently. Similarly, in the case of the pipe-like figure, the curvature of the boundary at the two ends of the neck is not all that different. Let us, then, propose a notion of significance for necks as the boundary support (given the same neck width). *The* significance *of a neck is established through the disparity of bending in the contour at its two ends, namely the absolute value of the sum of curvatures.*

What kind of a shape has a significant neck? When the two contour segments both bend in the same direction, as in the boomerang, one of the curvatures is negative

Figure 6.1: Neck, the narrowest region of the shape are often formed when two objects interpenetrate. However, it does not follow that necks lead to parts as the above counterexamples depict. What is missing is the integration of boundary support for parts.

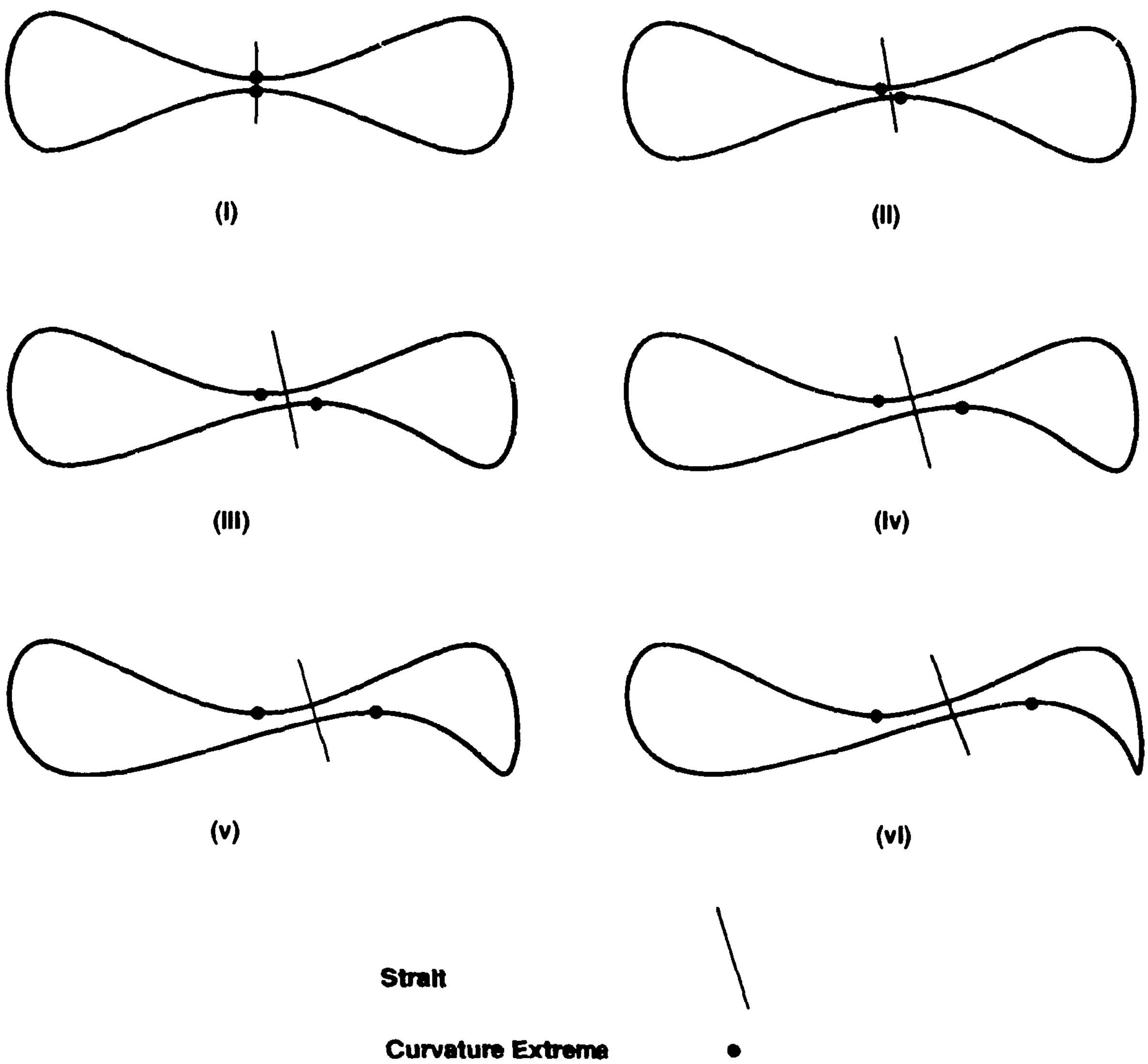

Figure 6.5: This figure illustrates six shape which are deformations of the shape in (i). In (i) the neck is in agreement with the curvature extrema. However, the neck and the curvature extrema are progressively more out of phase as the shape is deformed. Note that while in (i) the shape is seen as having two parts the shape in (vi) is more often seen to be a single object that is bent. It appears that for "parts" one needs agreement between the boundary support substantial difference in bending (as is the case with negative curvature extrema) and the regional support (necks).

and the other positive. As such the sum is nearly zero. Similarly, in the case of the pipelike figure, the two curvatures are slight, leading to a small sum. In contrast, when the contour segments at the two end points move away from each other, then curvatures are both of the same sign, leading to a large magnitude sum. In fact, when the two curve segments curve away from each other, this sum is largest when the two curvatures are at their extreme. In other words, it appears the strongest necks are produced when the end points of a neck are negative curvature extrema. This is in agreement with the transversality principle set forth by Hoffman and Richards [36], which states when two shapes are made to interpenetrate, at the point of their intersection, they will form negative curvature minima (or singularities). Recall, however, that not all negative curvature extrema give rise to parts. Shapes in figure 6.3 all have significant necks since the necks are doubly concave with extrema close to the neck.

To summarize, necks are determinants of shape parts. Their significance is established by the disparity in curvature across the neck. Therefore, the strongest necks are those with small widths and negative curvature minima as end points. This represents an integration of a region-concept, the neck, with a boundary-concept, its significance. A neck is representable in the language of shocks:

Theorem 6.1 *Each neck yields a second order shock.*

Proof Let the width of the neck be Δ and let the shape evolve for time $\Delta/2$. At this time, the two ends of the neck must come together. Since the shape is wider on at least one side, not all points of the boundary will have vanished on this side. By definition, then, this is a second-order shock. ∎

To illustrate how second order shocks gives rise to necks and therefore parts, consider the evolution in figure 6.6 of a set of overlapping discs. Each image is a point in the reaction-diffusion space which is reconstructed to compare to the original shape (see chapter 7), figure 6.7 displays its hierarchy of parts. Similarly, figure 6.8 depicts the evolution of the doll forward in time whose representation in the reaction-diffusion space ?? is reconstructed backwards in time (see chapter 7). The hierarchy of parts may be seen in figure 6.9, where the significance of a part is in its survival duration: the parts that last are the significant ones

6.2 PROTRUSIONS as Boundary Deformations

One of the ways of modifying a shape is to deform the boundary of the shape. For example, consider the circle and its protrusion in figure 5.1. Recall from chapter 5 that a single deformation of a boundary creates a curvature extremum While protrusions give rise to positive curvature maxima, indentations give rise to negative curvature minima. We generically refer to these boundary deformations as ***protrusions***.

Both forms of protrusion give rise to first-order shocks according to lemma 2.1, depending on the sign of β_0. Therefore, each type of protrusion (protrusion or indentation) appears only to the left or to the right of the time axis During the course of evolution in the eaction-diffusion space, small shocks disappear in larger ones. In contrast to Gaussian smoothing for which a small spike in the shape seriously affects the global properties of the shape, the formation of first order shocks is local to a segment of the curve. As such, a hierarchy of 'bumps' can be built The introduction of furthe: bumps at a small scale only affects that level; larger protrusions are not affected at all The scale of the bump then is dependent on how long it survives. We will see in chapter 7 that first-order shocks represent the boundary as deviations from a circular arc Finally, the protrusion is a ***boundary*** concept and is ***local*** to the shape

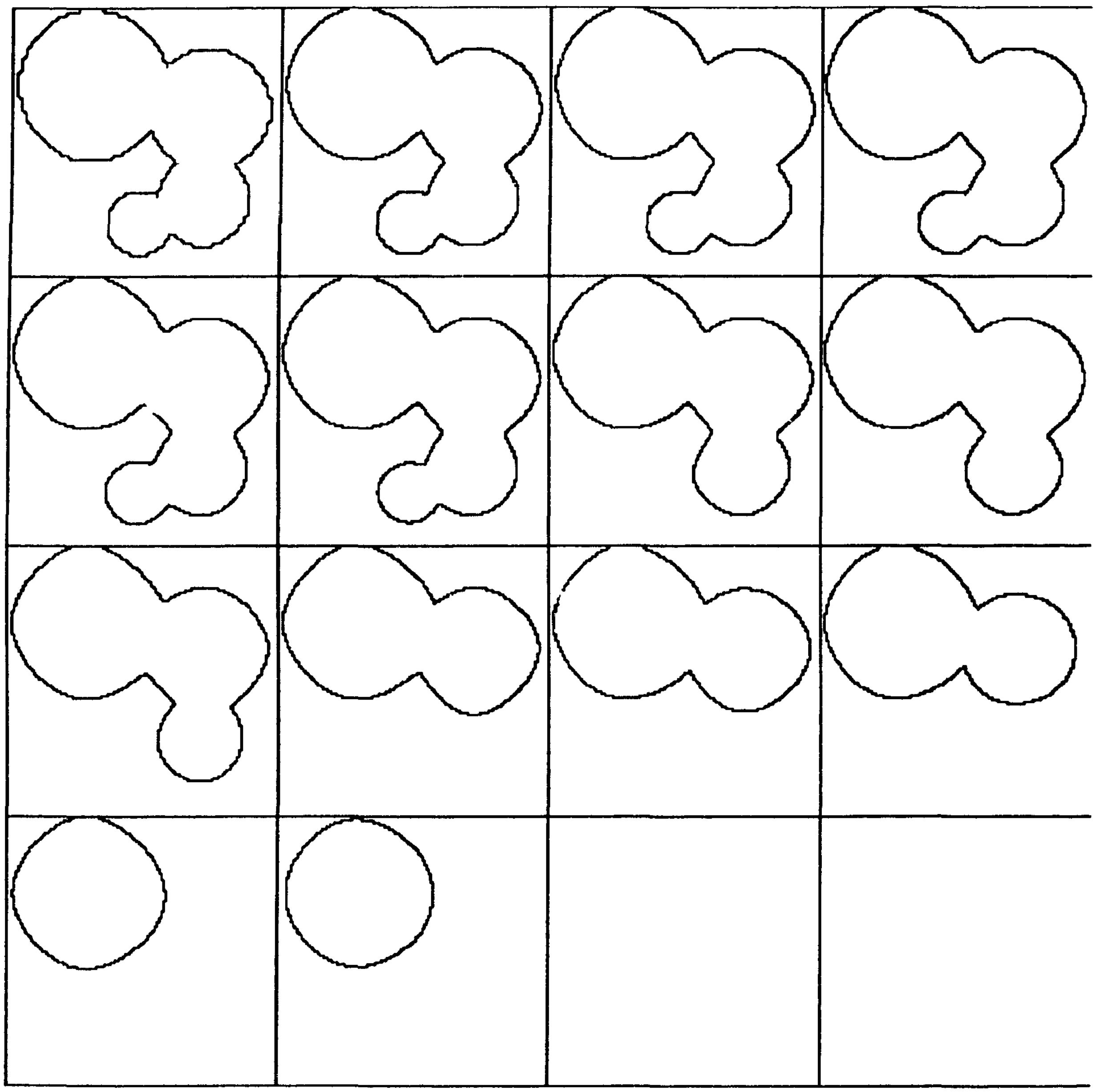

Figure 6.6: This figure depicts the evolution of a shape made of overlapping discs in the reaction-diffusion, having been reconstructed back in time. Note the shape decomposed into parts in a hierarchical fashion.

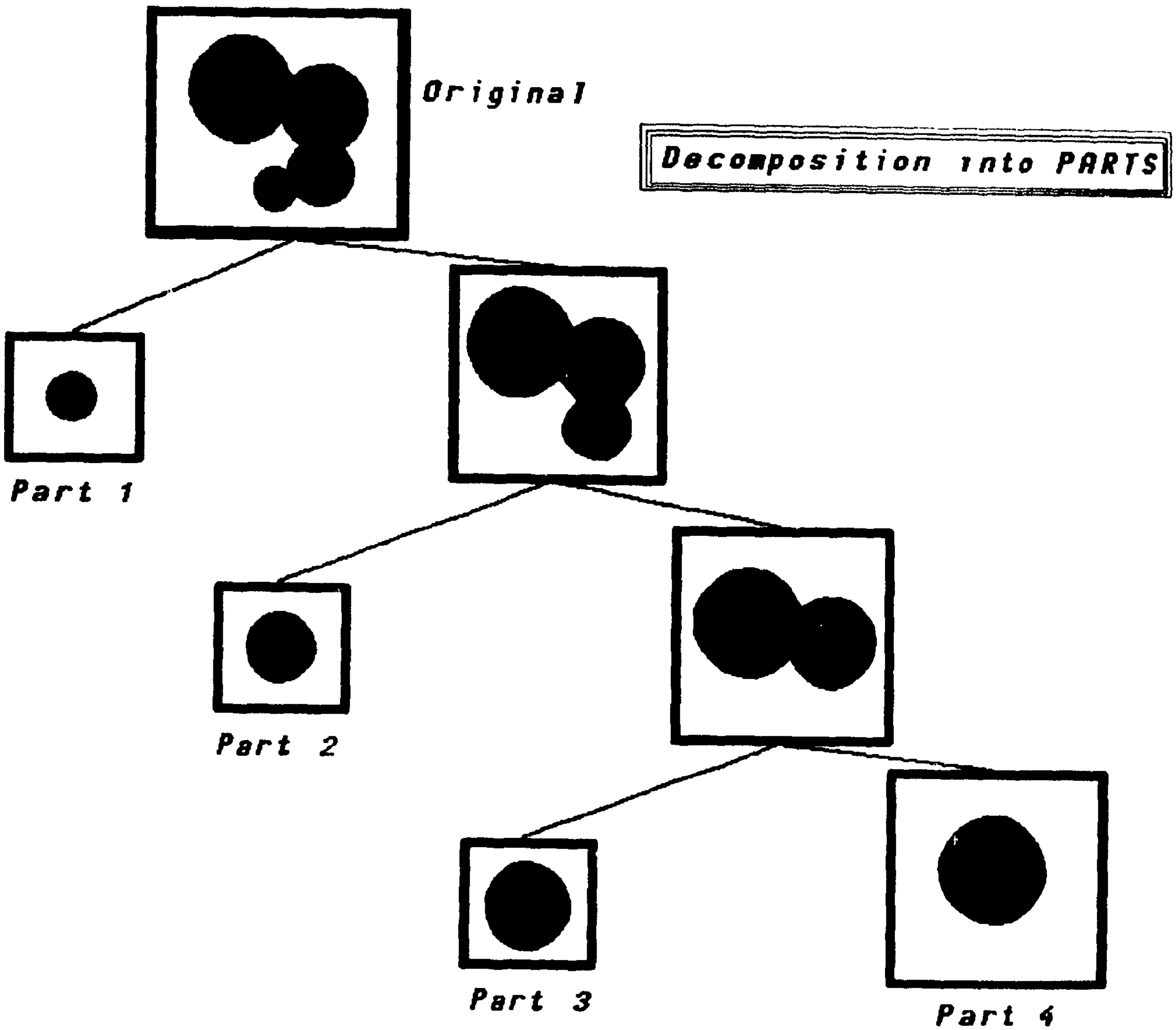

Figure 6.7: A hierarchy of significance for parts. !

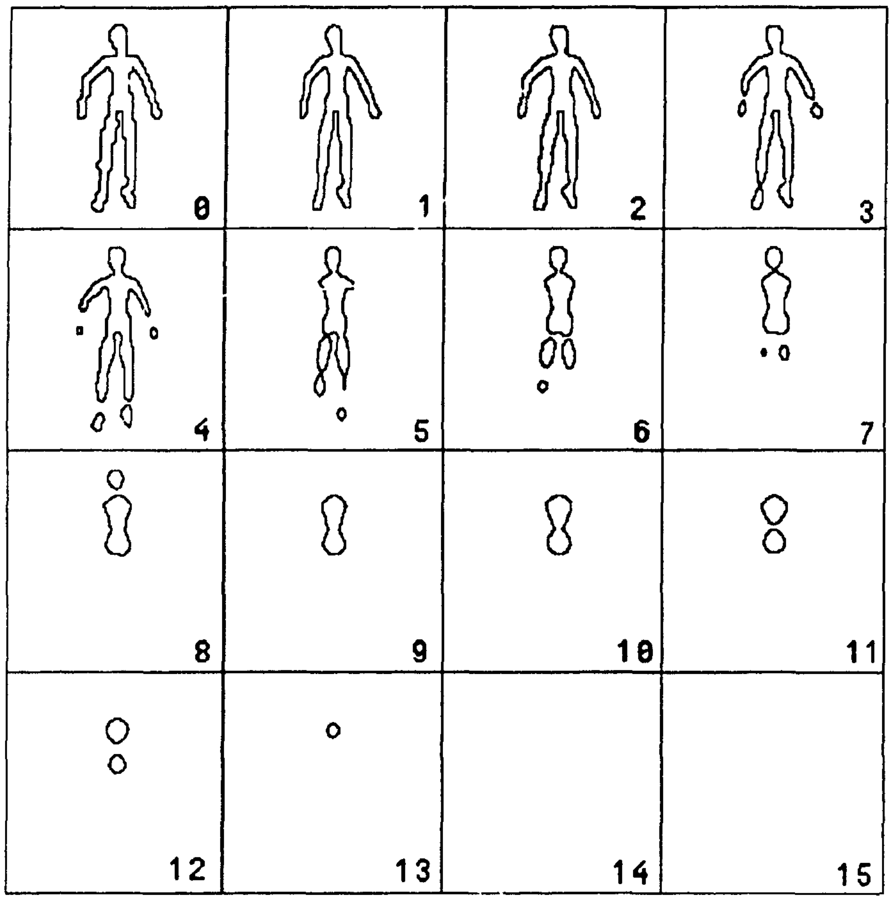

Figure 6.8: This figure depicts the evolution of a doll in time. Each step is a sample in the reaction-diffusion space that is reconstructed backwards in time (entropy space-space, see chapter 7. During the evolution the doll decomposes into parts. Those parts that appear later in time are more significant. figure 6.9.

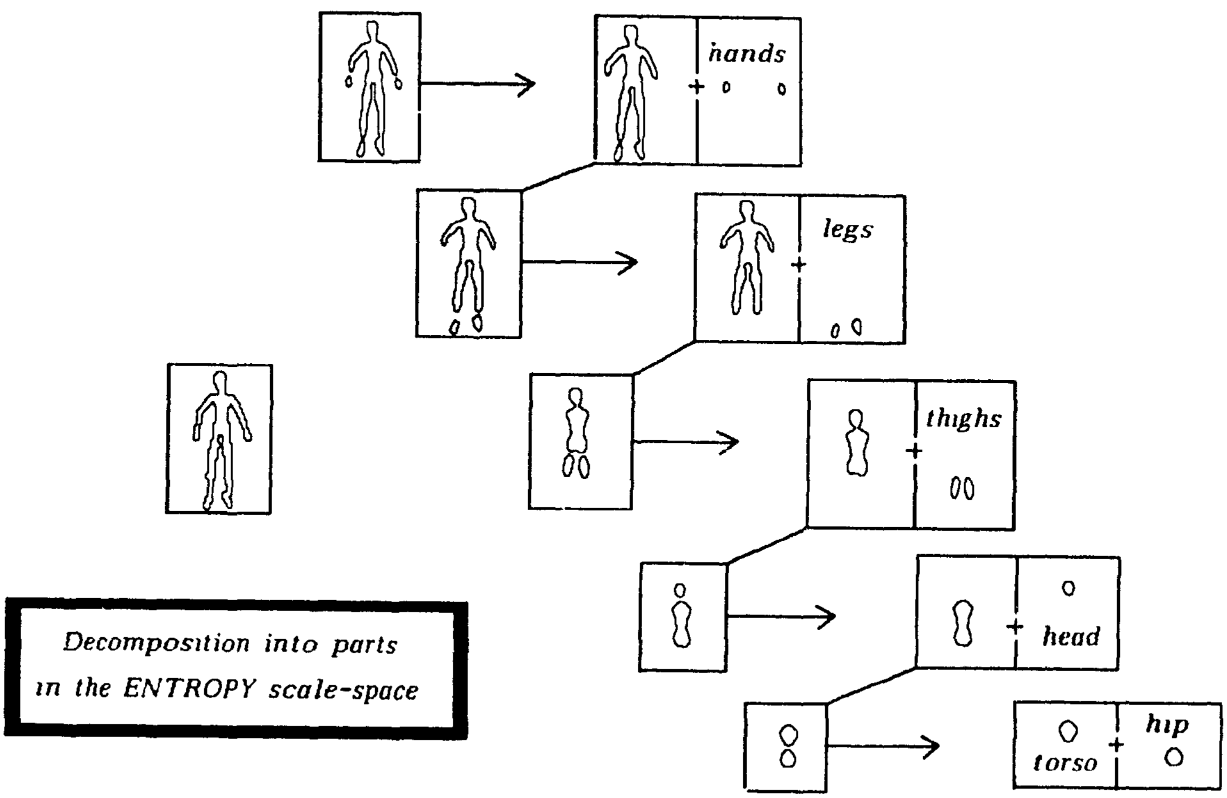

Figure 6.9: The parts of a doll can be arranged in a hierarchy of significance based on their survival in time. Note that the "hands" appear first and disappear quickly, while the "torso" appears last.

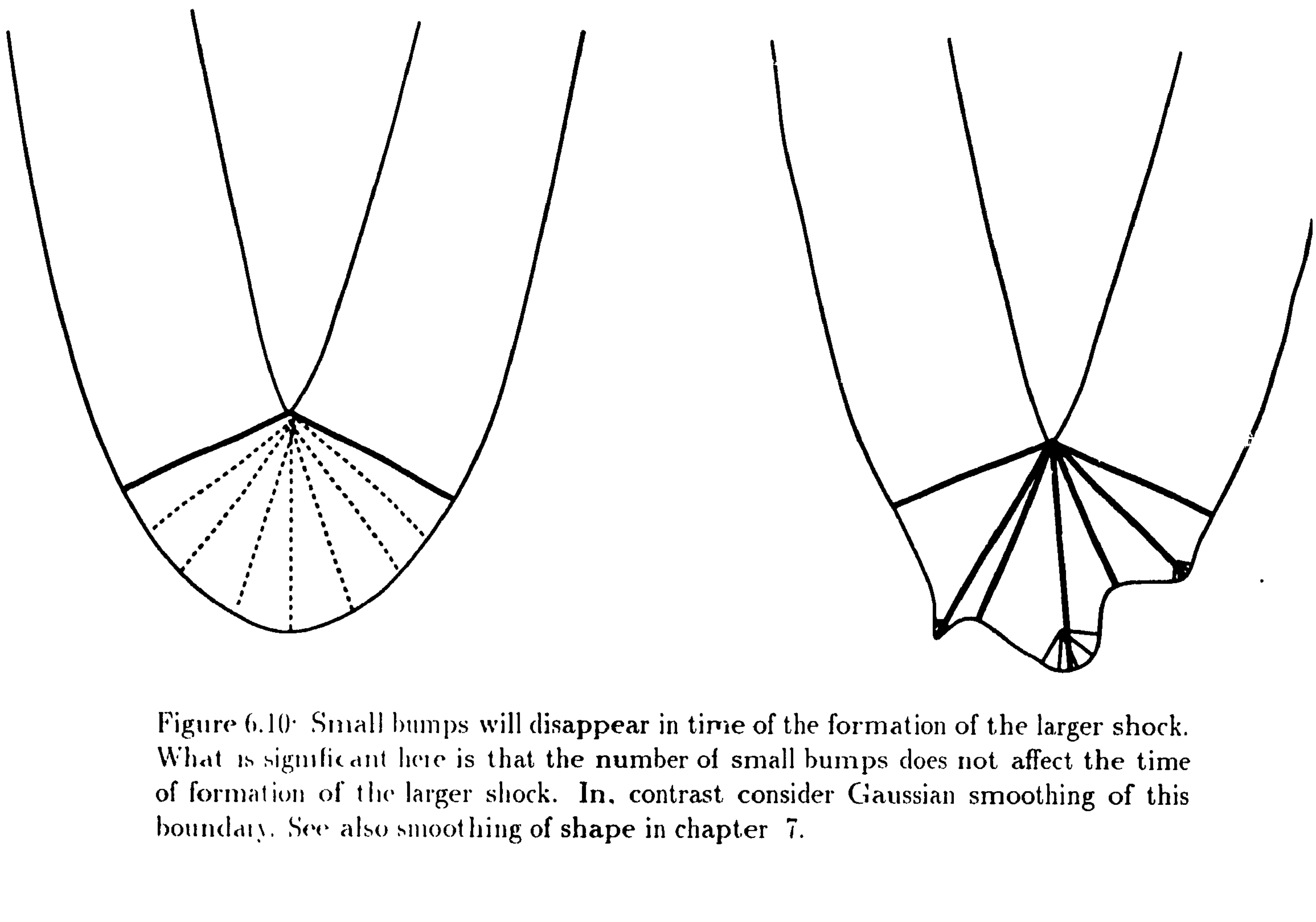

Figure 6.10: Small bumps will disappear in time of the formation of the larger shock. What is significant here is that the number of small bumps does not affect the time of formation of the larger shock. In, contrast consider Gaussian smoothing of this boundary. See also smoothing of shape in chapter 7.

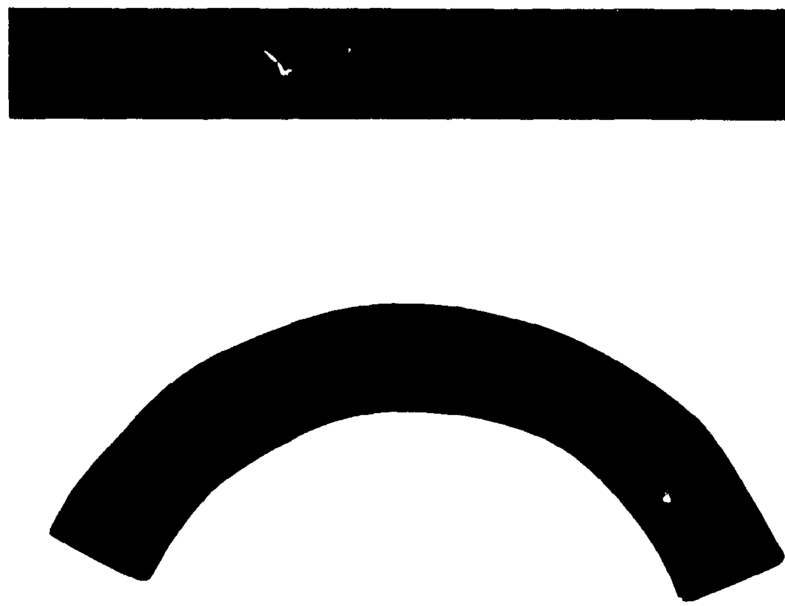

Figure 6.11: A shape may be modified by bending it. This is similar to the snake which may be considered as a bent rod.

6.3 BENDS as Regional Deformations

Another way of modifying the shape of an object is to *bend* the shape along its axis. Consider the rectangle of figure 6.11 which is bent to form an arc. Note that this single-part shape with no protrusions leads to third order shocks. The axis formed by the locus of third-order shocks represents the amount of bending of the shape. Other operations which affect the locus of third order shocks are stretching and squashing of the shape. A bend is significant when the amount of bending is high. A bend is closely related to the symmetry of a shape, since the locus of third-order shocks is part of the symmetric axis transform. Note that a bend is a *region* concept and that is *global*.

6.4 A Hierarchy of Significance

In order to differentiate between smaller and larger features of a shape, it becomes necessary to have a notion of significance associated with these features. A *neck* or a *part* is significant when the width of the neck is small and the curvature disparity across the neck is large. In the reaction-diffusion space, a neck will lead to a topological split along one of the pure reaction axes. Time determines the significance of each part, in that a part that lasts longer is more significant. Diffusion, on the other hand, pulls out a neck towards blurring the shape into a circle. As such, with more diffusion, the neck forms later in time. With enough diffusion the neck does not form at all. This is a measure of strength for the neck and for whether the shape contains two parts.

Protrusions, on the other hand, smooth away with diffusion. The effect of time on protrusions is to merge smaller ones into larger ones. Again, time becomes a measure of significance for protrusions: those that form last are the most significant ones.

Bends, are global concepts and their significance is established by the curvature in the locus of third order shocks.

6.5 Shocks and Shape

A representation of shape should be in a language that is natural for it, and we have argued that the language of parts, protrusions and bends is just such a candidate. Since shocks are intimately connected to these elements, a database of the shocks of the shape is a representation for shape in the following way. Fourth order shocks at some time and location assert that a seed should be placed at that location and time. That seed then grows protrusions according to its first-order shocks. Second-order shocks suggest that two adjacent parts be connected, and this shock subsequently grows to a neck. Finally, a group of third order shocks represent the bending of

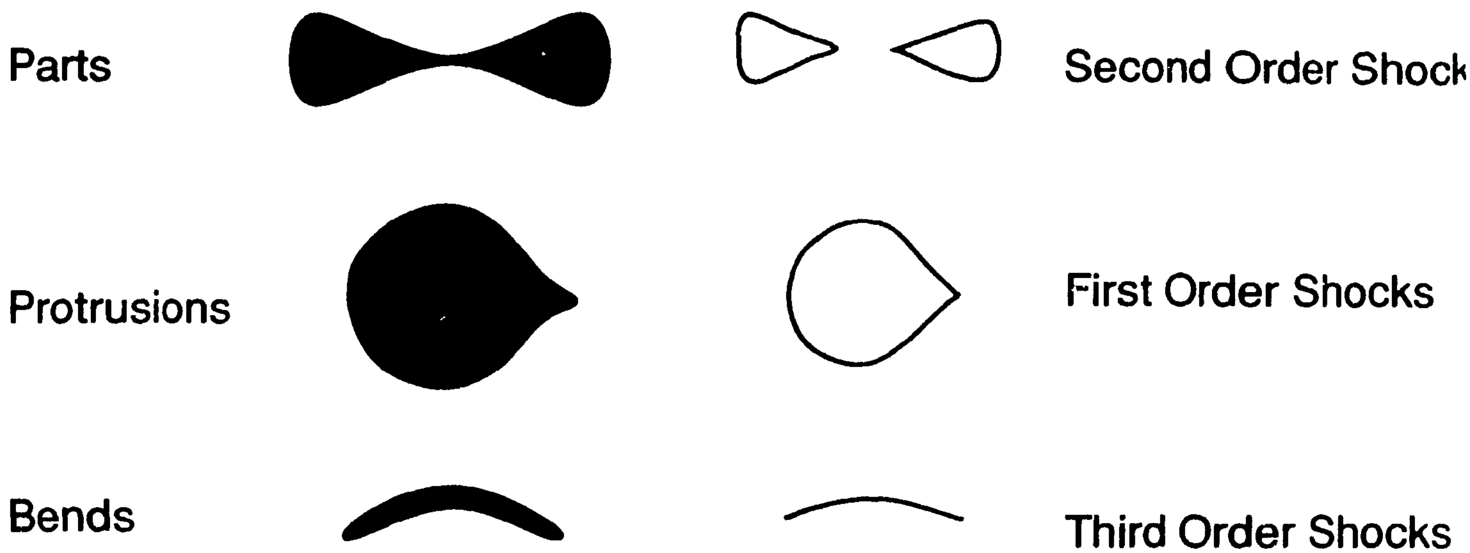

Figure 6.12: This figure illustrates the relationship between the computational elements of shape and shocks.

some element, which is made by growing them backwards in time, figure 6.12. Many questions remain to be answered: how shocks evolve in time? What types of shocks can merge and what do they lead to? These are currently under examination and several interesting results have emerged that we shall be reporting on separately from this thesis.

Chapter 7

The Entropy Scale Space for Shape

Events in the world occur at different scales, and as such, qualitative understanding of a sensory signal, such as an image, should reflect these different scales. To cite the classical example, fingers exhibit structure at a finer scale than hands, hands are finer than limbs, and so on. Thus there is a connection between scale and size, and, for many applications in computer vision, scale size became synonymous with operator size. Big operators select structure at large scales, and small operators select structure at fine scales: one need only recall the tree image in [57] to recall the force of this argument; see also [72, 57, 43, 95] as well as the psychophysical support they were engaging [16, 89].

But confounding these assessments of structure is noise, which suggests a different interpretation of operator size: big operators smooth large fractions of the image, while small operators smooth only tiny fractions. This confounding is clear for the "hand" above, in respect of which the "fingers" are just noise. Witkin [91] put these two interpretations together by suggesting a continuum of operators in a kind of *scale space*. Structure was captured by signal extrema, and these were computed not over a few neighborhood sizes, but over a *continuum* of neighborhoods, established by convolution against Gaussians of increasing extents. The behaviour of extrema as the signal is smoothed out yields the qualitative description of the signal. In addition, a hidden bonus emerged in the form of a significance hierarchy on the extrema, in the sense that the extrema that survive larger smoothing extents are considered more significant. This is analogous to the fingers being smoothed out before the hand. The space of the signal and its continuously smoothed versions is the *scale space* for the signal.

7.1 Gaussian Smoothing Annihilates Structure

The question thus arises of how to "smooth" the signal so that only increasingly "significant" features survive further smoothing. Koenderink showed that, given assumptions of *causality, homogeneity, and isotropy*, the diffusion equation is the only sensible way of embedding a signal in a family of simpler signals with the requirement that structure is not created [42, 44]. From a different perspective Babaud et.al. independently showed that the Gaussian is the unique smoothing kernel that does not create structure in that, with increased smoothing, no new zero-crossings are created [4]. Yuille and Poggio extended this result to two dimensions [93] and Hummel and Moinoit showed that zero-crossings, when supplemented with gradient data along the zero-crossing boundaries, are sufficient to reconstruct the original signal.

While these theorems and the popularity of Gaussian scale-spaces attest to its functionality in certain domains, it does not always provide "semantically meaningful" descriptions of images [66]. Rather, the above notions of structure are often not the natural ones, and Gaussian scale spaces may lead to more problems than they solve. For example, in an edge-detection Gaussian scale-space, the true location of edges is not available. Instead, the true location is estimated by tracking edges across the scale space. Furthermore, the edges, which are very high in information content, become blurred out in the Gaussian representation. This point is illustrated even more powerfully in the domain of shape, and exemplified by the depiction of "don Quixote" in figure 7.1. Ideally a scale-space representation of this profile should relate the structure of "the man on the horse with a lance " to that of 'the man on the horse" in much the same way as a qualitative description of a car with a radio antenna ought to be very closely related to the representation of the same car without the antenna, figure 8.1. Unfortunately, in the Gaussian scale-space representation of the shape, the lance (or the antenna) assumes a role much more significant than it has in the original image In fact, the longer the lance is, the more it dominates and distorts the remainder of the shape [1].

7.2 The Three Components of a Scale-Space

To review current scale-space structures in one common language, consider a scale-space as a structure composed of three elements:

- A *signal*, e.g. an intensity image;
- A *feature* that corresponds to some interesting structure, e.g. a curvature extremum, or a point of inflection; and,
- A *process* that annihilates information in a way that gradually removes low significance structure *without* affecting higher significance structure. While the process leaves high-order structure intact, it should not create new structure.

Figure 7.2 reviews and summarizes the several common scale-spaces in the above framework For example, Asada and Brady partition a curve into certain curvature-based multiscale primitives [1] Their approach is to detect significant changes in

[1]see [1] for an illustration of the "dumbbell" problem

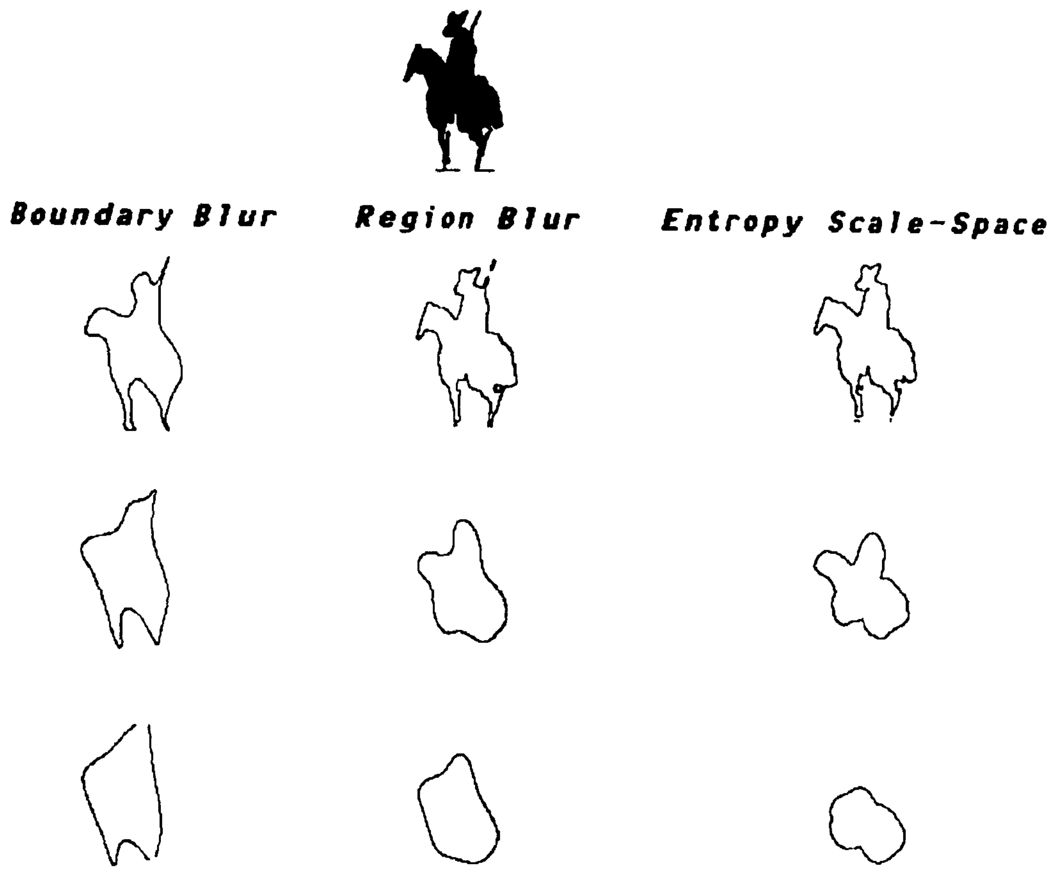

Figure 7.1: A depiction of don Quioxte. The left column illustrates three instances of the process of blurring the boundary coordinates; the middle column displays effects of blurring the characteristic function of the interior of the shape. On the right, three steps along one axis of the entropy scale-space is shown. Note, that while the lance as well as other features of the shape are distributed throughout the shape by Gaussian smoothing, this does not happen in the entropy scale-space. Here, small features like the lance are removed without affecting the larger structures.

	Signal	Feature	Process
Witkin	Intensity	Zero-crossings in Derivatives	Gaussian Smoothing
Mokhtarian & Mackworth	Boundary Coordinates	Inflection Points	Gaussian Smoothing
Richards et. al.	Boundary Orientation	Curvature Extrema	Gaussian Smoothing
Asada & Brady	Boundary Curvature	Extrema & Inflection Points	Gaussian Smoothing
Koenderink	Interior Chracteristic Function	Inflection Points	Gaussian Smoothing + Thesholding
Pizer et. al.	Interior Chracteristic Function	Symmetric Axis	Gaussian Smoothing + Normalized Thesholding

Figure 7.2: This figure reviews some of the proposed scale spaces. Note that the use of Gaussian smoothing is prominent.

curvature by observing its behaviour as it is convolved with a Gaussian. In our terms, the *signal* is curvature as a function of arc-length, the *features* are curvature extrema, and the *process* for removal of information is Gaussian smoothing. As another example, Mokhtarian and Mackworth abstract the general structure of boundaries found in Landsat images by convolving the coordinates of the curve with a Gaussian [60]. The zero-crossings of curvature are then located and studied over a range of scales [24]. This representation of zeros of curvature over scale is suitable to register the image to a map. In this case, the *signal* corresponds to the coordinates of the curve, the *features* to the zeros of curvature, and the *process* of annihilating information is again Gaussian smoothing. To illustrate further, consider the scale-space proposed for the Symmetric Axis Transform (SAT) [68], where a hierarchy of significance is placed on the symmetric axis by blurring the image. In this case, the signal is the two-dimensional intensity image, the *features* are the symmetric axis, and the *process* of annihilating information is two-dimensional Gaussian smoothing. Yet another example is the work of Witkin et. al., who considered the general problem of signal matching. Here, the problem is formulated as minimizing an energy functional by tracking the global minima from coarse scale to fine scale [90]. In this case, the *signal* is the general signal under consideration, the *feature* is the set of energy minima, and the *process* is again Gaussian smoothing.

The various properties of the Gaussian and its popularity show that it plays an important role in building a notion of scale. However, Gaussian smoothing amalgamates information regarding small scale structure with information of larger scale structure linearly. In fact, under certain smoothness assumptions, one can show that Gaussian blur does not annihilate information in a signal, but merely redistributes it [38]! Rather, the resulting simplicity of a blurred signal is due to quantization. Nevertheless, Gaussian blur remains an important component of a scale-space.

7.3 Nonlinear Annihilation of Structure

Thus, for Gaussian scale spaces, the "cure" almost seems worse than the "problem"; once the lance has been blurred together with don Quixote, it is almost impossible to remove it. Now, the situation is starting to look rather bleak, since the uniqueness theorems would seem to exclude other smoothing options for building scale-spaces. However, these theorems in fact make strong smoothness assumptions and do not hold when the scale space is extended to include non-differentiable or even non-continuous signals. Perona and Malik relax the homogeneity assumption and suggest that the candidate paradigm for generating a multiscale description should satisfy *causality*, *immediate localization*, and *piecewise smoothing* [66]. As before, causality requires that spurious detail should not be generated while passing from coarse to fine; immediate localization requires sharp scale-invariant placement of boundaries; and piecewise smoothing encourages intraregion over interregion smoothing. To alleviate the latter problem, they suggest that diffusion be location dependent, or anisotropic, for edge-detection.

Others have argued that much stronger nonlinearities are necessary. For example, morphological operations are another, very different approach to extracting structure, and several researchers have suggested morphological scale spaces: [52, 17, 56]

There is an immense conceptual transition from Gaussian smoothing to mathematical morphology; somehow, to be generally applicable, scale spaces must be extended to include these extremes. We now propose a formal mathematical framework for accomplishing this extension.

7.4 Entropy Scale Space

To review, a scale-space should capture essential structure while progressively eliminating small features. Although a linear smoothing method such as Gaussian blurring captures structure in a meaningful way for certain domains, it has shortcomings in others [92]. We suggest a scale space based on our two different basis motions, a *constant motion* along the normal and a *curvature motion* along the normal. A scale space arises in the sense that these processes annihilate information in two completely different and complementary ways.

Curvature motion is equivalent to the diffusion equation, or equivalently blurring of the boundary coordinates using Gaussian smoothing; see theorem 7.1. Based on this connection, therefore, curvature motion enjoys properties of Gaussian smoothing, in particular the property that structure can only be annihilated. Recall that recent results state that all embedded curves converge to a circle before they vanish [28, 35, 87]. Note that this process is *linear*, *global*, and spreads information with *infinite speed*.

Theorem 7.1 *Consider the family of curves $C(s,t)=(x(s,t),\, y(s,t))$ satisfying*

$$\begin{cases} \frac{\partial C}{\partial t} & = -\kappa(s,t)\vec{N} \\ C(s,0) & = C_0(s), \end{cases} \tag{7.1}$$

where $C_0(s) = (x_0(s), y_0(s))$ is the initial curve, s is some arbitrary parameter along the curve, t is time, κ is curvature, and $\vec{N}$ is the normal. Then the coordinates satisfy the diffusion equation

$$\begin{cases} \frac{\partial x}{\partial t} & = \frac{\partial^2 x}{\partial \tilde{s}^2} \qquad x(\tilde{s},0) = x_0(\tilde{s}) \\ \frac{\partial y}{\partial t} & = \frac{\partial^2 y}{\partial \tilde{s}^2} \qquad y(\tilde{s},0) = y_0(\tilde{s}), \end{cases} \tag{7.2}$$

where $\tilde{s}$ is the arc-length parameter along the curve.

Proof: Recall from section 2.1 that,

$$\kappa \quad := |\frac{\partial \vec{T}}{\partial \tilde{s}}|, \tag{7.3}$$

$$\vec{N} \quad := \frac{-\frac{\partial \vec{T}}{\partial \tilde{s}}}{|\frac{\partial \vec{T}}{\partial \tilde{s}}|} \tag{7.4}$$

Therefore

$$\kappa\vec{N} = -\frac{\partial\vec{T}}{\partial\tilde{s}}. \tag{7.5}$$

Since,

$$\vec{T} =:= \frac{\partial\mathcal{C}}{\partial\tilde{s}}, \tag{7.6}$$

we conclude that

$$\kappa\vec{N} = -\frac{\partial^2\mathcal{C}}{\partial\tilde{s}^2}. \tag{7.7}$$

Leading to

$$\begin{cases} \frac{\partial\mathcal{C}}{\partial t} & = \frac{\partial^2\mathcal{C}}{\partial\tilde{s}^2} \\ \mathcal{C}(s,0) & = \mathcal{C}_0(s), \end{cases} \tag{7.8}$$

In terms of coordinates this is simply the diffusion (heat) equation.

$$\begin{cases} \frac{\partial x}{\partial t} = \frac{\partial^2 x}{\partial\tilde{s}^2} & x(\tilde{s},0) = x_0(\tilde{s}) \\ \frac{\partial y}{\partial t} = \frac{\partial^2 y}{\partial\tilde{s}^2} & y(\tilde{s},0) = y_0(\tilde{s}). \end{cases} \tag{7.9}$$

It is well-known that the kernel for this equation is the Gaussian [88]. Hence, one may generate coordinates (x, y) at time t by simply convolving the initial coordinates with a Gaussian whose extent increases with time t. ∎

Constant motion, on the other hand, simplifies shape nonlinearly and more like mathematical morphology. It is based on the concepts of *shocks* and *entropy* and in contrast to previous one, is *nonlinear*, *local*, and spreads information with *finite speed*. The following theorem asserts that as scale increases the shape becomes simpler in the sense that the total absolute curvature is nonincreasing [11]. More specifically, no new zero-crossings of curvature may be created, therefore as before, structure can only be annihilated as the following theorem shows.

Theorem 7.2 *Let $\mathcal{C}(s,t)$ be a solution of*

$$\begin{aligned} \frac{\partial\mathcal{C}}{\partial t} &= \beta(\kappa(s,t))\vec{N} \\ \mathcal{C}(s,0) &= \mathcal{C}_0(s). \end{aligned}$$

$t \in [0, t')$. Suppose that $\beta_\kappa \leq 0$ and $\kappa_{\tilde{s}}(\tilde{s}, t) \neq 0$ for all $\tilde{s}$ and $0 \leq t \leq t'$. Then,

$$\bar{\kappa}(t) \leq \bar{\kappa}(0).$$

This theorem was proved in section 2.4.2.

To illustrate why we view shocks as "black holes of information", let us consider the system 4.4 and the initial condition 4.5. Up to the time of shock formation the process is reversible in that the signal may be recovered by tracing the characteristics back in time. As such the information content of the signal remains the same up to the formation of a shock. However, at any point past shock formation, the process is irreversible [19]. In the context of gas dynamics, this irreversibility and the fact that entropy must increase across a shock (and therefore loss of information) has long been recognized [78, 50] Any attempt to recover the initial signal will be successful only for those characteristics that can be traced back in time; that is, any point other than the shock itself. However, the shock point maps to a region of the initial signal, namely its *domain of dependence* [29]. Therefore, information contained in this section of the signal is irreversibly lost, see figures 4 1, 4 2. It is with this view that we have termed a shock a "black hole" of information: with increasing time, increasingly larger sections of the signal map onto the shock, irrecoverably lost. Other sections of the signal, however, can be recovered fully and exactly. This is, therefore, a local process whose domain increases with time and eventually becomes global

An interesting question is what happens to the lost section of the signal upon recovery. The nonshock points can be retrieved by running the *same* process backwards in time [2]. However, the process of running a shock backwards in time leads to a rarefaction wave. The rarefaction wave generates a continuous solution connecting the two disparate ends. For the case of shape, this will be equivalent to arc of circle

[2] For the diffusive-type conservation laws (e g heat equation) this process is ill-conditioned however for the wave-type (e g our case) this process has proven extremely robust

approximation, figures 4.5 and 4.6.

Shocks interact by merging to form more significant shocks. The significance of a shock is in the contour or the parts that it maps to. The longer a shock survives, the more its back projection extends. This is precisely the hierarchy that is required for a scale-space. Therefore,

Definition 7.1 *The* Entropy Scale Space *is generated from the reaction-diffusion space in the following way. each point of the entropy scale-space is the result of reconstructing the shape at the corresponding point by running the process backward in time with the same reaction and zero diffusion.*

Roughly speaking, we reconstruct the reaction part to undo the shock into a circular arc. In fact, this is a process of replacing local portions of shape by circular arcs.

7.5 Examples

We illustrate the entropy scale space for don Quixote of figure 7.1, and the four pears presented by Richards et. al. The pears sequence contains four pears and is interesting because the shapes contain various combinations of texture and noise.

To illustrate the figures, recall that the entropy scale space is a two dimensional space. One axis reflects relative amounts of reaction to diffusion. the other is time. We use logarithmic sampling of both axes [42] There are no parameters so that tuning is not necessary The diffusion extreme is the equivalent of Gaussian blurring and gives expected results. The reaction extreme removes structure locally without affecting the global shape. It is equivalent to the morphological operation of opening/closure with a ball as the structuring element.

In the first figure, one slice through the entropy scale-space representation for each of the four pears is shown together to demonstrate the potential for building

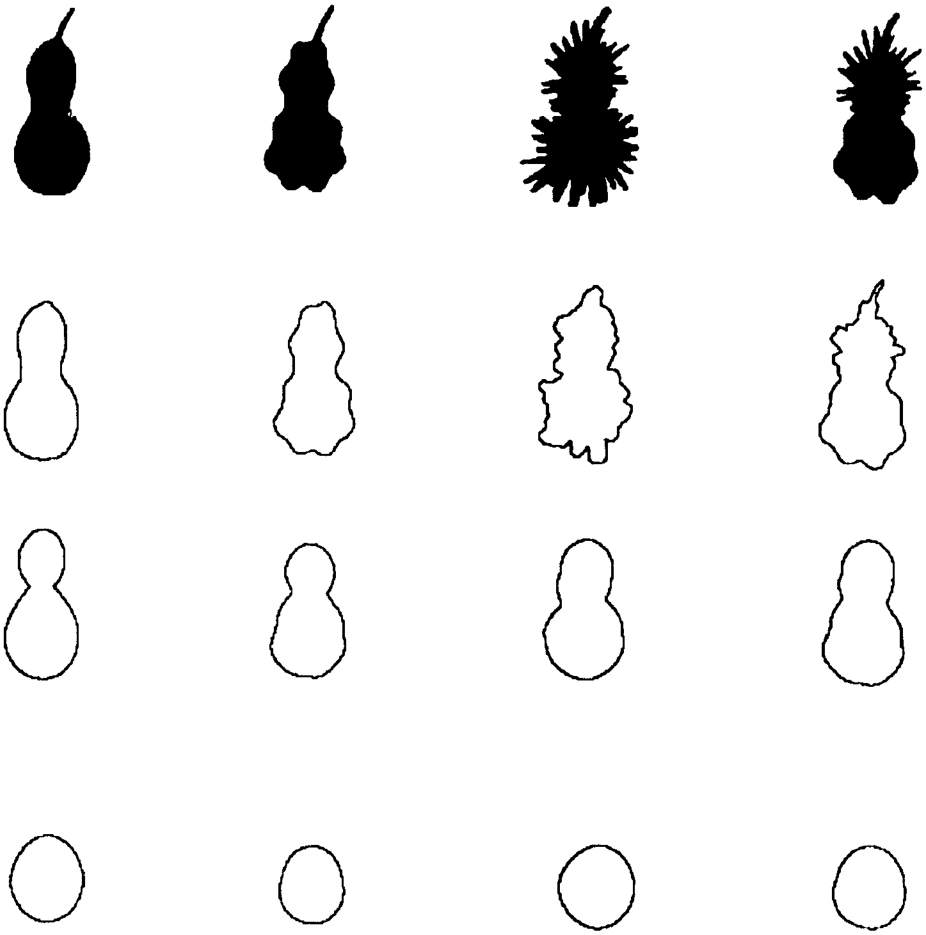

Figure 7.3: Samples from a slice through the entropy scale-space are displayed for four pears. Note that the similarity that emerges with increased smoothing provides a basis for building a similarity measure between shapes.

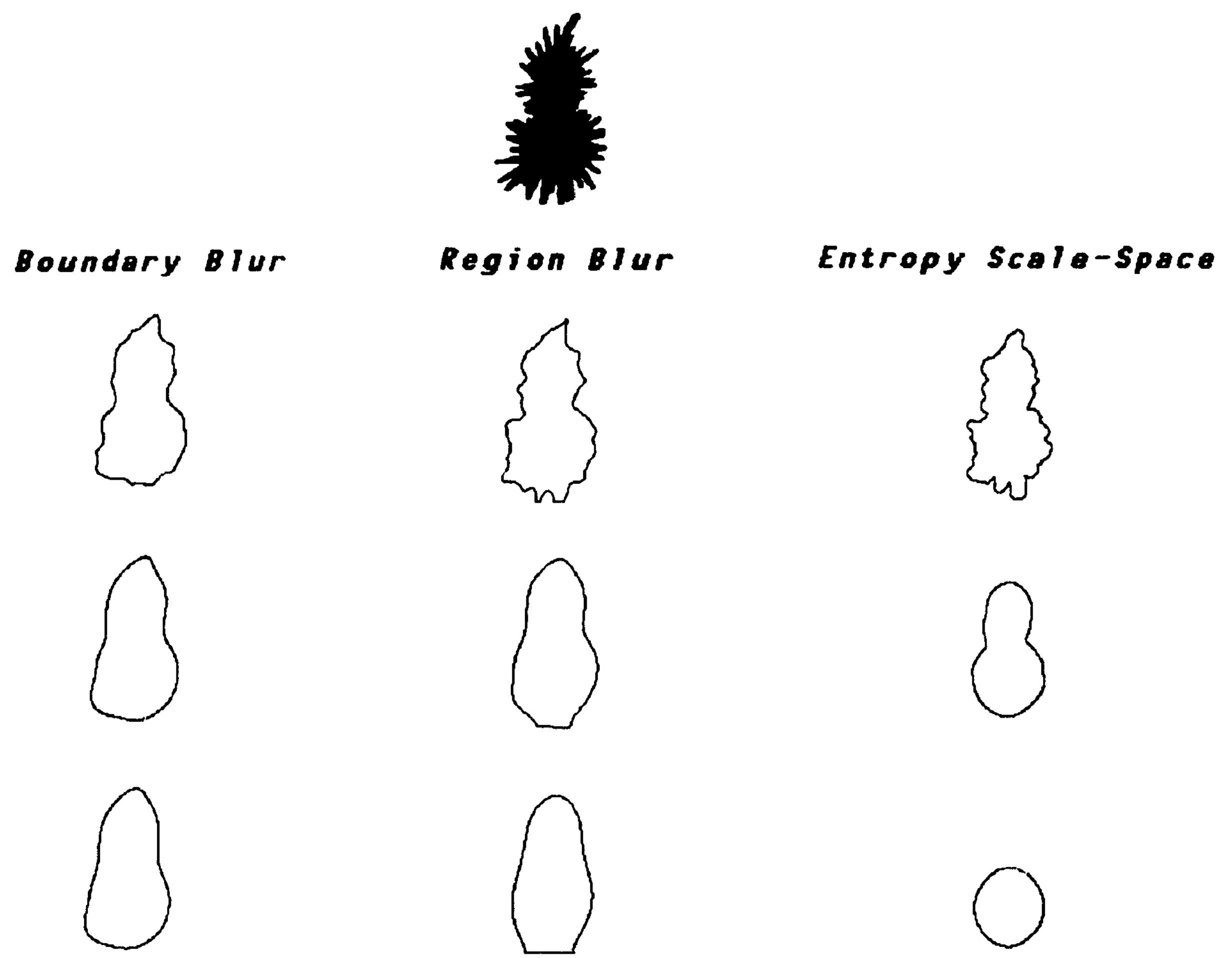

Figure 7.4: Samples of the "electric pear" are taken and displayed in columns. The left column corresponds to the smoothing the boundary coordinates, the middle column to smoothing the region characteristic function. Finally, the right column displays samples from one slice of the entropy scale-space.

a measure of similarity and a topology on shape. This is then contrasted with the results based on boundary-based and region-based Gaussian blur. Finally, the portion of the entropy scale-space is shown for several images. These images show that the entropy scale-space is a promising framework within which to build a topology for shape.

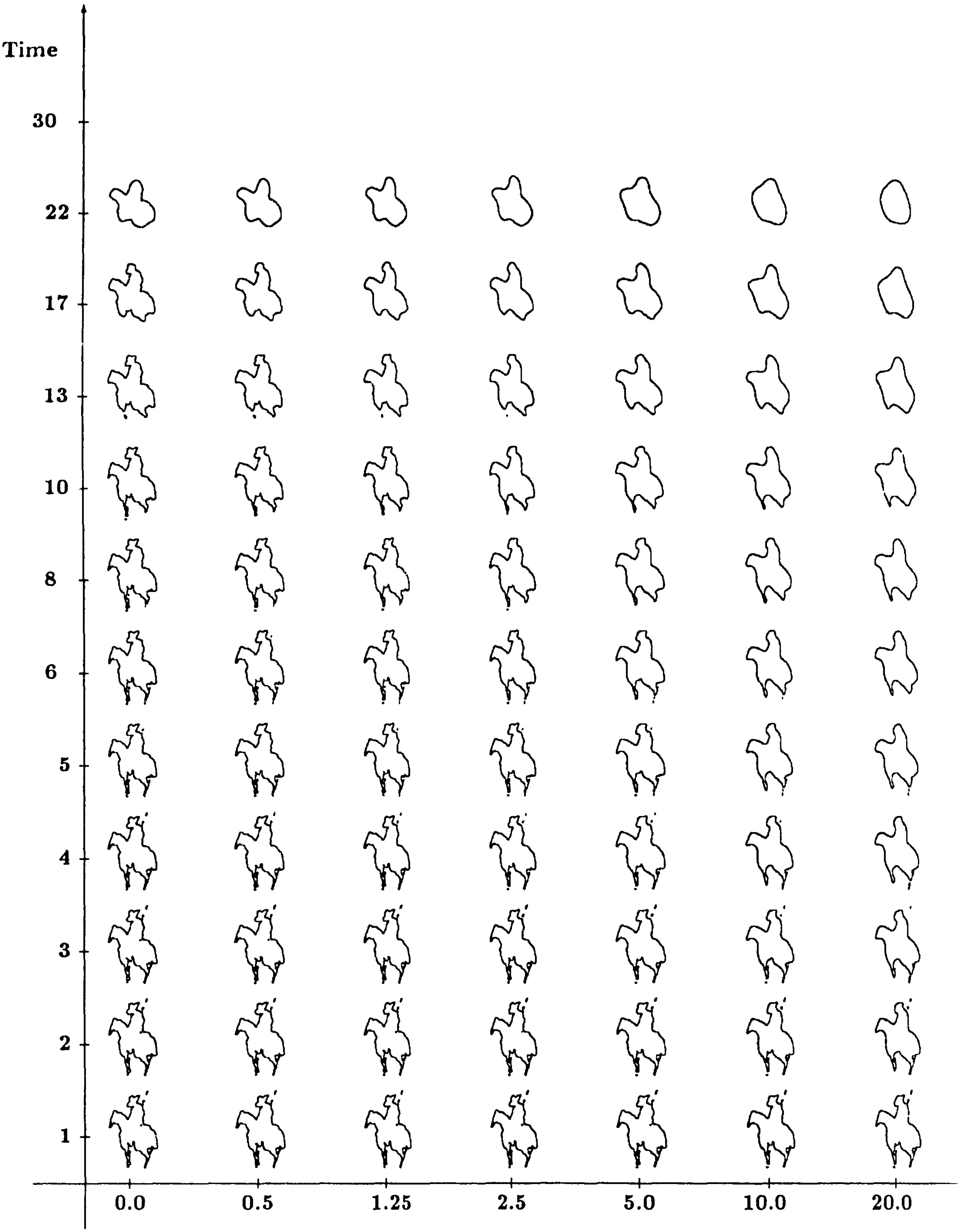
Time
30
22
17
13
10
8
6
5
4
3
2
1
0.0
0.5
1.25
2.5
5.0
10.0
20.0

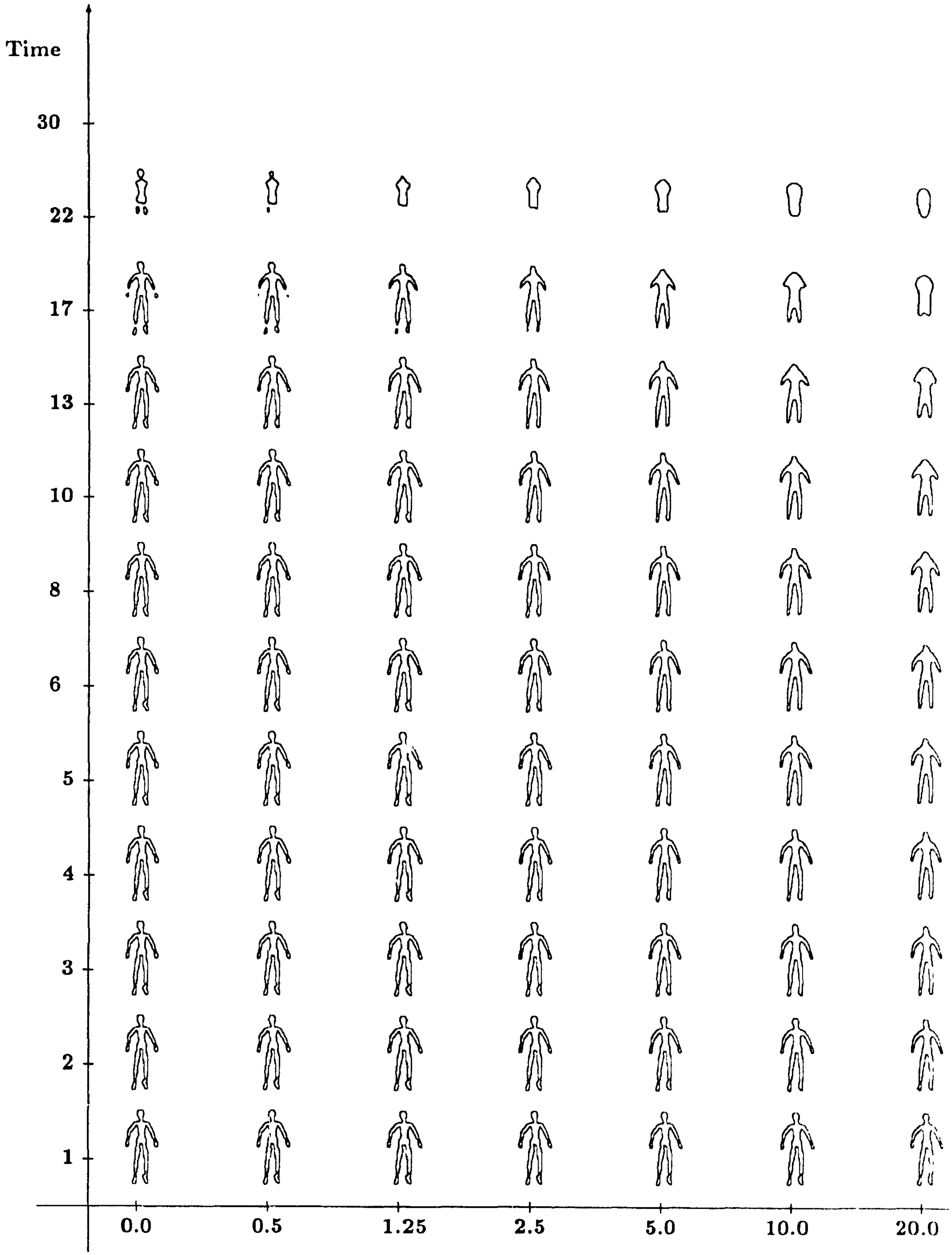
Time
30
22
17
13
10
8
6
5
4
3
2
1
0.0
0.5
1.25
2.5
5.0
10.0
20.0

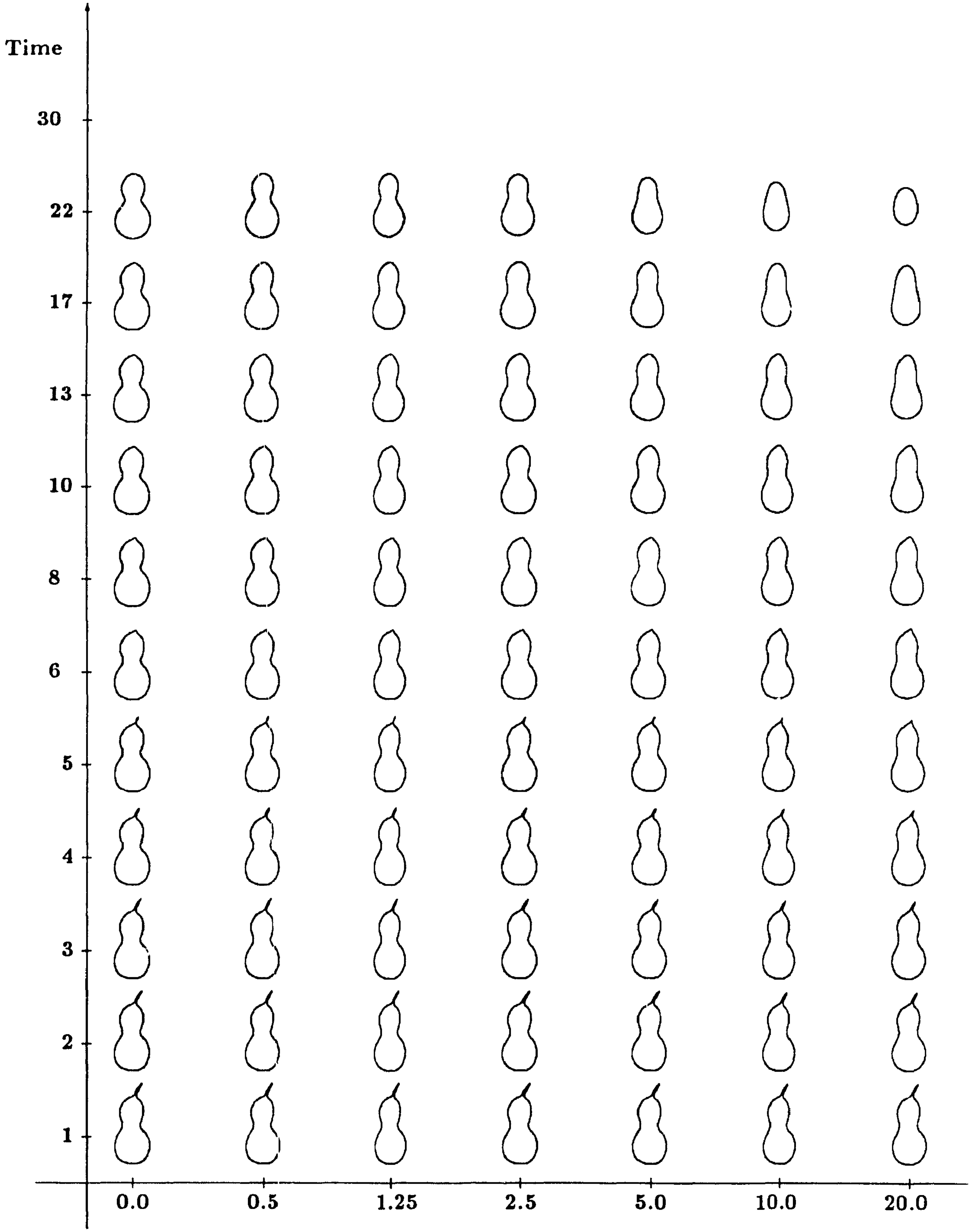

Time
30
22
17
13
10
8
6
5
4
3
2
1
0.0
0.5
1.25
2.5
5.0
10.0
20.0

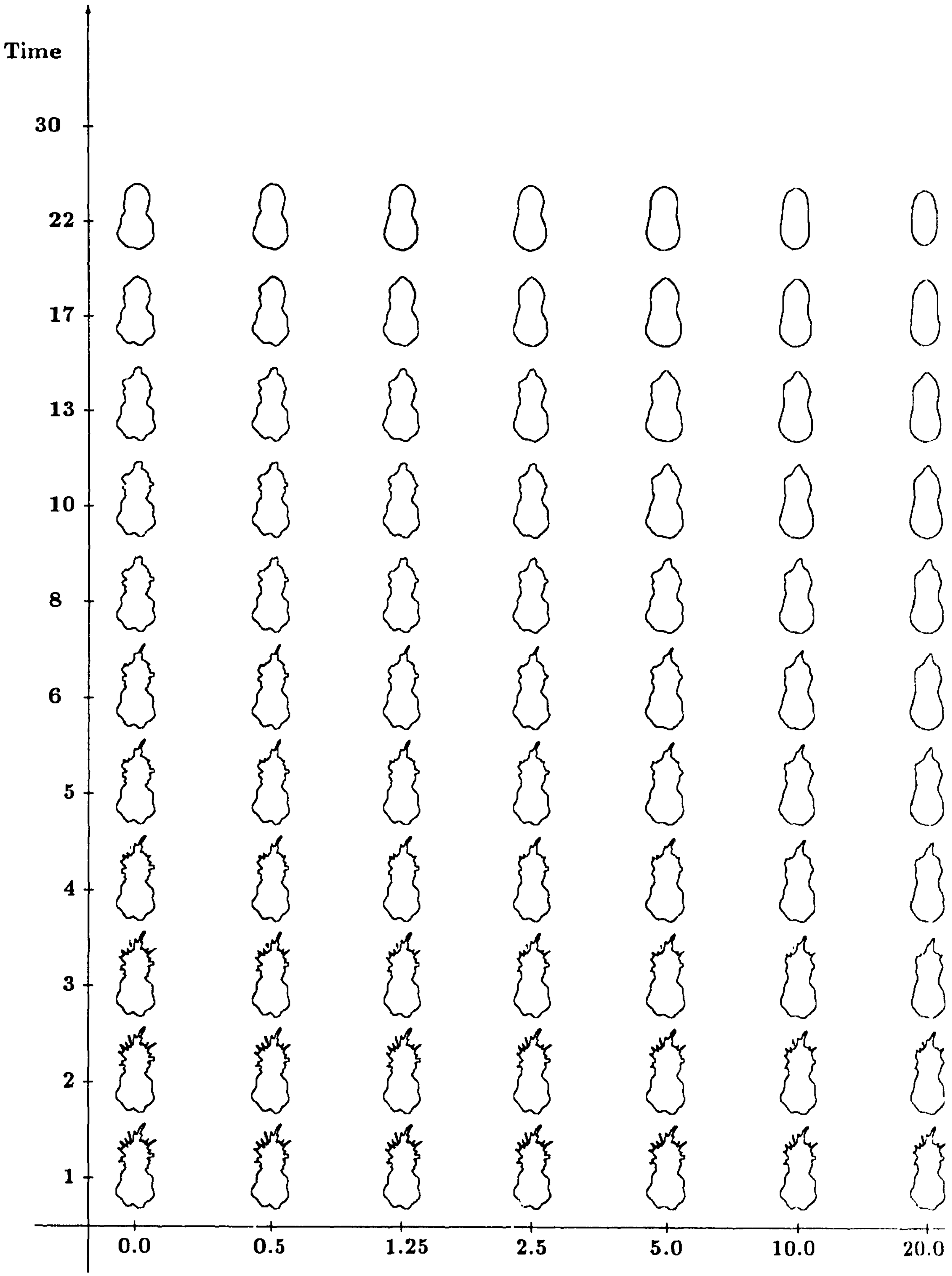
Time
30
22
17
13
10
8
6
5
4
3
2
1
0.0
0.5
1.25
2.5
5.0
10.0
20.0

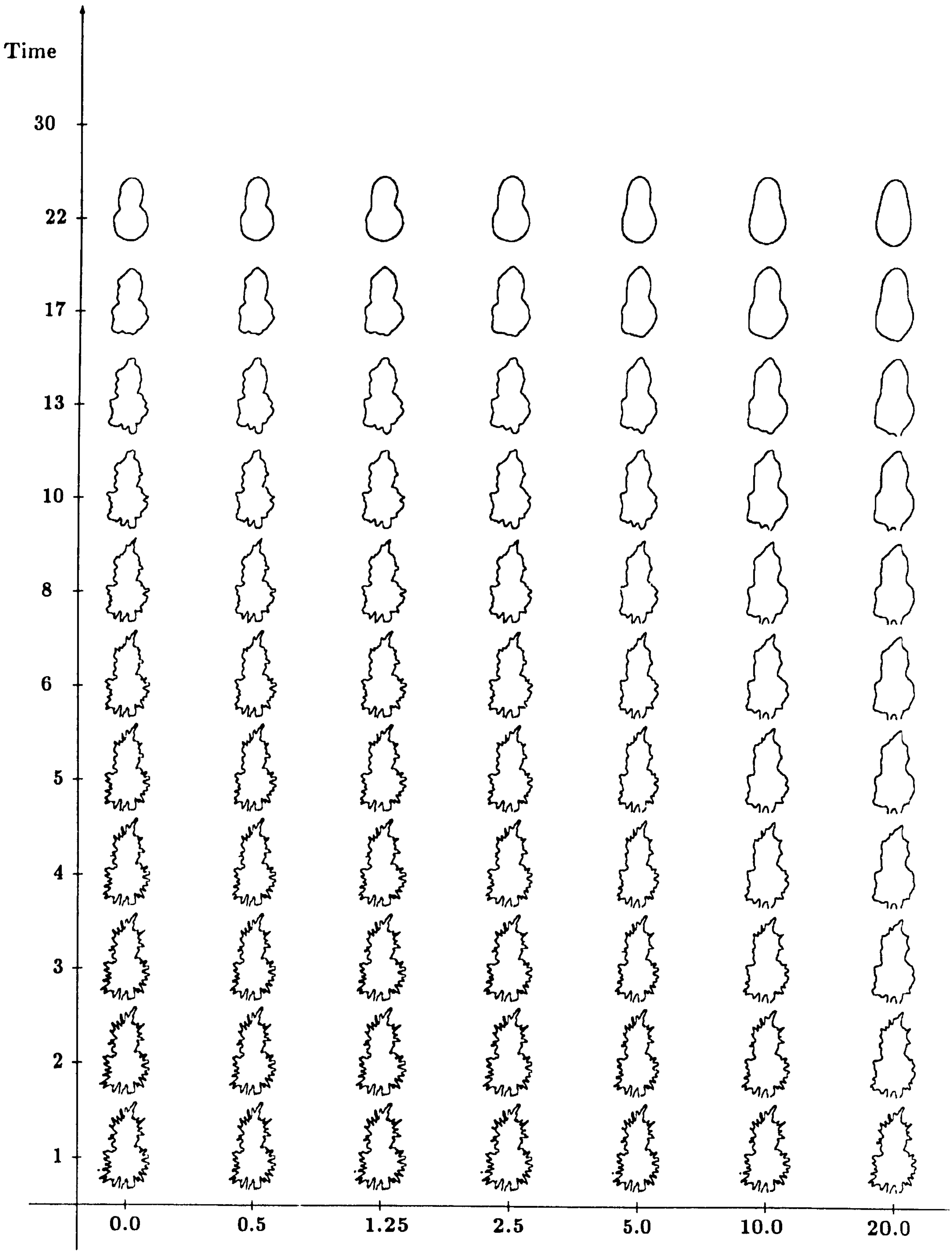
Time
30
22
17
13
10
8
6
5
4
3
2
1
0.0
0.5
1.25
2.5
5.0
10.0
20.0

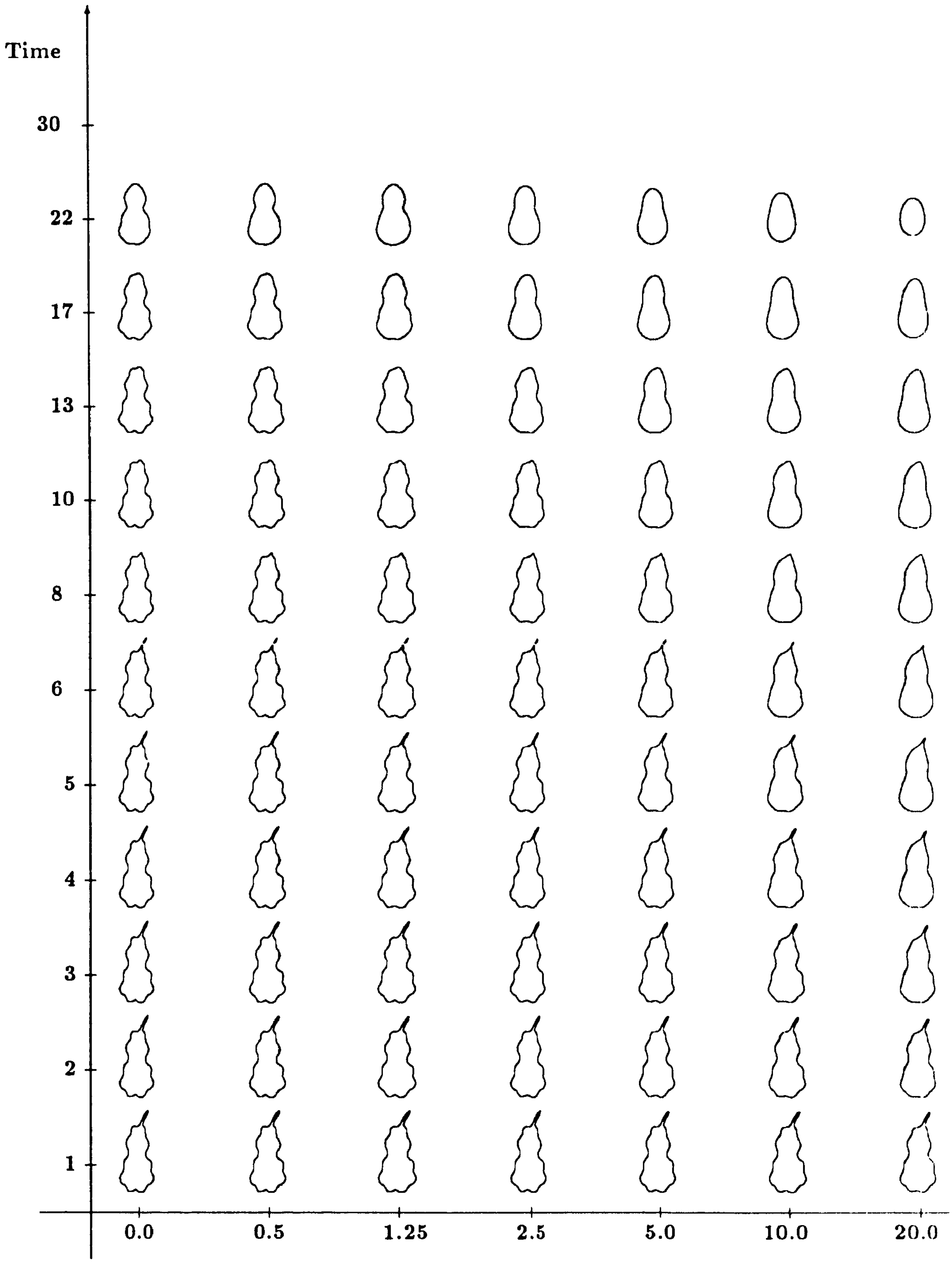
Time
30
22
17
13
10
8
6
5
4
3
2
1
0.0
0.5
1.25
2.5
5.0
10.0
20.0

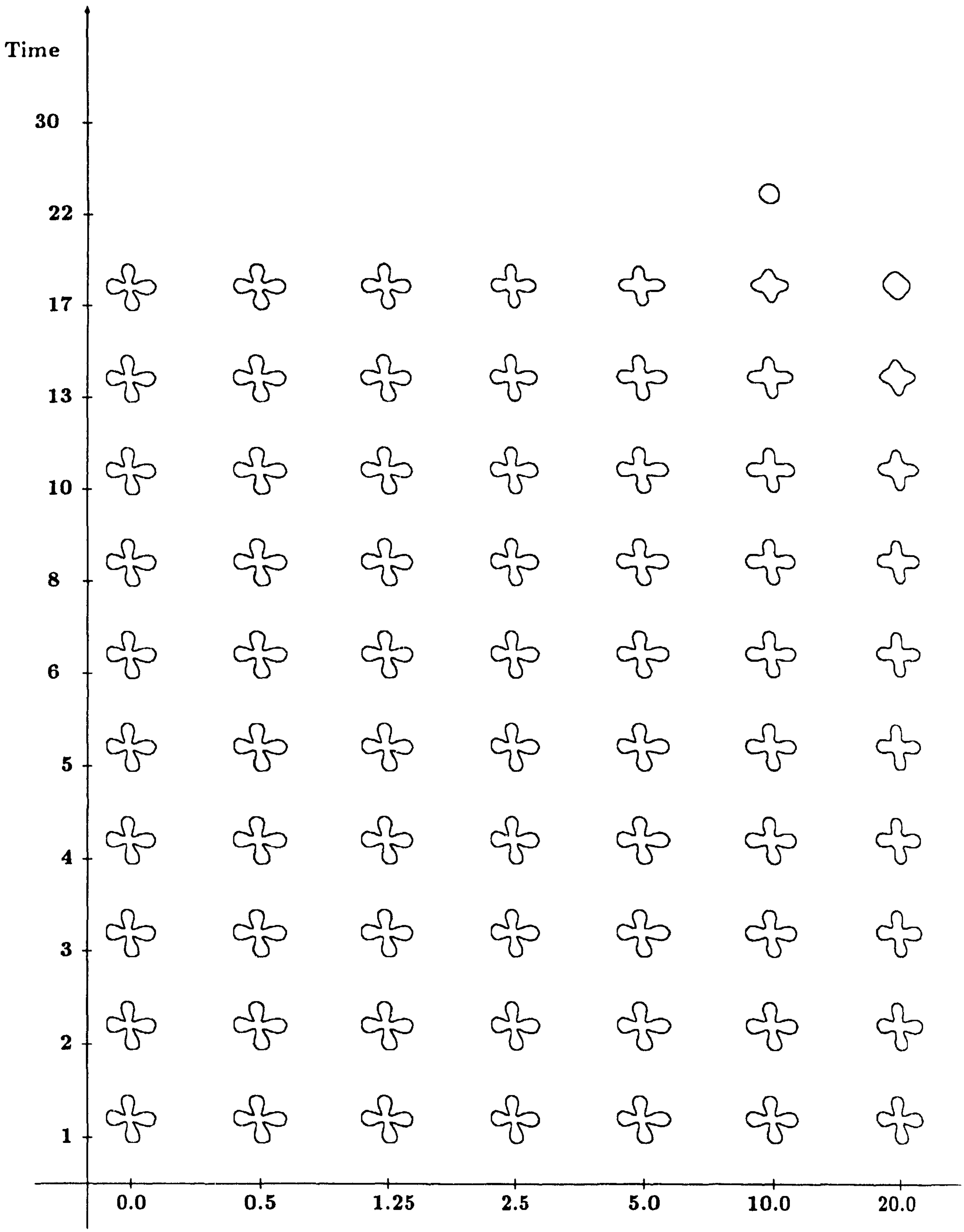
Time
30
22
17
13
10
8
6
5
4
3
2
1
0.0
0.5
1.25
2.5
5.0
10.0
20.0

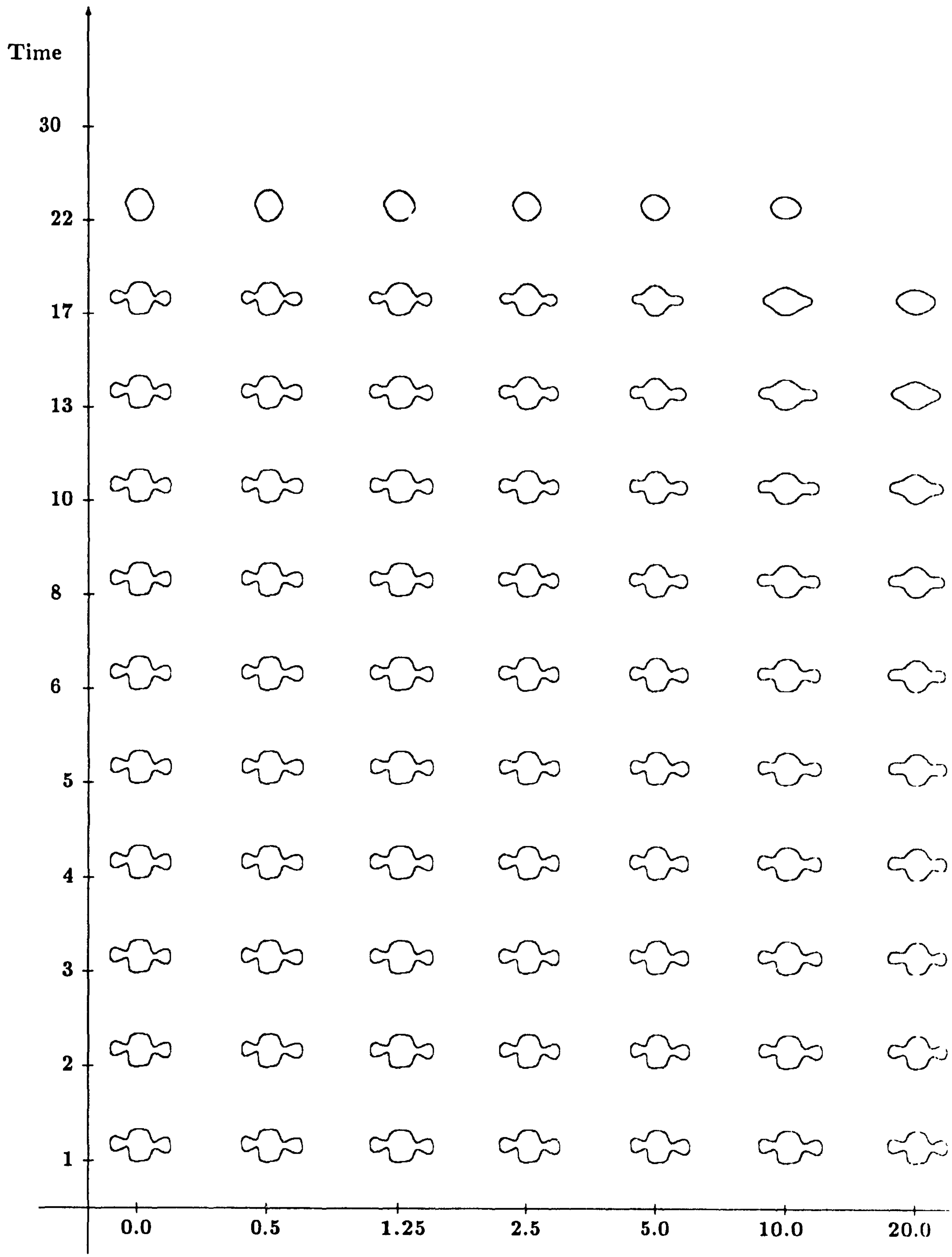
Time
30
22
17
13
10
8
6
5
4
3
2
1
0.0
0.5
1.25
2.5
5.0
10.0
20.0

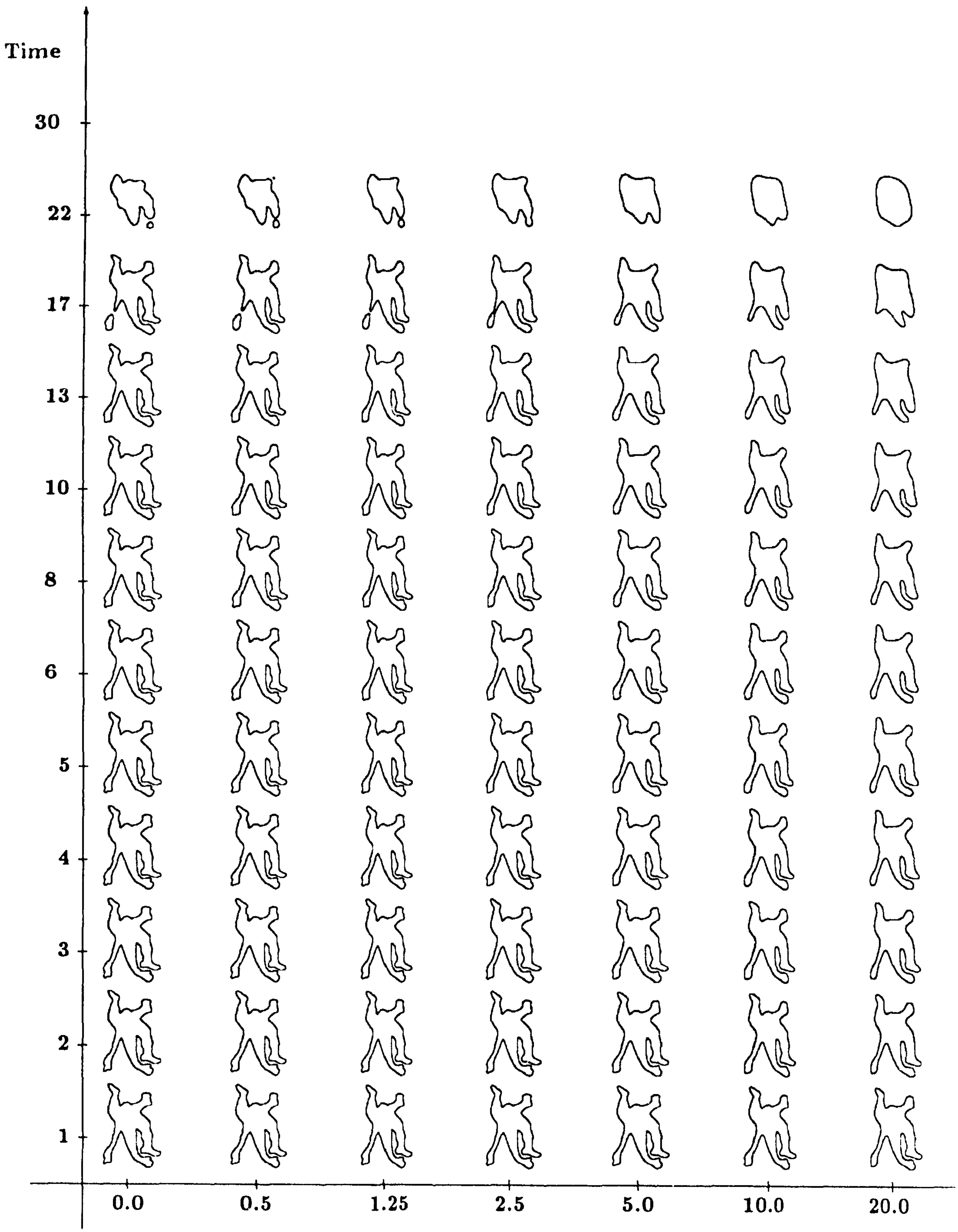
Time
30
22
17
13
10
8
6
5
4
3
2
1
0.0
0.5
1.25
2.5
5.0
10.0
20.0

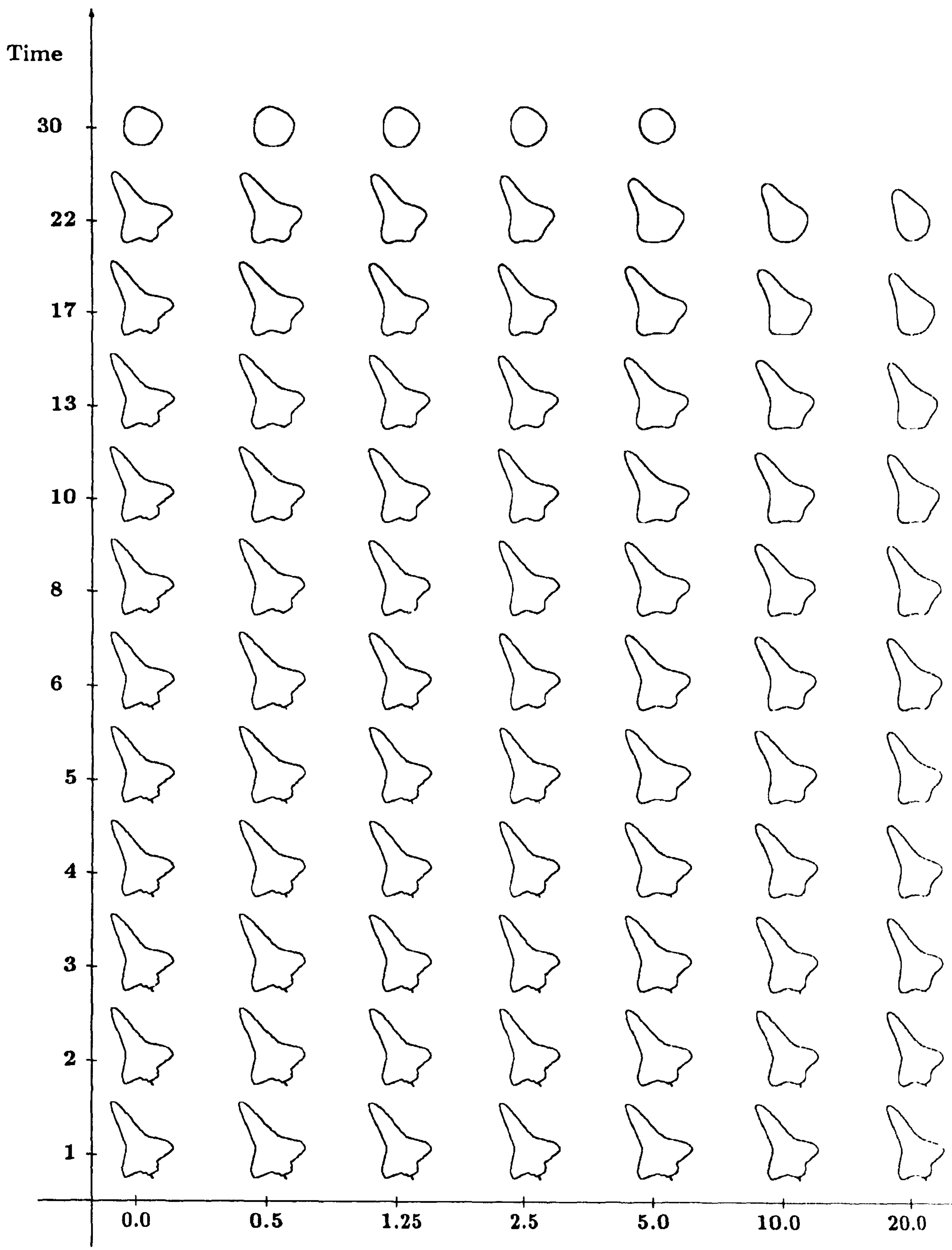

Time
30
22
17
13
10
8
6
5
4
3
2
1
0.0
0.5
1.25
2.5
5.0
10.0
20.0

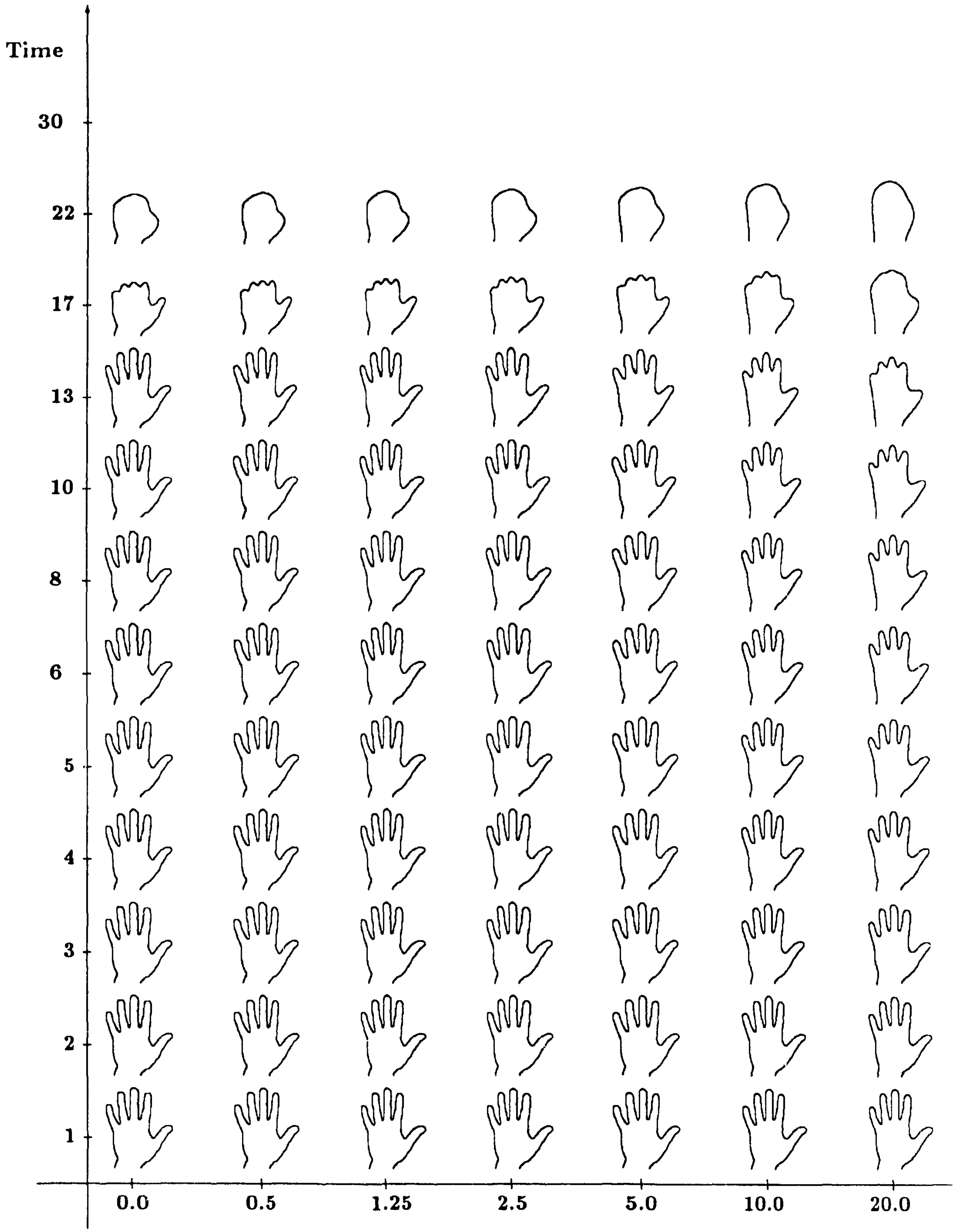
Time
30
22
17
13
10
8
6
5
4
3
2
1
0.0
0.5
1.25
2.5
5.0
10.0
20.0

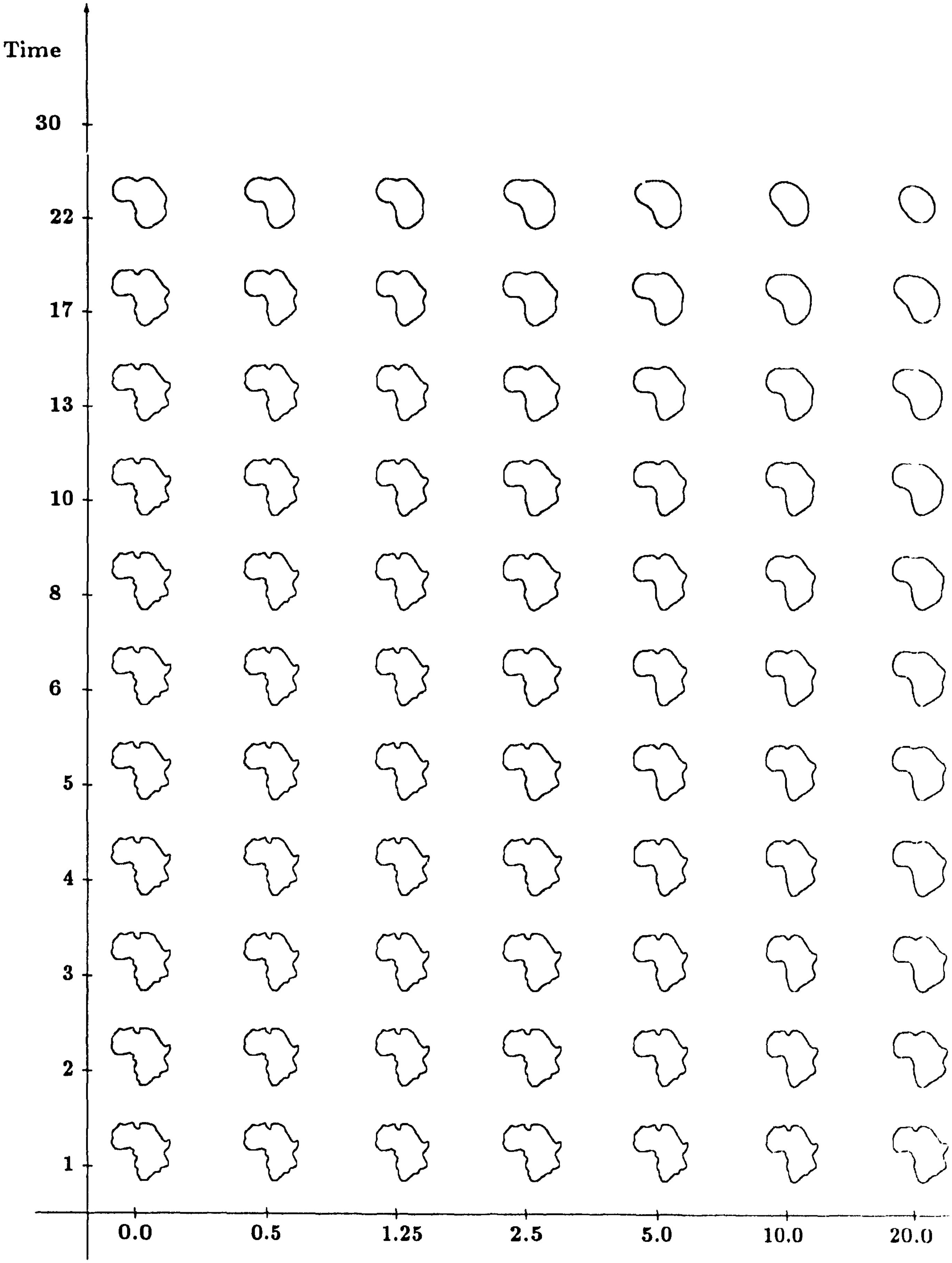

Time
30
22
17
13
10
8
6
5
4
3
2
1
0.0
0.5
1.25
2.5
5.0
10.0
20.0

Chapter 8

The Shape Triangle

In the previous chapter, *parts*, *protrusions*, and *bends* were proposed as computational elements of shape. Parts are components of *composition*, protrusions are *boundary deformations*, and bends are *region deformations*. We now assign a process to compute each of these elements and focus on effects at a single scale. Each process defines a corner in the *shape triangle*. In this chapter, we explore the relationship and the interaction between these *shape processes*. We propose that these processes in cooperation and in competition describe the shape; that is they locate the shape in the shape triangle.

8.1 The Many Faces of Shape

The essence of shape is in its relationship to its many similar neighboring shapes. In other words, one might describe a shape as a similar shape with some alteration. For example, "a car with its antenna raised" is very, intimately connected to "a car with its antenna down" figure 8.1. A description of shape ought to capture this relationship, or otherwise, as the antenna is raised the description could become drastically different. Furthermore, the interpretation of this description is not unique,

Figure 8.1: Our perception of a car does not change drastically as its antenna is raised. Similarly, the change in representation of objects when a small feature is added should be slight.

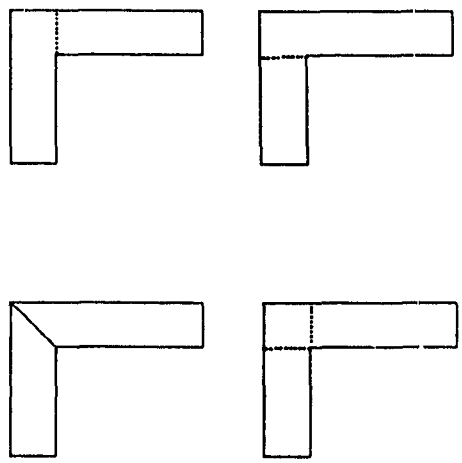

Figure 8.2: The elbow may be partitioned in many ways [36]. This ambiguity is not necessarily undesirable: connectivity of shape is the essence of it

in that there are often many ways of interpreting a shape, figure 8.2. In this chapter, we explore the multiple interpretations of shapes, and show that, contrary to popular opinion, this is not an undesirable effect. In fact, to force a shape into a discrete interpretation is to ignore the relationships between shapes in effect to ignore the natural topology of shape

To illustrate this multiple interpretation of shape, we have done a number of qualitative psychophysical experiments. Each experiment involves a sequence representing gradual alteration of one shape to another The goal is to correlate the change in percept with the geometrical aspects of shape.

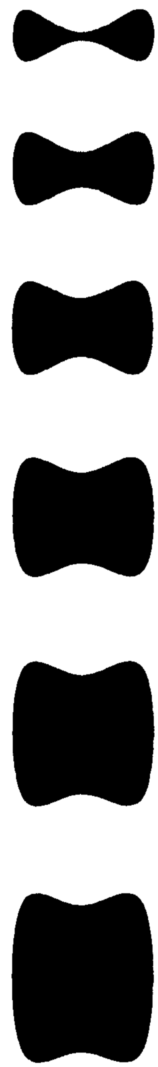

Figure 8.3. The sequence is generated by altering the top shape by expanding a portion of each of its lateral boundaries. As such, the number, order, and the spacing of non-lateral extrema remains intact. Nevertheless, there is a change in percept from the top shape as having two parts to the bottom shape as a rectangle with a deformed boundary.

As the first example of this multiple interpretation of shape, consider figure 8.3 where the top shape is progressively changed so that, during this sequence, the top and bottom portions of the boundary remain intact, while the lateral boundary segments are stretched. Observe how the percept of the shapes comprising the sequence varies: While the shape on the top (bowtie) is often perceived as having two parts, the shape on the bottom (trainwheel) is most often seen as a single object. In other words, the shape on top is seen to be an object where two parts came together and were attached. In contrast, the object on the bottom is perceived as a rectangle whose boundary was modified. For shapes in between both explanations are plausible to varying degrees: they can either be seen as a glued pair or as a deformed rectangle. Schemes which are purely based on the location and ordering of the curvature extrema would tend to miss this change of percept.

As a second example, consider shapes in figure 8.4 where the shape sequence is constructed as above. Here, the shape on top is recognized as a snake, or perhaps a worm, while the shape on the bottom can be recognized as a lasagna noodle. The shape of the snake may be interpreted as a bending of its body, sometimes straight and other times bent. In contrast, the lasagna-noodle shape may best be explained as the result of deforming the boundary of some rectangle by cutting along its edges. Note that it is difficult to see the bottom shape as a bent rod, or the top shape as a rectangle with modified boundary. Again, the change represents increased spacing between two pairs of curvature features (extrema or inflection points) without changing either the number, order, or the spacing of other curvature features. A boundary-based scheme without regional grouping of curvature extrema again would likely miss this change in percept.

As a third example, consider the sequence of shapes in figure 8.5 which is generated by displacing the bottom portion of the boundary. In this case, the bottom portion is displaced by sliding it under the top portion. Again, the change is between

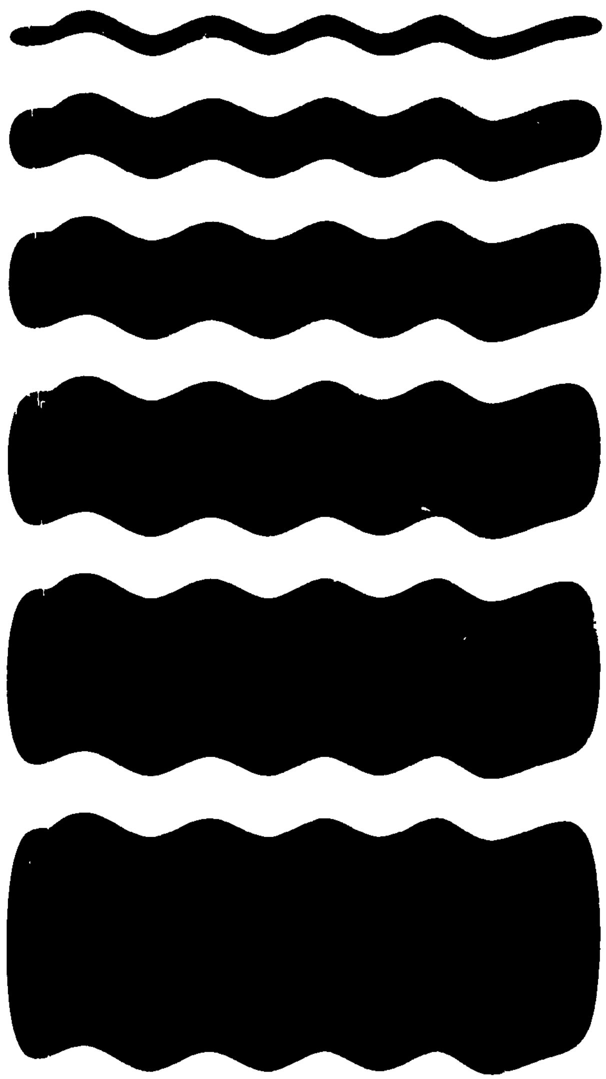

Figure 8.4: This sequence is generated by stretching the lateral boundary which does not affect the number, order, and spacing of other boundary features. The change in percept is one of a bent stick (top) to a rectangle with a deformed boundary (bottom).

two boundary points only and all other points are not affected. Observe that the top shape (sausage) is most frequently judged to have six parts while the bottom shape (auger) is seen to be a single object. The bottom shape is instead seen as a bent stick, while this is unlikely to be the case for the top shape. This change of percept can be explained as a grouping of boundary features through the region: in the first case two negative curvature extrema group to form a neck. In contrast, in the second case positive curvature maxima and negative curvature minima group to claim the shape as a bending of a rectangle.

As another example, consider the modification of shapes in figure 8.6 where, as before, portions of the boundary are stretched. Note that while the shape on the top (cross) is seen to have four parts (sometimes five parts were reported), the shape on the bottom is judged as having three parts (rolling pin). The intermediate shapes are sometimes seen as having three parts and other times as four or five. In other words, while in the extremes the perception is clear, for shapes in between multiple interpretations are possible.

8.2 The Shape Triangle

The multiple perceptions and interpretations of shape are not undesirable. In fact, we argue that without the power to support multiple and simultaneous interpretations of shape, our perceptions would violently change as shapes were modified, e.g. consider any sequence of the previous section. Since we live in a changing world where movement of parts, growth, occlusion, etc. is not uncommon, representations that support multiple interpretations are necessary.

Descriptions of shape are indeed related to other shapes. In chapter 6 we proposed three computational elements for shape: *parts* for composition, *protrusions* for boundary deformations, and *bends* for region deformation. In general, a shape may be

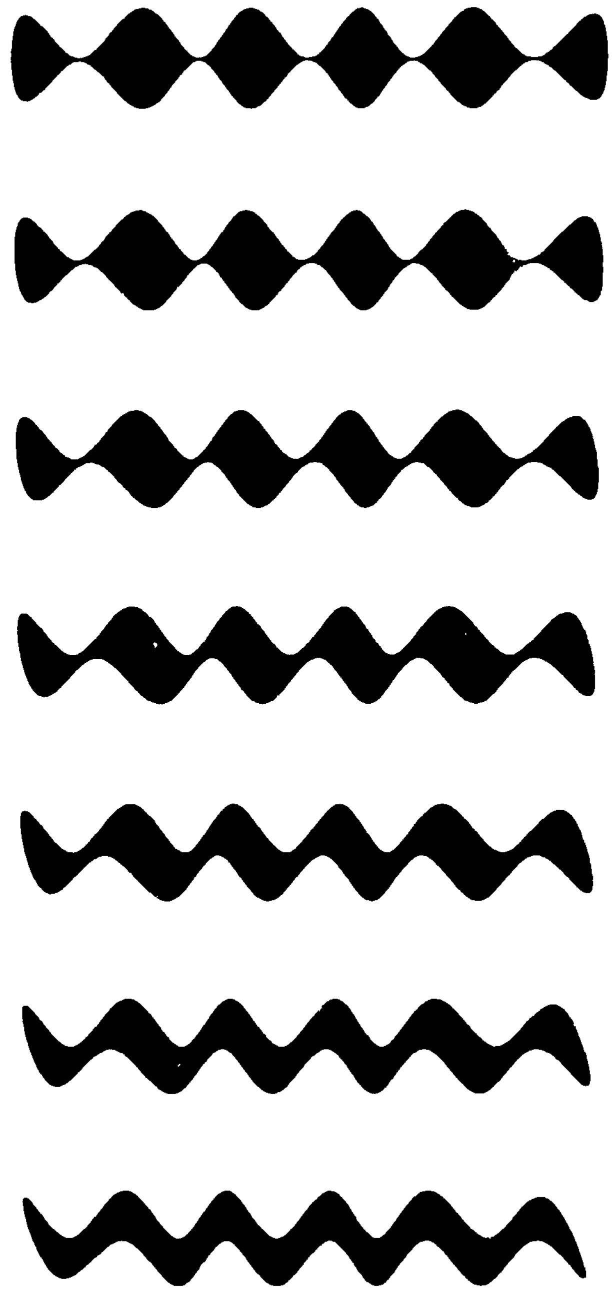

Figure 8.5: This sequence is generated by shifting the bottom portion of the boundary under the top portion. The change percept changes from an object with six parts to a that of a bent stick. Again, this change of percept can not be explained by purely boundary-based methods.

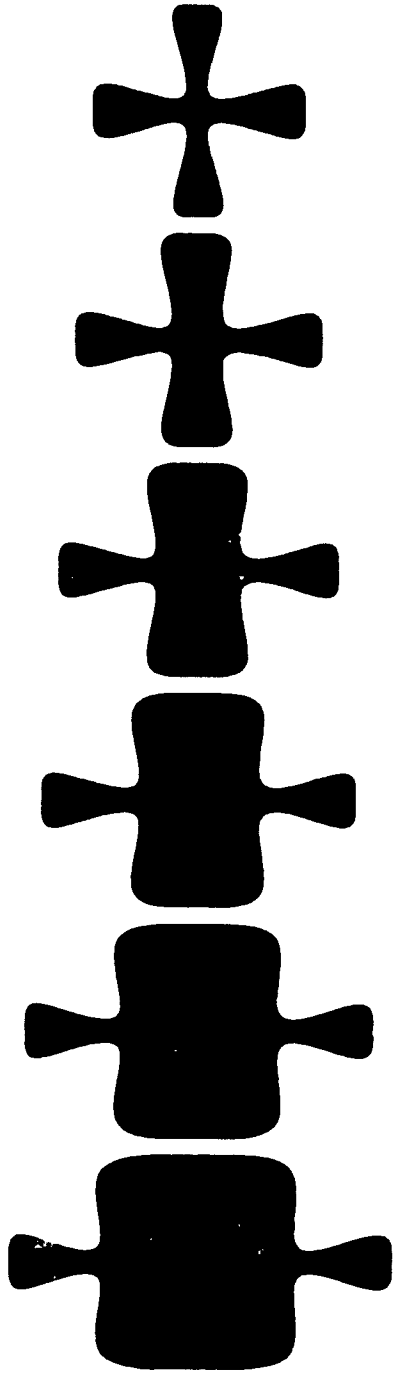

Figure 8.6

The percept changes from the "iron cross" to that of a "rolling pin" when the top shape is transformed to the bottom one. The sequence is generated by stretching the top and portions of the boundary.

transformed in any combination of these three shape processes. These processes form a *basis* for arbitrary transformations and we conceptually assign each to the corner of a **shape triangle**, figure 8.7. A shape, then, is placed somewhere in the triangle between other shapes in the corners. This is our representation for a simple shape: more complicated shapes involve a more complex sequence of these three processes with multiple layers of scale.

8.3 The Shape Triangle

The shape triangle represents three dimensions of shape: compositions, boundary deformations, and region deformations.

To illustrate the idea of the shape triangle, consider the sequence in figure 8.3 and the analysis of the (bowtie) versus the (trainwheel) in the shape triangle. While the bowtie has a strong part component, the boundary deformation process is giving a weak interpretation, figure 8.8. In contrast, the boundary process gives a strong interpretation of the trainwheel, the part gives a weak interpretation of the trainwheel, figure 8.9. How can these interpretations be derived from the reaction-diffusion space? For the bowtie, the reaction process gives parts due to a topological split and formation of a second order shock. Increasing the diffusion ratio only delays the time of shock (second order) formation. It is only for large diffusion values that this shock does not form. The trainwheel has a different representation in the reaction-diffusion space, since second order shocks do not form, or at best form for only very small diffusion values.

Let us now consider the sequence in figure 8.4 where the two extremes, the snake and the noodle have different representations in the shape triangle. For the snake, the bend process claims a strong interpretation, while the boundary process gives a weak one, figure 8.10. In contrast, for the noodle, the bend process gives a weak

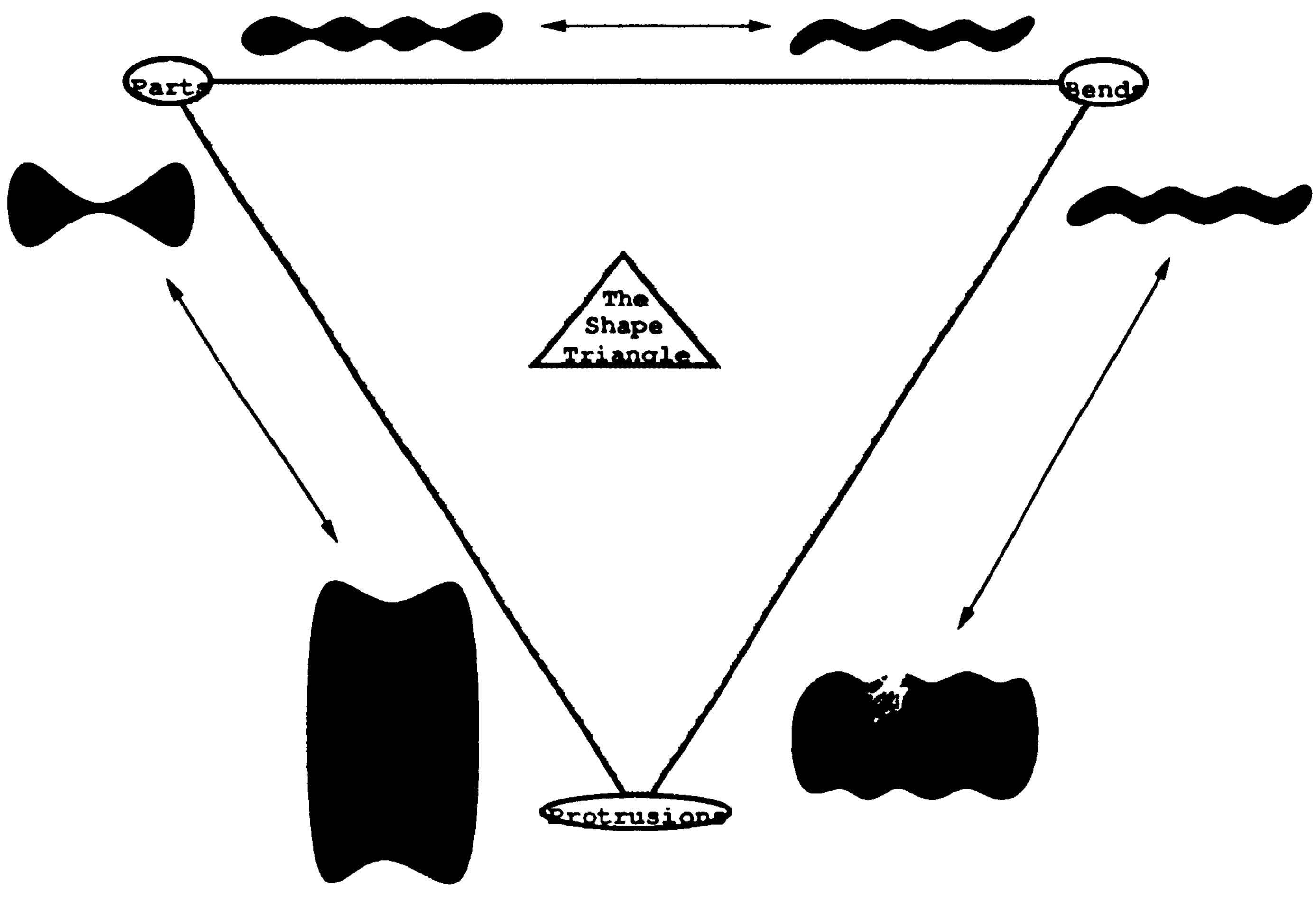

Figure 8.7: The Shape Triangle is triangular in shape.

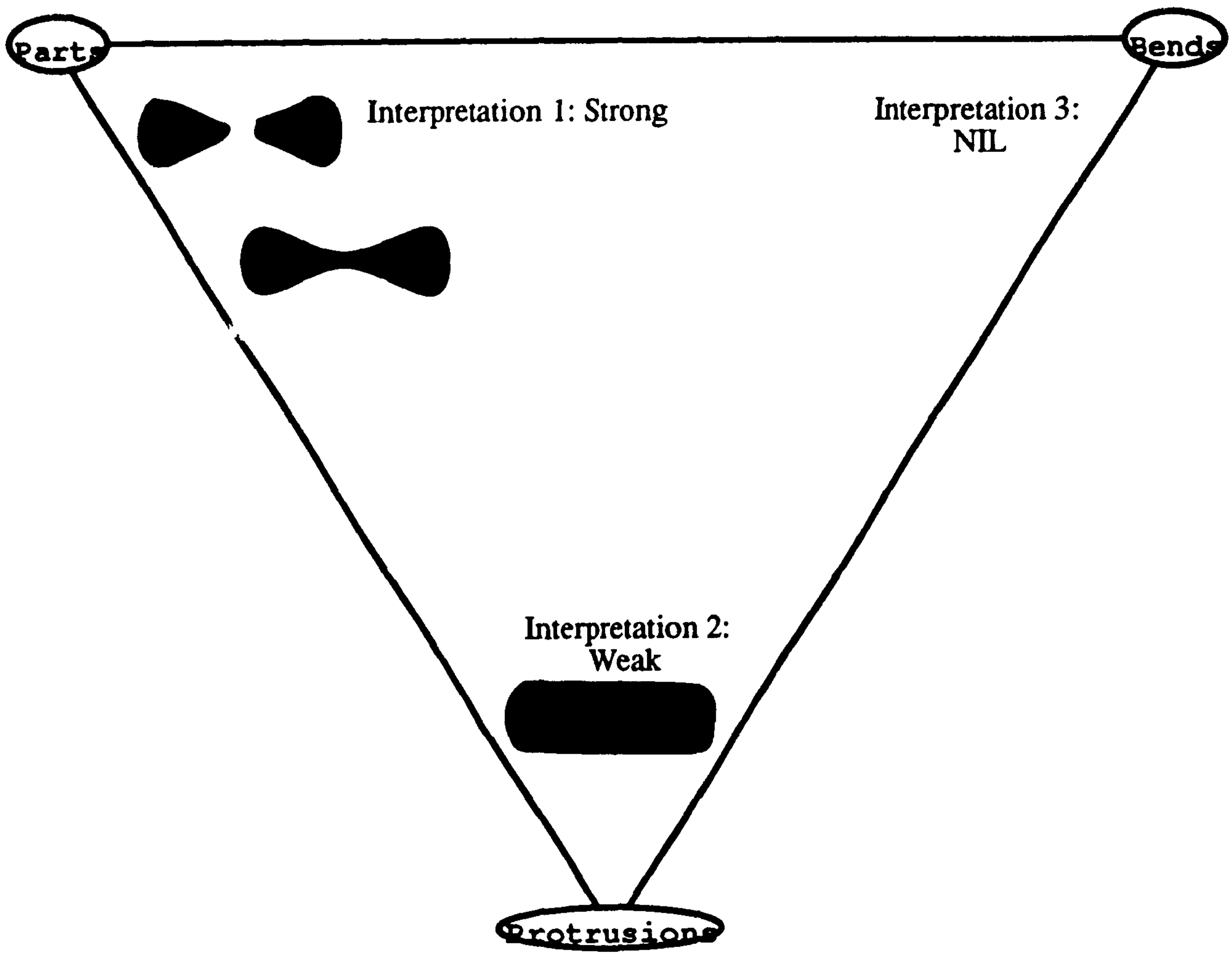

Figure 8.8: The bowtie shape has a strong part interpretation, but a weak boundary interpretation.

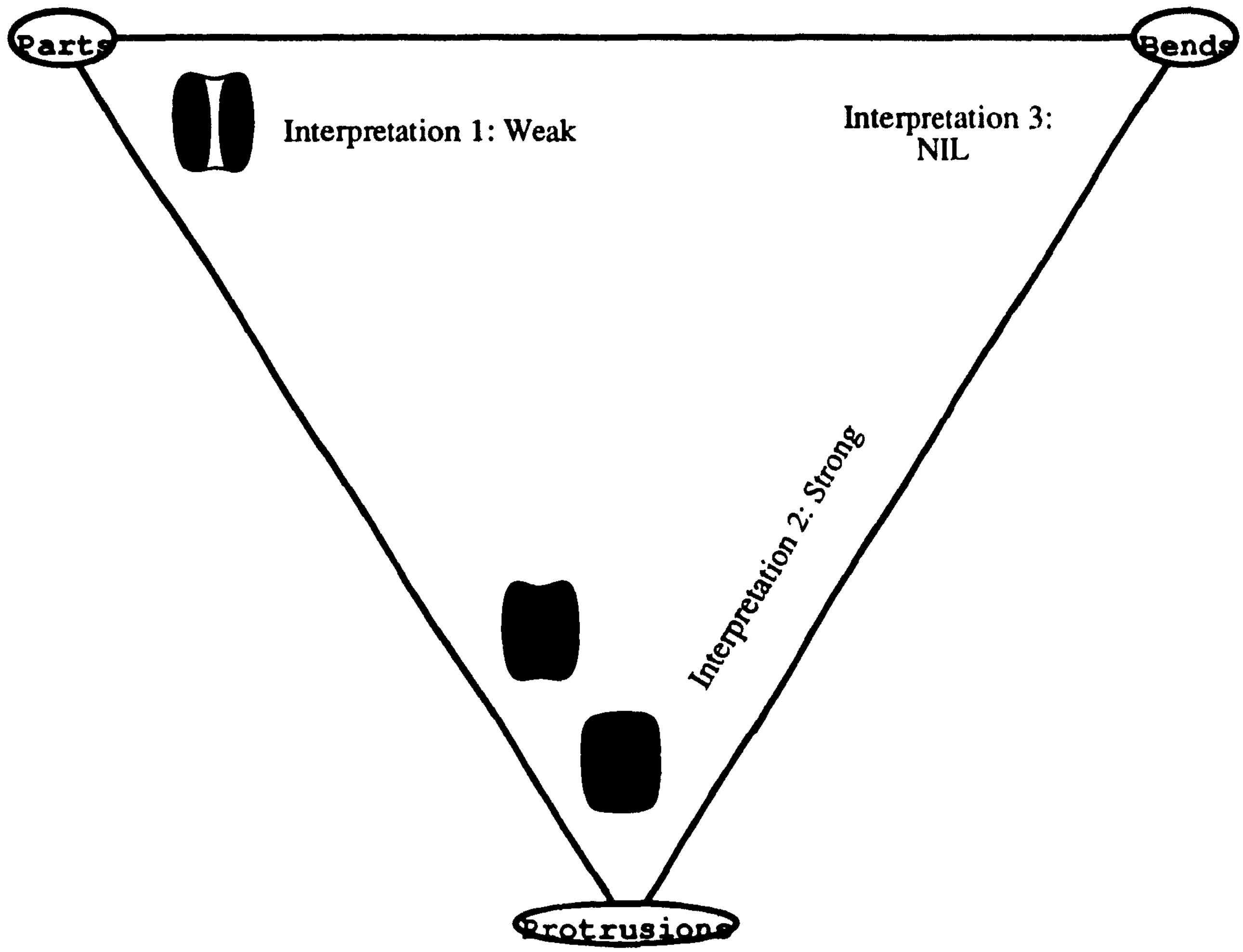

Figure 8.9: The trainwheel shape has a weak part interpretation, but a strong boundary interpretation.

interpretation, while the boundary process asserts a strong interpretation, figure 8.11. To relate this to shocks, for the snake third order shocks form quickly, while for the noodle first order shocks form.

Finally, to depict the competition along the third axis of parts-bends, consider the sequence in figure 8.5 The sausage has a strong part interpretation, while the snake has a strong bend interpretation. To summarize, figure 8.12 depicts the tension between the three processes of shape. At this point, we present the following proposal.

Proposal 8.1 (**shape triangle**) *Shape is explained as the interaction of three shape processes. One shape process (parts) in biased to "see" parts and composition. It very optimistically searches for possibilities of compositions and reports its parts. The second shape process (protrusions) concentrates on the boundary and is entirely biased to see shapes as simpler shapes whose boundary was deformed The third shape process (bends), is region-oriented and reports of modifications of the shape through its axis. Through competition and cooperation these processes explain a shape as a series of operations on simple shapes.*

While we showed in this chapter how the shape triangle can support shape descriptions, and indicated intuitively how it can be derived from the reaction/diffusion space, it remains to study them with the same mathematical precision utilized in earlier parts of this thesis.

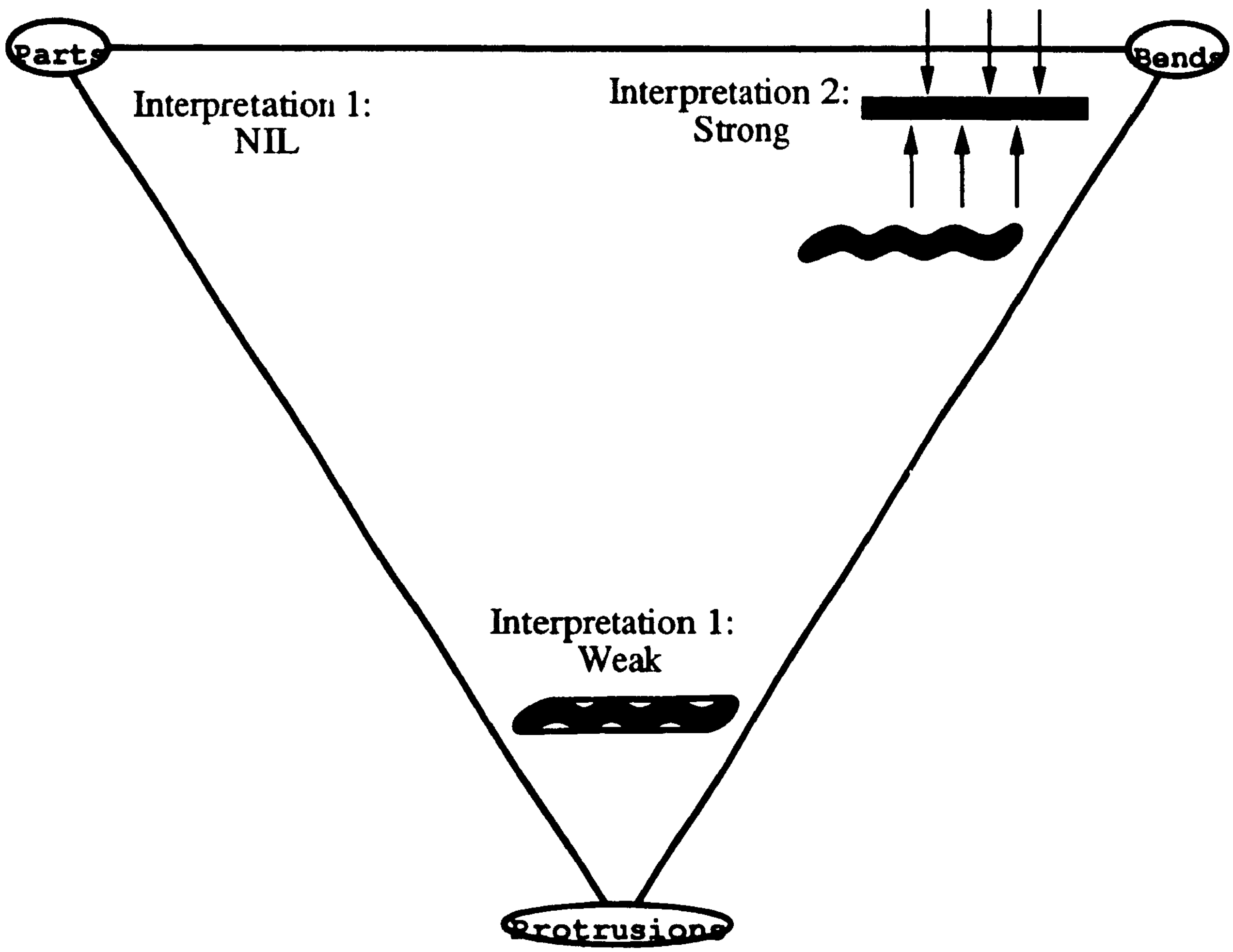

Figure 8.10 The snake is interpreted strongly as a bend, but is weakly interpreted as the result of boundary deformation.

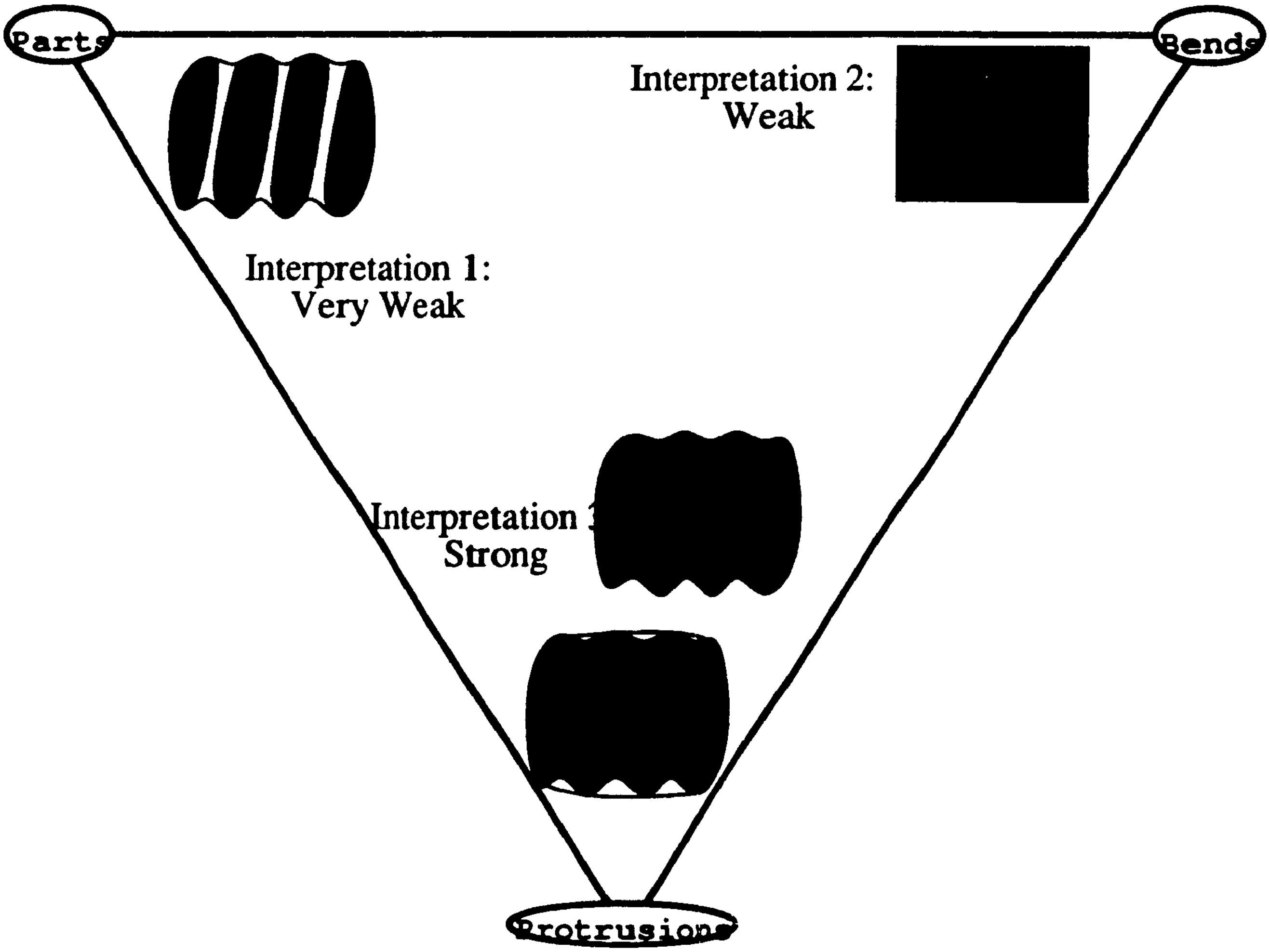

Figure 8.11: The Lasagnia noodle is given a strong vote by the protrusion process but is given a weak one by the bend process.

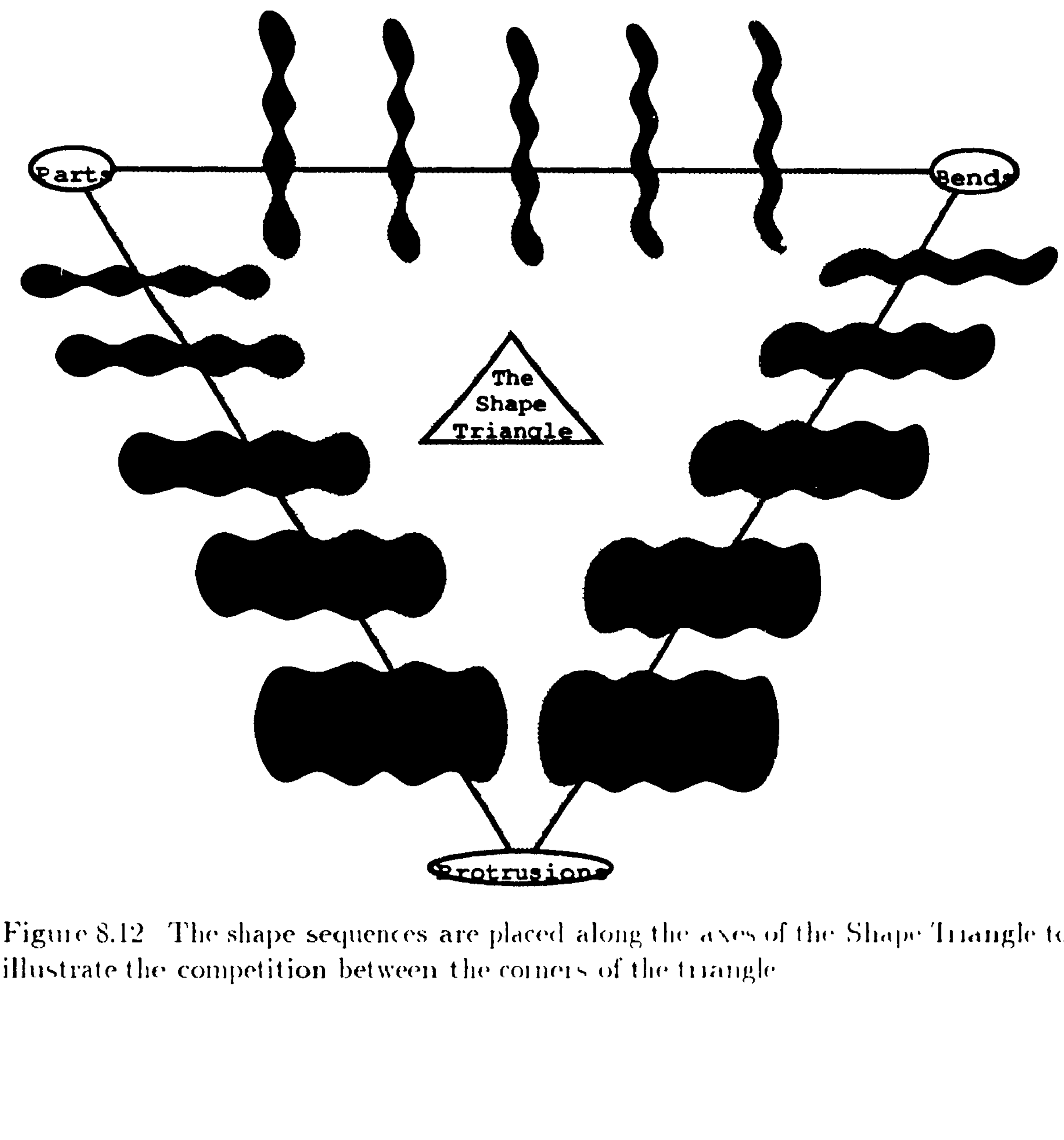

Figure 8.12 The shape sequences are placed along the axes of the Shape Triangle to illustrate the competition between the corners of the triangle

Chapter 9

Conclusion

We have presented the beginning of a theory of shape based on the dynamic evolution of curves. We were motivated by the need for a new geometry, which lead to a classification of deformations into constant motion and curvature motion. While constant motion satisfies a conservation law, curvature motion plays the role of viscosity. Viewed differently, constant and curvature motion satisfy a reaction-diffusion system The two extremes of reaction and diffusion bring out complementary properties of shape. Most importantly, the reaction-diffusion equations lead to entropy satisfying singularities called shocks It is the classification of these shocks that inspired our proposal that parts, protrusions, and bends be considered as the computational elements of shape. The shocks were studied in a reaction-diffusion space, which is spanned by time and the ratio of reaction to diffusion, and leads to a natural notion of approximation and scale. Scale lead in turn to another space, the entropy scale-space, which, provided the final support for the shape triangle. This final structure suggested a representation for shapes in which three shape processes cooperate and compete for an interpretation of shape

Our work is by no means complete While we have provided a new approach to study shape, the final mapping from the shape triangle into formal shape descriptions requires much additional research. The metric and topology remain to be specified in mathematical detail, and the application to object matching in computer vision remains to be implemented. However, we feel confident that foundation has been properly laid, and that these next tasks can be accomplished in the near future

Bibliography

[1] H. Asada and M. Brady. The curvature primal sketch. *IEEE PAMI*, 8:2–14, 1983.

[2] F. Attneave. Some informational aspects of visual perception. *Psych Review*, 61:183–193, 1954.

[3] F. Attneave and M. D. Arnoult. The quantitative study of shape and pattern perception. *Psychological Bulletin*, 53(6):452–471, 1956.

[4] J. Babaud, A. P. Witkin, M Baudin, and R. O Duda Uniqueness of the gaussian kernel for scale-space filtering. *PAMI*, 8(1):26–33, January 1986.

[5] D. Ballard Strip trees: A hierarchical representation for curves. *Comm ACM*, 24(5):310–321, May 1981.

[6] D H. Ballard and C. M. Brown. *Computer Vision*. Prentice Hall, New Jersey, 1982.

[7] G. Barles. Remarks on a flame propagation model. Technical Report No 464, INRIA Rapports de Recherche, December 1985.

[8] E. Ben-Jacob, N Goldenfield, J Langer, and G Schon. Dynamics of interfacial pattern formation. *Physical Review Letters*, 51(21):1930–1932, 1983.

[9] I. Biederman Recognition by components. *Psych. Review*, 94:115–147, 1987.

[10] T. Binford. Inferring surfaces from images. *Artificial Intelligence*, 17:205–244, 1981.

[11] H. Blum. Biological shape and visual science. *J. Theor. Biol.*, 38:205–287, 1973.

[12] H. Blum. A geometry for biology. *Annals of N.Y. academy of Sciences. Mathematical Analysis of Fundamental Biological Phenomena*, 213:19–30, 1974.

[13] R. Bolles and R. Cain. Recognizing and locating partially visible objects: The local-feature-focus method. *International Journal of Robotics Research*, 1(3):57–82, 1982.

[14] F. L. Bookstein. *The Measurement of Biological Shape and Shape Change*. Springer-Verlag, 1978.

[15] R. Brooks. Symbolic reasoning among 3-d models and 2-d images. *Artificial Intelligence*, 17:285–348, 1981.

[16] F. W. Campbell and J. G. Robson. Applications of fourier analysis to the visibility of gratings. *J. Physiol (London)*, 197:551–556, 1968.

[17] M.-H. Chen and P.-F. Yan. A multiscale approach based on morphological filtering. *PAMI*, 11(7):694–700, July 1989.

[18] E. Conway and E. Hopf. Hamilton's theory and generalized solutions of the Hamilton-Jacobi equation. *Journal of Mathematics and Mechanics*, 13(6):939–986, 1964.

[19] . F. K. Courant, R. *Supersonic Flow and Shock Waves*. Interscience Publishers, 1948.

[20] M. Crandall. The semigroup approach to first-order quasilinear equations in several space variables. *Israel J. Math.*, 12:108–132, 1972.

[21] M. Crandall and P. Lions. Viscosity solutions of Hamilton-Jacobi equations *Trans. Amer. Math. Soc.*, 277:1–42, 1983

[22] M. P. do Carmo. *Differential Geometry of Curves and Surfaces.* Prentice Hall, New Jersey, 1976.

[23] A. Douglis. An ordering principle and generalized solutions of certain quasilinear partial differential equations. *Comm. Pure. Appl. Math.*, 12:87–112, 1959.

[24] G. Dudek. Shape representation from curvature. Ph.D. dissertation, Dept. of computer science, University of Toronto, Toronto, Canada, 1990.

[25] W. J. Firey. Shapes of worn stones. *Mathematika*, 21:1–11, 1974.

[26] H. Freeman. Computer processing of line drawing images. *Computer Surveys*, 6(1):57–98, March 1974.

[27] M. Gage. On an area-preserving evolution equation for plane curves. *Contemp. Math.*, 51:51–62, 1986.

[28] M. Gage and R. S. Hamilton. The heat equation shrinking convex plane curves. *J. Differential Geometry*, 23:69–96, 1986

[29] P. Garabedian. *Partial Differential Equations.* John Wiley and Sons, 1964

[30] P. Gardenier, B. McCallum, and R. Bates. Fourier transform magnitudes are unique pattern recognition templates. *Biological Cybernetics*, 54:385–391, 1986.

[31] J. Gibson. *The Perception of the Visual World.* Riverside Press, 1950.

[32] J. Glimm and P. D. Lax. Decay of solutions of systems of hyperbolic conservation laws. *American Math. Soc. Memoir, 101*, 1970

[33] E. Gombrich. *Art and Illusion.* Princeton, Bollingen, 1956

[34] G. Granlund. Fourier processing for handprinted character recognition. *IEEE Transaction on Computing*, c-21:195–201, 1972.

[35] M. A. Grayson. The heat equation shrinks embedded plane curves to round points. *J. Differential Geometry*, 26:285–314, 1987.

[36] D. D. Hoffman and W. A. Richards. Parts of recognition. *Cognition*, 18:65–96, 1985.

[37] E. Hopf. The partial differential equation $u_t + uu_x = \epsilon u_{xx}$. *Comm. Pure Appl. Math.*, 3:201–230, 1950.

[38] R. Hummel, B. B. Kimia, and S. W. Zucker. Deblurring gaussian blur. *Computer Vision, Graphics, and Image Processing*, 38:66–80, 1987.

[39] IEEE Computer Society. *Second International Conference on Computer Vision*, Tampa, Florida, December 1988.

[40] F. John. *Partial Differential Equations*. Springer-Verlag, 1971.

[41] B. B. Kimia, A. Tannenbaum, and S. W. Zucker. On the evolution of curves via a function of curvature, I: The classical case. *JMAA*, To appear, 1990.

[42] J. J. Koenderink. The structure of images. *Biol. Cybernetics*, 50:363–370, 1984.

[43] J. J. Koenderink and A. J. van Doorn. Visual detection of spatial contrast: Influence of location in the visual field, target extent and illuminance level. *Biological Cybernetics*, 30:157–167, 1978.

[44] J. J. Koenderink and A. J. van Doorn. Dynamic shape. *Biol. Cyber.*, 53:383–396, 1986.

[45] S. Kruskov. First-order quasilinear equations with several space variables. *Math. USSR Sb.*, 10:217–273, 1970.

[46] J. Langer. Instabilities and pattern formation in crystal growth. *Reviews of Modern Physics*, 52(1):1–28, 1980.

[47] P. D. Lax. Hyperbolic systems of conservation laws II. *Comm. Pure Appl. Math.*, 10:537–566, 1957.

[48] P. D. Lax. *Shock Waves and Entropy*, pages 603–634. Academic Press, New York, 1971.

[49] P. D. Lax. *Hyperbolic Systems of Conservation Laws and the Mathematical Theory of Shock Waves*. SIAM Regional Conference series in Applied Mathematics, Philadelphia, 1973.

[50] P. D. Lax. Shock waves, increase of entropy and loss of information. Technical Report DOE/ER/03077-240, Courant Mathematics and Computing Library-R&D Report, 1981.

[51] M. D. Levine, P. B. Nobel, and Y. M. Youssef. Understanding blood cell motion. *Computer Graphics and Image processing*, 21(1):188–209, January 1983.

[52] F. Leymarie and M. D. Levine. Shape features using curvature morphology. In *Proceedings of the SPIE "Intelligent Robots and Computer Vision VIII: Algorithms and Techniques" Conference*, volume 1192, part 2, pages 536–547, Philadelphia, Penn., USA, November 1989.

[53] M. Leyton. Symmetry-curvature duality. *Computer Vision, Graphics, and Image processing*, 38:327–341, 1987.

[54] M. Leyton. A process grammar for shape. *AI*, 34:213–247, 1988.

[55] N. K. Link and S. W. Zucker. Sensitivity to corners in flow patterns. *Spatial Vision*, 12(3):233–241, 1987.

[56] P. Maragos. Pattern spectrum and multiscale shape representation. *PAMI*, 11(7):701-716, July 1989.

[57] D. Marr and E. Hildreth. Theory of edge detection. Technical Report MIT AI Memo 518, MIT AI Lab, 1979.

[58] D. Marr and K. H. Nishihara. Representation and recognition of the spatial organization of three dimensional structure. *Proceedings of the Royal Society of London*, B200:269–294, 1978.

[59] E. E. Milios. Recovering shape deformation by an extended circular image representation. In ICCV2 [39], pages 20–27.

[60] F. Mokhtarian and A. Mackworth. Scale-based description of planar curves and two-dimensional shapes. *IEEE PAMI*, 8:34–43, 1986.

[61] D. Mumford. The problem of robust shape descriptors. In *Proceedings of the First International Conference on Computer Vision*, pages 602–606, London England, 1987.

[62] O. Oleinik. Discontinuous solutions of nonlinear differential equations. *Amer. Math. Soc. Transl. Ser. 2*, 26:95–172, 1957.

[63] S. Osher and J. Sethian. Fronts propagating with curvature dependent speed: Algorithms based on Hamilton-Jacobi formulations. *Journal of Computational Physics*, 79:12–49, 1988.

[64] A. Pentland. Recognition by parts. In *First International Conference on Computer Vision*, London, England, June 1987. IEEE Computer Society.

[65] A. Pentland. Part segmentation for object recognition. *Neural Computation*, 1:82–91, 1989.

[66] P. Perona and J. Malik. Scale-space and edge detection using anisoropic diffusion. *PAMI*, 12(7):629-639, July 1990.

[67] E. Persoon and K. Fu. Shape discrimination using fourier descriptors. *IEEE Transaction on Systems, Man, and Cybernetics*, SMC-7:170-179, 1977.

[68] S. M. Pizer, W. R. Oliver, and S. H. Bloomberg. Hierarchical shape description via the multiresolution symmetric axis transform. *IEEE PAMI*, 9(4):505-511, 1987.

[69] U. Ramer. An iterative procedure for the polygonal approximation of plane curves. *CVGIP*, 1(3):244-256, 1972.

[70] W. Richards and D. Hoffman. Codon constraints on closed 2d shapes. *CVGIP*, 31(2):156-177, 1985.

[71] A. Rosenfeld and A. C. Kak. *Digital Picture Processing*. Academic Press, 1982.

[72] A. Rosenfeld and M. Thurston. Edge and curve detection for visual scene analysis. *IEEE Trans. Comput.*, C-20:562-569, 1971.

[73] H. Samet. Region representation: Quad trees from boundary codes. *Comm. ACM*, 23(3):163-170, March 1980.

[74] J. Sethian. *Numerical Methods for Propagating Fronts*, pages 155-164. Springer-Verlag, New York, 1985.

[75] J. A. Sethian. Curvature and the evolution of fronts. *Comm. Math. Physics*, 101:487-499, 1985.

[76] G. Sivashinsky. Nonlinear analysis of hydrodynamic instability in laminar flames - I. derivation of basic equations. *Acta Astronautica*, 4:1177-1206, 1977.

[77] J. Smith. Shape instabilities and pattern formation in solidification. A new mathod for numerical solution of the moving boundary problem. *Journal of Computational Physics*, 39:112–127, 1981.

[78] J. Smoller. *Shock Waves and Reaction-Diffusion Equations*. Springer-Verlag, New York, 1983.

[79] J. G. Snodgrass and M. Vanderwart. A standardized set of 260 pictures. Norms for name agreement, image agreement, familiarity, and visual complexity. *Journal of Experimental Psychology: Human Learning and Memory*, 6(2):174–215, 1980.

[80] S. Sobolev. *Partial Differential Equations of Mathematical Physics*. Pregamon Press, 1964.

[81] R. Thom. page 89. Edinburgh University Press, 1970.

[82] D. Thompson. *On Growth and Form*. Cambridge University Press, London, England, 1961.

[83] P. H. Todd. *Intrinsic Geometry of Biological Surface Growth*. Springer-Verlag, 1986.

[84] J. Von Neumann and D.Richtmyer. A method for the numerical calculation of hydrodynamic shocks. *Journal of Applied Physics*, 21:232–237, 1950.

[85] T. Wallace and P. Wintz. An efficient three-dimensional aircraft recognition algorithm using normalized fourier descriptors. *Computer Vision, Graphics, and Image Processing*, 13:99–126, 1980.

[86] D. Waltz. *Understanding Line Drawings of Scenes with Shadows*. McGraw-Hill, 1975.

[87] B. White. Some recent developments in differential geometry. *The Mathematical Intelligencer*, 11(4):41–47, 1989.

[88] D. Widder. *The Heat Equation*. Academic Press, 1975.

[89] H. R. Wilson and J. R. Bergen. A four mechanism model for threshold spatial vision. *Vision Research*, 19(1):19–32, 1979.

[90] A. Witkin, D. Terzopoulos, and M. Kass. Signal matching through scale space. *International Journal of Computer Vision*, 1(2):133–144, 1987.

[91] A. P. Witkin. Scale-space filtering. In *Proceedings of the 8^{th} International Joint Conference on Artificial Intelligence*, pages 1019–1022, Karlsruhe, West Germany, Aug. 1983.

[92] A. L. Yuille. The creating of structure in dynamic shape. In ICCV2 [39], pages 685–689.

[93] A. L. Yuille and T. A. Poggio. Scaling theorems for zero crossings. *PAMI*, 8(1):15–25, January 1986.

[94] C. Zahn and R. Roskies. Fourier descriptors for plane closed curves. *IEEE Transactions on Computers*, C-21:269–281, 1972.

[95] S. W. Zucker and R. Hummel. Receptive fields and the representation of visual information. *Human Neurobiology*, 5:121–128, 1986.

[96] L. Zusne. *Visual Perception of Form*. Academic Press, New York, 1970.